Aspects of Q-ball Theory

Olivier R. E. V. Lennon
St John's College
University of Oxford

A thesis submitted for the degree of
Doctor of Philosophy
Trinity 2021

Acknowledgements

Despite its origin as a quip against Robert Hooke, Newton was right in his statement that we see further by standing on the shoulders of others. My life has been particularly full of these people while I have researched and produced the document you find before you. I shall acknowledge them here, but must apologise in case I forget any names – names may be forgotten, but the presence in my life is not.

Firstly, I would like to thank my supervisor, John March-Russell, for his guidance throughout my years in Oxford, as well as for sharing his ideas with me – some which worked, some which didn't – during my time as his student. I am truly a better physicist for having had an insight into the way he thinks.

I give thanks to my collaborators on all my projects during my DPhil. Aside from my supervisor, this includes Fady Bishara, George Johnson, Rudin Petrossian-Byrne and Hannah Tillim. In particular, I have worked with Fady for the majority of my DPhil, and so I must thank him for, in some sense, being my second supervisor. Special thanks are also reserved for Jesse Liu here – we may not have formally collaborated on any projects, but my – sometimes late night – discussions with him over the years have truly helped my intellect grow.

I must also thank Prateek Agrawal and Edward Hardy for agreeing to be the assessors of this thesis, as well as my other assessors over the years: Pedro Ferreira, Joseph Conlon and Fabrizio Coala. In particular, Pedro offered encouraging and helpful comments in the past.

On a practical level, a doctorate is impossible to complete without adequate funding. I must thus acknowledge the Science and Technologies Facilities Council for funding the bulk of my studies. Additional funding has come in the way from grants from St John's College or work at St John's College, Linacre College and St Catherine's College, as well as from members of my family: Christine Lennon, Michael and Joanne Lennon, and Corinne Vigny.

As a student with a disability, my path through life in general, and, in particular, my studies, has been highly non-linear and fraught with interruption. I cannot overstate how much I appreciate those tasked with helping me steady myself. They are Andrew Knight, Nadia Drews and Jean Debarros. Quite simply, I would not be here if not for these people. Unfortunately, due to the nature of our relationships, I am out of contact with two of these, and soon will be with the third. Their contributions to my life will never be forgotten. I also want to thank Michelle Bosher, Eileen Marston, Elaine Eastgate, Carrie Leonard-McIntyre, Sara Scott, Rachel Steadman and Shelly

Jenkin for their help in navigating the hurdles faced by someone in my position. I am very grateful to Michelle in particular, who has always been on hand to help in any way she can, and has always gone above-and-beyond to do so.

My journey into physics started atypically. However, under the tutelage of Errol Simpson, I had my eyes opened to the beauty of human thought when applied to the underlying nature of our universe. He helped me to flourish, and was there at a time when I needed him most. Unbeknownst to me at the time, he fought for me behind the scenes against some opposition. He is a phenomenon of a person and, to this day, he remains an inspiration to me.

Throughout my DPhil studies, I have known many extraordinary people. An undoubtedly incomplete list of those who had the greatest impact throughout my time here are: Christopher Arran, Juvid Aryaman, Emma Beddall, James Bonifacio, Callum Brodie, Katharine Burnett, Kieran Campbell, Samantha Campbell, Elwin Carlos, Azaria Coupe, Chrislynn Ann D'lima, Fran Chadha-Day, Ajay Duncan, Helen Fletcher, Hannah Gerlach, George Green, Laura Grima, Tom Han, Mikayla Hunter, Rob Kemp, Marina Lambrakis, Samira Lindstedt, Jesse Liu, Ellie Milnes-Smith, Rita Nissim, Evan Odell, Meera Patel, Anthony Payne, Jess Prew, Sam Pugh, Susanna Riley, Paul Secular, Jessie See, Prashant Shah, Nasrin Sharifi, Eden Tanner, and Hannah Tillim. I may not be in contact with you all at the moment, but your presence in my life is remembered.

The COVID pandemic has provided a unique challenge to navigate in both my professional and personal life. Aside from many of the people listed already in these acknowledgements, I must additionally thank the first (now second) year physics students at St Catherine's College of the academic year 2020 - 2021, as well as the people around the world found in various Discord servers I have frequented over the last 18 months. They all helped keep me sane.

Special thanks must be reserved for my family, for providing unending support and love throughout my entire life. They are too numerous to list here but, in particular, I would like to thank: my mother, Christine Lennon; my father, Michael Lennon; my sister, Pascale Lennon; and my aunts, Angela Russell and Margaret Jones. They have been through a lot with me – particularly over the past 14 years – and I want them to know that I am eternally grateful. I would also like to take the opportunity to thank my partner, Samira Lindstedt, in a similar vein.

Finally, this thesis is dedicated to those we lost during the process of completing it: Patrick Joseph Lennon (1960 - 2018) and Mary Teresa Lennon (1938 - 2018). May their memories live on in the Bodleian Library archives forever.

Statement of Originality

To the best of my knowledge, this thesis is wholly my own work and contains no material previously published or written by another person, except where indicated in the text with a reference.

In terms of collaboration, the thick-wall analyses of Chapters 7 and 8 were performed in collaboration with Fady Bishara, George Johnson and John March-Russell and can be found in Ref. [18]. In particular, the numerical simulations were performed by Fady Bishara. The thin-wall analysis of Chapter 8 was performed in collaboration with Fady Bishara and can be found in Ref. [19]. In particular, the numerical simulations were performed by Fady Bishara. The remaining original works, as indicated in the text, of Chapters 2, 3, 4, 6 were performed solely by myself and are either unpublished or can be found in Refs. [100–102].

This thesis contains no material that has already been accepted, or is currently being submitted, for any degree or diploma or certificate or other qualification at the University of Oxford or another institution.

– Olivier Lennon, 2022

Abstract

Q-balls are an example of non-topological soliton that can appear in the spectrum of scalar field theories. They are semi-classical states that minimise the energy for a given Noether charge. If isolated from other sectors, these spherically symmetric objects are kept absolutely stable by energy and Noether charge conservation. Though the properties of Q-balls cannot be determined analytically in general, progress can be made in two opposite limits: the thin-wall (large charge) limit; and the thick-wall (small charge) limit. Q-balls are both interesting phenomenologically and as formal objects in their own right, as evidenced by the large body of work on this subject.

This thesis represents a study on the formal properties of field theories, with the aim to determine the subclass of models that admit Q-ball solutions. To that end, its goals are two-fold. Firstly, to constrain the theories that possess stable Q-ball states by: (i) determining the differential equations that govern the VEV of the constituent scalar in the thin-wall limit, together with the physical properties of the resulting Q-ball; (ii) constraining the small-field expansions that lead to stable thick-wall Q-balls by demanding that the minimum of energy be classically stable against decay to the underlying quanta of the scalar field. Secondly, to determine whether stable Q-balls, in both the thick- and thin-wall limit, can form from scalar mesons, arising from the breaking of an approximate chiral symmetry, in the SM and in a specific BSM theory. We will not discuss the phenomenology of these theories in this thesis.

The content of this thesis is laid out in three parts. Part I is concerned with Q-balls in theories possessing only one scalar field, and comprises Chapters 2 and 3, whereas Part II is concerned with theories with multiple scalar fields, and comprises Chapters 4-6. In these parts, we perform an analysis to determine the existence of Q-ball states, and any constraints required by the theories that possess them. In particular, in Part I, the thick-wall analysis presents us with necessary conditions, whereas in Part II, the thick-wall analysis presents us with sufficient conditions. Finally, Part III analyses theories when the underlying scalars of the theory are pseudo-Nambu-Goldstone bosons arising from the breaking of an approximate chiral symmetry, as in the Standard Model – this final part comprises Chapters 7 and 8. We show that stable Q-balls are not part of the spectrum of the leading-order Chiral lagrangian, but that they can arise in the class of BSM models we study.

The bulk of the original work of this thesis can be found in Refs. [18, 19, 100–102], with the remaining work unpublished.

Contents

Chapter 1

The Standard Model and Beyond

1.1 Introduction

Much like Newton unified the motions of the heavens with that of a terrestrial apple, the aim of any mathematical model of physics is to unify many disparate phenomena into a single, theoretical framework. Specifically, if the theory is to determine the fundamental nature of the universe, then it must describe the matter contained within it, together with the interactions between matter in its various guises.

The current paradigm of four, fundamental forces of nature, together with matter formed from the quarks and leptons, and (fundamental) mass generation via the Higgs mechanism, has been very successful in describing a wealth of universal phenomena – from, for example, the anomalous magnetic moment of the electron and the running of the coupling constants with energy scale, to the dynamics of black holes and the expansion of the known universe. These phenomena are described by, not one but, two theoretical frameworks: the Standard Model (SM) of Particle Physics, and General Relativity (GR).

However, this is not believed to be the end of the story. Cracks in this structure are known to exist, not least due to the fact that a compelling, single framework still eludes us. Both theoretical inconsistencies and experimental puzzles have yet to be definitively explained: for example, the masses of the neutrinos; the existence of a non-luminous component of matter which holds galaxies together; the observed matter-anti-matter asymmetry; the acceleration of the expansion of the known universe; the hierarchy between the gravitational (Planck) and weak scales; a resolution to the strong-CP problem; hierarchies in the Yukawa couplings; and whether or not the gauge couplings unify.

This thesis will be concerned with one direction of theoretical progress in alleviating these issues, namely, in models Beyond-the-SM (BSM). Specifically, this is a thesis

on the formal properties of theories of complex scalar fields invariant under groups of symmetries that can exist in BSM theories, but not on their phenomenology. Consequently, we open this chapter on a discussion of symmetries in field theories, with a focus on the theorems associated to Noether and Goldstone. We then discuss the theoretical structure of the SM, together with a subset of its known open theoretical and experimental issues.[1] We pay particular emphasis to the light meson sector of the SM, as this will become highly relevant later in the thesis. We then introduce the exotic object that will concern us for the rest of this thesis: Q-balls, which are objects that can arise in extensions to the SM with scalar sectors. Finally, we close this chapter by outlining the rest of this thesis.

1.2 The Theorems of Noether and Goldstone

As this thesis represents a study into the consequences of symmetries on the spectrum of theories, it behooves us to discuss the theory of symmetry in the context of field theories. In this section, we will review what is meant by a symmetry in a field theory, along with the associated theorem affiliated to Noether. We will then discuss Goldstone's theorem which is associated to the spontaneous breaking of a symmetry by the vacuum state of the theory. We will explore these in the context of scalar fields, both for simplicity and because these are the main focus of the original work in this thesis. It should be noted that the ideas of this section generalise to more complex fields, such as vector or spinor fields.

1.2.1 Noether's Theorem

A complex scalar field, $\Phi(\vec{x}, t)$, is a complex-valued function of spacetime coordinates that transforms trivially under the Lorentz group of symmetries. A classical theory of these scalar fields is described via an action, S, which is usually defined via another functional, the Lagrangian density, $\mathcal{L}$.[2] For a theory of a single, complex scalar field, these are related through

$$S = \int \mathrm{d}^4x \, \mathcal{L}(\partial_\mu \Phi^*, \partial_\mu \Phi, \Phi^*, \Phi), \tag{1.1}$$

[1] Note, we will not discuss the structure of GR any further, except to mention it in passing when discussing the unification of it with the framework of the SM.

[2] Quantum mechanically, the action appears as the exponent in the path integral formulation. However, as the objects of study in this thesis – Q-balls – are described semi-classically, it will suffice to only consider the classical action here. Moreover, some quantum field theories possessing conformal symmetries do not have an action formulation, but this is very far out of the scope of this thesis.

where we have implicitly taken $\hbar = c = 1$, as we will do for the rest of this thesis, and we take the spacetime to be flat and in $3+1$ dimensions, such that its isometries are described by the Poincaré group of transformations. The integral is implicitly taken over all of spacetime. The Lagrangian density, a functional of the degrees of freedom of the model and their spacetime derivatives, can also be an explicit function of the spacetime coordinates, however we will not consider this here. Classically, the action is real-valued and, therefore, so must be the Lagrangian density.[3] It is therefore clear why both the field and its complex conjugate must be present in the Lagrangian density – that we take these as separate degrees of freedom is customary and signifies that a complex scalar field on its own has two (real) degrees of freedom.

The equation of motion, or, Euler-Lagrange equation, describing the evolution of the complex scalar field is found by invoking the principle of least action, namely, that first order variations of the action, associated to variations of the field that vanish at spatial infinity, vanish. It can be proven that the Euler-Lagrange equation is then given by

$$\partial_\mu \left(\frac{\partial \mathcal{L}}{\partial(\partial_\mu \Phi)} \right) - \frac{\partial \mathcal{L}}{\partial \Phi} = 0, \tag{1.2}$$

and similarly for the complex-conjugate of the scalar field.

A classical field theory is said to possess a symmetry if the action describing it is invariant under a group of transformations.[4] Note, it is sufficient for the Lagrangian density to be invariant under the group of transformations. However, some symmetries, such as spacetime translation invariance, are only made manifest when considering the action – if the Lagrangian density transforms by a total derivative, the action is then left invariant. Since we will be concerned with symmetries of the Lagrangian density throughout this thesis, we merely consider this sufficient condition in what follows.

There is a deep theorem relating symmetries of a theory to its conserved quantities, named after its discoverer: Noether's theorem. If a theory is invariant under a group of transformations, then associated to that symmetry is a conserved current density, known as a Noether current density. For our theory of a complex scalar field, this is defined as

$$j^\mu = \lim_{\alpha \to 0} \left(\frac{\partial \mathcal{L}}{\partial(\partial_\mu \Phi)} \frac{\delta \Phi}{\alpha} + \frac{\partial \mathcal{L}}{\partial(\partial_\mu \Phi^*)} \frac{\delta \Phi^*}{\alpha} \right), \tag{1.3}$$

[3] Quantum mechanically, this requirement can be relaxed as the path integral computes the complex probability amplitude, and so the action does not need to be real.

[4] It should be noted that symmetries of the classical model do not necessarily translate to the quantum model, whereby these classical symmetries can be broken by quantum effects, or, "anomalies".

where $\delta\phi$ is the (leading-order) perturbation of the field under the transformation associated to the symmetry. We see that

$$\partial_\mu j^\mu = 0, \tag{1.4}$$

by application of the Euler-Lagrange equations, given in Eq. (1.2). We implicitly sum over repeated indices, and will continue to do so throughout this thesis. It is in this sense that, by obeying this continuity condition, the current density is conserved. Moreover, we may associate a conserved charge, Q, to the Noether current density, defined through

$$Q \equiv \int \mathrm{d}^3x\, j^0, \tag{1.5}$$

such that

$$\frac{\mathrm{d}Q}{\mathrm{d}t} = 0, \tag{1.6}$$

by virtue of the boundary conditions of the field theory, i.e., nothing is flowing out or in through the boundary at spatial infinity.

1.2.2 Goldstone's Theorem

A symmetry is said to be spontaneously broken if the vacuum of the theory, i.e., the global minimum of the potential,[5] does not possess the symmetries of the model. The classic example is of a theory with a "wine-bottle" potential – also known as the linear sigma model – defined for a single complex scalar field as

$$\mathcal{L} = \partial_\mu \Phi^* \partial^\mu \Phi + \mu^2 \Phi^* \Phi - \lambda(\Phi^* \Phi)^2. \tag{1.7}$$

This theory is invariant under a global $U(1)$ symmetry, made manifest by the invariance of the Lagrangian under the transformation

$$\Phi \to e^{i\alpha}, \tag{1.8}$$

where $\alpha \in \mathbb{R}$. The potential,

$$U(\Phi^*, \Phi) = -\mu^2 \Phi^* \Phi + \lambda(\Phi^* \Phi)^2, \tag{1.9}$$

[5] If there is a process that breaks the symmetry to a local minimum, it is highly likely that there would be a tunnelling process to the global minimum of the potential. However, if the local minimum is long-lived, one can consider this a practical case of spontaneous symmetry breaking, even if it doesn't strictly adhere to the definition.

also exhibits this symmetry about the field value $\Phi = 0$. However, this stationary point of the function represents a maximum. The global minimum of the potential is a collection of points defined through

$$|\Phi_0| = \sqrt{\frac{\mu^2}{2\lambda}}. \tag{1.10}$$

The vacuum thus has the manifold structure of a circle. That the theory will naturally want to be in its vacuum state means that the $U(1)$ symmetry of the theory is spontaneously broken. In this particular model, the vacuum of the theory does not possess any residual, unbroken symmetry. However, in general, the symmetry can be broken from one group to a smaller, non-trivial group.[6]

We now seek to shift the field such that it describes variations about the vacuum of the theory, as opposed to the origin of symmetry. For simplicity, we recast the complex scalar in terms of two real scalar degrees of freedom, ϕ_1 and ϕ_2, defining

$$\Phi = \frac{1}{\sqrt{2}}(\phi_1 + i\phi_2), \tag{1.11}$$

such that

$$\mathcal{L} = \frac{1}{2}\delta_{ij}\partial_\mu\phi^i\partial^\mu\phi^j + \frac{1}{2}\mu^2\delta_{ij}\phi^i\phi^j - \frac{\lambda}{4}\lambda(\delta_{ij}\phi^i\phi^j)^2. \tag{1.12}$$

Given that the vacuum manifold is that of a circle, we pick a direction such that

$$\phi_0^i = (0, v) \tag{1.13}$$

where

$$v = \frac{\mu}{\sqrt{\lambda}}, \tag{1.14}$$

as found above. Defining a set of shifted fields, π and σ, through

$$\phi^i = (\pi, v + \sigma) \tag{1.15}$$

the Lagrangian density of the theory now becomes

$$\mathcal{L} = \frac{1}{2}\partial_\mu\pi\partial^\mu\pi + \frac{1}{2}\partial_\mu\sigma\partial^\mu\sigma - \frac{1}{2}(2\mu^2)\sigma^2 - \mathcal{O}(\sigma^3, \pi^2\sigma), \tag{1.16}$$

where we ignore the terms cubic and higher in the fields as they do not concern our discussion here. Note, only one of the fields possesses a mass (quadratic) term when we consider the theory about its vacuum. That the other field is massless is the essence of Goldstone's theorem, which states, in general, that to each broken

[6] A smaller group here means one with fewer generators.

generator of a symmetry group undergoing spontaneous symmetry breaking, there is an associated massless scalar mode, referred to as a Nambu-Goldstone boson (NGB) when considered from the point-of-view of particles. Explicitly, if the group $\mathcal{G}$, with $N_{\mathcal{G}}$ generators, spontaneously breaks to the group $\mathcal{H}$, with $N_{\mathcal{H}}$ generators, then there will be a number $N_{\mathcal{G}} - N_{\mathcal{H}}$ of massless degrees of freedom associated to that breaking in the theory. Moreover, these NGBs cannot acquire a mass from any order of quantum corrections – for a discussion of this see, for example, Ref. [117].

There are two methods of evading the massless modes inherent in Goldstone's theorem. The first is to make the theory, and associated symmetry, more complex, namely, to consider a local (gauge) symmetry, together with initially massless vector (gauge) fields. In this scenario, the massless degrees of freedom associated to the field that spontaneously breaks the gauge symmetry are "eaten" by the gauge fields. These vector fields then gain a degree of freedom, promoting them to massive vector (Proca) fields. This is precisely the mechanism associated to the Higgs boson found in the SM.

The second is to simply have a symmetry that was only approximate, that is, manifest only when some parameter is tuned to zero. If this parameter is sufficiently small, the massless modes gain a small mass and are kept naturally light. This can also be checked experimentally – if there are massive bosons discovered with the structure of NGBs, then the explicit symmetry breaking term is small enough. In this case, the NGBs are referred to as pseudo-NGBs (pNGBs). This is the mechanism associated to the light mesons of the SM.

1.3 The Standard Model of Particle Physics

The Standard Model of Particle Physics is a renormalisable quantum field theory in $3+1$ dimensions. It is invariant under the $SU(3)_C \times SU(2)_W \times U(1)_Y$ gauge group, where we use C, W, and Y to denote colour, weak-isospin, and hypercharge, respectively.[7] It mathematically describes the coupled dynamics of three sectors: left- and right-handed chiral spinors, denoting matter; vector gauge bosons, mediating the forces; and the Higgs scalar. Each of these states is charged under the overall gauge group, though sometimes trivially. The latter of these – the Higgs – is introduced, along with an appropriate potential, to spontaneously break $SU(2)_W \times U(1)_Y \rightarrow$

[7] In some sense, the SM describes "3/4" of nature, by virtue of describing three of the known fundamental forces of nature, with the other "1/4" coming from the description of gravity in GR.

$U(1)_{EM}$, i.e., to the familiar electromagnetic interaction, and with Yukawa couplings to generate a bare mass for those states that are massive.

This is summed up classically by the Lagrangian density – famously described as fitting on a coffee mug – given by

$$\mathcal{L} = -\frac{1}{4}F_{\mu\nu} \cdot F^{\mu\nu} + i\bar{\psi}_i \not{D}\psi_i + y_{ij}\psi_i H^c \psi_j + \text{h.c.} + |D_\mu H|^2 - V(H), \tag{1.17}$$

where we have made judicious use of notation to hide the complexity of the model. Below, we briefly outline the theoretical structure of the SM.[8]

1.3.1 The Gauge Structure

The gauge group structure can be roughly split into two parts: the strong and electroweak sectors. The strong sector of quantum chromodynamics (QCD) is associated to the group $SU(3)_C$. The eight gauge bosons, or "gluons", furnish the adjoint representation of this gauge group and, due to the non-Abelian nature of the group, self-interact at tree-level by virtue of terms in the field-strength tensor. The one-loop beta function for QCD in the SM,

$$\beta_0 = \frac{\partial g}{\partial \mu} \propto -\frac{1}{3}\left(11 - \frac{2}{3}n_f\right), \tag{1.18}$$

where g is the QCD coupling strength, and μ is the energy scale. In QCD, $n_f = 6$ is the number of flavours of quark, and so the beta function is negative. This means that the gauge coupling strength reduces with growing energy and, consequently, QCD is asymptotically free at high – ultra-violet (UV) – energies. Correspondingly, the Landau pole of the theory is at low – infra-red (IR) – energies, which purportedly leads to confinement of matter charged under QCD into "colour neutral states".

The electroweak sector represents weak isospin (also known as the weak force) and hypercharge, and is associated to the product group $SU(2)_W \times U(1)_Y$. This gauge group structure is spontaneously broken below the weak scale by the Higgs mechanism – see below – to the subgroup $U(1)_{EM}$. Through this process, the gauge field bosons $W^\pm$ – associated with $SU(2)_W$ – together with the Z^0 – an admixture of the W^0 of $SU(2)_W$ and the B of $U(1)_Y$ – gain a mass. The need for this breaking comes from the requirement of a gauge-invariant mass term for the weak bosons associated to the theory. The remaining gauge boson, γ – also an admixture of the W^0 and the B – remains massless and is the familiar photon of quantum electrodynamics. Due to the

[8] It shall have to remain brief as a full rundown of its structure would be far longer than a doctoral thesis allows.

Abelian nature of $U(1)_{EM}$, the photon does not self-interact at tree-level, but can do so at loop-level. Moreover, unlike QCD, the $U(1)$ gauge groups possess a Landau pole in the UV and so does not confine in the IR.[9]

1.3.2 The Matter States

The matter sector of the SM splits into two types of state: the quarks, which are colour-charged, and the leptons, which are colour-neutral. Moreover, the matter states are represented by chiral fermions owing completely to the fact that the weak force only interacts with left-handed chiral fermions, thus rendering their right-handed counterparts neutral under the weak force and therefore offering parity violation to the SM. Curiously, the matter sector is repeated twice more – into three copies, or "generations", in total – with the only difference being their masses. As such, there are: three flavours of "up-type" quark – up, charm, top; three flavours of "down-type" quark – down, strange, bottom; three leptons charged under $U(1)_{EM}$ – electron, muon, tau; and three leptons uncharged under $U(1)_{EM}$ – electron neutrino, muon neutrino, tau neutrino.

If we define the notation, $(C, W)_Y$, to denote the representations of the matter states under colour, weak-isospin, and hypercharge, then the SM comprises three copies of

$$q = (3, 2)_{1/6}, \quad u^c = (\bar{3}, 1)_{-2/3}, \quad d^c = (\bar{3}, 1)_{1/3}, \quad l = (1, 2)_{-1/2}, \quad e^c = (1, 1)_1, \tag{1.19}$$

where the index c denotes the charge conjugate of the state,[10] and q, u, d, l, e refer to the quark, up, down, lepton and electron states, respectively. Note, mass terms in the SM are of Dirac form – see below when we discuss neutrino oscillations. These terms mix left- and right-handed parts. Since neutrinos appears massless in the SM, under the assumption that all mass terms are of Dirac form, the neutrino possesses no right-handed state. However, this does not preclude the neutrino possessing a Majorana mass term – see below.

The matter sector contains a wealth of global $U(1)$ symmetries associated to particle number. Specifically, overall quark number is conserved – named baryon number, such that each quark has a baryon number of $1/3$ – as are individual lepton numbers associated to each $SU(2)_W$ doublet – electron number, muon number and tau number.

[9]The weak gauge group does possess a Landau pole in the IR, but the Higgs mechanism takes over at an energy higher than this and so it is not relevant.

[10]By convention, we use the charge conjugate here instead of the right-handed states.

As stated above, the strong force confines at low energies such that only colour singlets can be observed. As such, the quarks "hadronise" into colour neutral bound states with the appropriate description no longer being the quark theory of the SM. The effective theory most appropriate for the mesons of this sector is chiral perturbation theory – we return to this below in Section 1.3.4.

The weak isospin quantum number, T_3, is defined in analogy with quantum mechanical spin: to each doublet under $SU(2)$, $T_3 = +1/2$ is associated with one state – the electron neutrino and up quark – and $T_3 = -1/2$ is associated with the other state – the electron and down quark. The quantum number, or electromagnetic charge, associated to the representation under $U(1)_{EM}$ is then defined through

$$Q = T_3 + Y, \tag{1.20}$$

where Y is the hypercharge quantum number of the state.

The matter states gain fundamental masses through Yukawa interactions with the Higgs doublet – see below. Similarly to the gauge bosons of the weak force, this was needed in order to have gauge invariant mass terms. Associated to these interactions are the Yukawa couplings, y_{ij}. In the quark sector of Eq. (1.17), we have hidden an additional object in these couplings – the CKM matrix. This structure explains the mixing of weak eigenstates of quarks into mass eigenstates.[11] Furthermore, this provides CP-violation to the SM, alongside the parity violation found in the weak sector. The relative mixing angles of the CKM matrix, together with the individual Yukawa couplings associated to each species, must be determined experimentally. However, only a subset of these have thus far been measured in interactions between the Higgs and the matter states. This structure – as far as we are aware – is not present in the lepton sector. In the SM, the neutrino sector possesses vanishing Yukawa couplings as they are massless.

1.3.3 The Higgs Sector

The final sector of the SM incorporates the Higgs mechanism. This facilitates the spontaneous symmetry breaking of the gauge group $SU(2)_W \times U(1)_Y \to U(1)_{EM}$ by introducing a complex scalar doublet, $H = (1, 2)_{1/2}$, together with a potential whose global minimum lies away from zero field,

$$V(H) = -\mu^2 H^\dagger H + \lambda (H^\dagger H)^2. \tag{1.21}$$

[11] This mixing explicitly breaks the $U(1)$ symmetries associated to individual quark numbers.

The number of generators before and after the spontaneous symmetry breaking are four and one, respectively. Thus, by Goldstone's theorem, we might expect three massless degrees of freedom. However, as stated above, in breaking a gauge symmetry and coupling the scalar field to gauge fields through the covariant derivative,

$$D_\mu H = (\partial_\mu - i g_W W_\mu^a \tau^a - i\frac{1}{2} g_Y B_\mu) H, \tag{1.22}$$

these massless degrees of freedom are "eaten". Thus, the gauge fields – $W^\pm$ and Z^0 – pick up masses. As the Higgs is represented by a complex scalar doublet, it contains four degrees of freedom. The final one remains massive, and this is the Higgs boson.

A key component of the Higgs mechanism is in the Yukawa interactions of the Higgs with the matter states of the theory,

$$y_{ij} \psi_i H^c \psi_j + \text{h.c.}. \tag{1.23}$$

When the Higgs gains a VEV, we can shift the field in the same way as in Section 1.2.2. Loosely, we can set $H = h + v$ in the above. We thus see that we obtain one set of terms denoting the couplings between the matter states and the Higgs, and one set of terms that become mass terms for the fundamental matter states. Thus, the Higgs is the origin of fundamental mass.

Though the unambiguous observation of the Z^0 in 1983 all but confirmed the existence of the Higgs mechanism, the Higgs boson was finally discovered in 2012. However, in order to fully confirm that this Higgs is the SM Higgs, it is necessary to observe the direct coupling of the Higgs with each of the particles through its Yukawa couplings and covariant derivative. As it stands, this Higgs represents the only instance of a fundamental scalar particle in nature.

1.3.4 The Chiral Lagrangian

As a particular example of pNGBs that will concern us later in this thesis, we will now consider in more detail the formal structure of the meson sector of the SM. Discussions of chiral perturbation theory (ChPT) can be found in many textbooks. We present a treatment which follows those given in Refs. [64, 127], as well as the review given in Ref. [118].

In the massless limit, the left- and right-handed quarks lose their coupling through the mass terms in the QCD Lagrangian:[12]

$$\mathcal{L}_{\text{quarks}} = i\bar{q}_L \not{D} q_L + i\bar{q}_R \not{D} q_R, \tag{1.24}$$

[12]The left- and right-handed quarks do still talk to each other via their gauge interactions, however.

where q is in the fundamental representation of SU(N_f), containing N_f quark flavours. Note, we ignored the kinetic terms for the gauge fields above as they are irrelevant for our discussion: we are only concerning ourselves with the quark content of QCD. This Lagrangian is invariant under a global symmetry group

$$U(N_f) \times U(N_f) = SU(N_f)_L \times SU(N_f)_R \times U(1)_V \times U(1)_A. \tag{1.25}$$

The two $U(1)$ symmetries are vector and axial symmetries, respectively. In particular, $U(1)_V$ corresponds to baryon number conservation. In the full SM, containing weak interactions, this is an anomalous symmetry, i.e., valid classically, but broken by quantum effects. It is also trivially realised in the meson sector. We shall ignore this in the present discussion. The $U(1)_A$ symmetry is always anomalous due to QCD, and so we will ignore this, too. We shall thus presently focus on $SU(N_f)_L \times SU(N_f)_R$.

The $SU(N_f)_L \times SU(N_f)_R$ symmetry is spontaneously broken when $\langle \bar{q}q \rangle = \Lambda^3_{\rm QCD}$, that is, the quark condensate acquires a VEV and hadrons form below the confinement scale. The symmetry breaks to the vector symmetry, $SU(N_f)_L \times SU(N_f)_R \to SU(N_f)_V$, with the axial symmetry, $SU(N_f)_A$, being spontaneously broken. The vector symmetry rotates left- and right-handed fields in the same way, with the broken axial symmetry not doing so. As such, it would seem that the dynamics of confinement triggers chiral symmetry breaking, and so the chiral symmetry breaking scale, Λ_χ, is parametrically similar to the confining scale in the SM: $\Lambda_\chi \sim \Lambda_{\rm QCD}$.[13] Below the Landau pole, therefore, the relevant states are those which are colour-neutral and composite, with the chiral Lagrangian an effective theory valid up to the chiral symmetry breaking scale.

The basic idea of ChPT is to build a low-energy effective field theory, valid below the confinement scale, of composite states of quarks. The exact details of the spontaneous symmetry breaking are ignored, with only the symmetry breaking pattern, $SU(N_f)_L \times SU(N_f)_R \to SU(N_f)_V$, used. The theory is ordinarily constructed only considering the above global symmetry; other local symmetries can be incorporated in the standard way by promoting derivatives to covariant derivatives.

We consider a set of scalar fields, organised into a unitary matrix, $\Sigma_{ij}(x)$,

$$\Sigma(x) \equiv \exp\left(2i\frac{\pi^a(x)\tau^a}{f}\right), \tag{1.26}$$

where $\pi^a(x)$ are fields in the adjoint representation of $SU(N_f)$, τ^a are the generators, and f is some dimensionful constant, chosen so that the $\pi^a(x)$ fields are canonically

[13] However, whether these are indeed separate dynamics or inherently linked in QCD is still an area of research – see Ref. [51] and discussion therein.

normalised. This is must be measured experimentally – in the $SU(2)$ ChPT, this is known as the pion decay constant. We take the Σ field to transform linearly under $SU(N_f)_L \times SU(N_f)_R$:

$$U \to LUR^\dagger. \tag{1.27}$$

Writing $L = \exp\left(i\theta_L^a \tau^a\right)$ and $R = \exp\left(i\theta_R^a \tau^a\right)$, then, for infinitesimal transformations, the π^a fields transform as

$$\pi^a \to \pi^a + \frac{f}{2}(\theta_L^a - \theta_R^a) - \frac{1}{2} f^{abc}(\theta_L^b + \theta_R^b)\pi^c + \cdots, \tag{1.28}$$

where f^{abc} are the structure constants for the unbroken subgroup. Notice, for $\theta_L^a = \theta_R^a$, the π^a fields transform in the adjoint representation of the unbroken subgroup. Under the axial transformations, $\theta_L^a = -\theta_R^a$, the π^a fields transform non-linearly, shifting at leading order. This shift symmetry forbids a mass term for the π^a fields.

We now justify the leading-order chiral Lagrangian, which is a theory describing the Σ fields. Any invariant term not containing any derivatives necessarily is a function of $\Sigma^\dagger\Sigma = \mathbb{1}$, and so does not contribute to the dynamics of the theory. All terms must thus contain a derivative and, therefore, mass terms for the π^a are forbidden, which is consistent with π^a being a NGB. Furthermore, by Lorentz invariance, each term must have an even number of derivatives. The Lagrangian of $\mathcal{O}(p^2)$ we may write down, invariant under global $SU(N_f) \times SU(N_f)$, charge conjugation and parity is

$$\mathcal{L}_\chi = \frac{f^2}{4} \mathrm{tr}\left(\partial_\mu \Sigma \partial^\mu \Sigma^\dagger\right). \tag{1.29}$$

This is the unique leading-order Chiral Lagrangian. Notice, the normalisation of the first term is set in order to canonically normalise the π^a fields.

As we stated above, the π^a fields are pNGBs, so they require mass terms. To embed these into the theory, we must return to the (massless) QCD Lagrangian and employ the "spurion trick". We modify this Lagrangian by coupling the massless quarks to external, classical currents. These are fields that are non-dynamical ("spurious fields" or "spurions"). This is particularly useful in modelling how the quarks couple to external fields, such as the electroweak field. The usefulness to ChPT is that we introduce mass terms in this way. This is reasonable, since fundamental masses arise from coupling to the Higgs field. The trick is to demand that these currents transform under $SU(N_f) \times SU(N_f)$ in such a way to keep the Lagrangian invariant under the symmetry. In particular, the spurion from which the masses of the quarks arise gains a VEV, thus explicitly breaking the remaining $SU(N_f)_V$. This is similar

in spirit to our discussion so far: we use symmetry breaking patterns, and fields invariant under the original symmetries, to build a theory valid below the symmetry breaking scale.

As we are only seeking to determine the leading-order chiral Lagrangian, we will only consider the spurious fields that allow us to write down a real mass term – other spurious fields can be invoked to determine higher order terms in the chiral Lagrangian or mass with an imaginary part. The modification to the massless Lagrangian is given by

$$\begin{aligned}\mathcal{L} &= \mathcal{L}^0_{\text{QCD}} - \bar{q}sq \\ &= \mathcal{L}^0_{\text{QCD}} - \bar{q}_R s q_L - \bar{q}_L s q_R,\end{aligned} \tag{1.30}$$

where $\mathcal{L}^0_{\text{QCD}}$ is the massless QCD Lagrangian, and s is a classical $N_f \times N_f$ Hermitian matrix field known as a spurion. If $q_L \to Lq_L$ and $q_R \to Rq_R$, then for this theory to be invariant under $SU(N_f)_L \times SU(N_f)_R$ we require that this field transforms as

$$s \to RsL^\dagger. \tag{1.31}$$

We may now construct a chiral Lagrangian that includes the contribution from this spurion. Identifying the mass matrix M with s, we may write the chiral Lagrangian of $\mathcal{O}(p^2)$, invariant under global $SU(N_f) \times SU(N_f)$ chiral transformations, charge conjugation and parity, as:

$$\mathcal{L}_\chi = \frac{f^2}{4}\text{tr}\left(\partial_\mu \Sigma \partial^\mu \Sigma^\dagger\right) + \frac{B_0 f^2}{2}\text{tr}\left(M(\Sigma^\dagger + \Sigma - 2)\right). \tag{1.32}$$

where B_0 is a coefficient to be determined experimentally. It can be related to the scale Λ_χ by $\Lambda_\chi^3 \sim B_0 f^2$. Note, with a view to the future of this thesis, we have also scaled the mass term such that zero field corresponds to zero potential, as is customary in Q-ball physics.

Note, in our section on Goldstone's theorem, we stated the parameter that explicitly breaks a symmetry to produce pNGBs had to be small, but that this smallness was defined observationally. It is found that, in the SM, the chiral Lagrangian is valid for the up, down and strange quarks. If we include heavier quarks, it does not reproduce what is observed, and thus we conclude that the masses of these heavier quarks are too large.

1.4 The Problems with the Standard Model

Despite its success in describing a wide range of phenomena, it is believed that the SM remains incomplete. In this section, we highlight some of the experimental and theoretical concerns in order to justify the study of BSM physics.

1.4.1 Experimental Puzzles

In this subsection, we describe a subset of the experimental results that disagree with the predictions of the SM.

Neutrino Oscillations

In the SM, the neutrinos are massless. However, the observation that neutrinos oscillate between species implies otherwise. This happens because of a mismatch between the gauge eigenstates under the weak force, and the mass eigenstates. The neutrinos travel in mass eigenstates – and so have different quantum mechanical phase – but are measured through their interaction with the weak force, and so mix. Previously, it was believed that three lepton numbers were individually conserved, i.e., electron number, muon number and tau number. However, neutrino oscillations explicitly break this conservation. An open question is whether the mass is of Dirac form, which mixes left- and right-handed states,

$$m\bar{\nu}\nu = m(\bar{\nu}_L\nu_R + \bar{\nu}_R\nu_L), \tag{1.33}$$

or of Majorana form,

$$\frac{1}{2}m(\bar{\nu}^c\nu + \bar{\nu}\nu^c) = \frac{1}{2}m(\bar{\nu}^c_L\nu_L + \bar{\nu}_L\nu^c_L), \tag{1.34}$$

in which the neutrinos are their own antiparticle. Many plausible underlying UV theories exist to imbue the neutrino with either of these masses.

Dark Matter

Perhaps the most tantalising hint of BSM physics comes from the hypothesised existence of dark matter (DM). The first evidence for a non-luminous component to matter came from observations by Zwicky in the 1930s [145]. He found that the Coma Cluster of galaxies contained more mass than was expected from its luminosity. This observation was ignored for many decades before the now classic observation of the rotation curves of the Andromeda galaxy in the 1970s by Rubin and Ford [121]. The orbital velocity of objects outside the main disk of the galaxy were measured as a function of distance from the galactic centre. It was found that, instead of going like $r^{-1/2}$, the velocity curve was constant well outside of the galactic disk. This suggests

an additional dark component to matter beyond the visible disk[14] distributed as a spheroidal "halo", as evidence by lensing experiments (see, for example, [138]). Today, the observational evidence for DM on all scales is vast [56, 67] (see also [63, 105] and references therein) and includes, but is not limited to, the rotation curves of many galaxies [21], strong- and weak-gravitational lensing [39, 111, 137, 138], observations of the Bullet Cluster [28], large-scale structure [45], and anisotropies in the CMB [20, 79–81, 129].

The matter discrepancy cannot be baryonic in nature, due to limits from Big Bang Nucleosynthesis (BBN) [112]. Specifically, the relative abundance of the light elements (D, ^{3}He, ^{4}He, and ^{7}Li) are constrained by very well understood SM processes in the early universe [141]. It is now known that if DM exists as some new mass state, it comprises 26.8% of the energy content of the observable universe, with ordinary (baryonic) matter only comprising 4.9% [5]. The mass of this state is rather unconstrained. A conservative upper bound of $m_{\rm DM} \lesssim 100\, M_\odot$ comes from looking at the disruption of wide binaries [144]. A lower bound comes merely from the demand that it form halos. If it is bosonic in nature, the DM can be packed into the same point in phase space and so can be treated as a classical field that acts as DM on lengthscales above the de Broglie wavelength, leading to a lower bound of $m_{\rm boson} \gtrsim 10^{-22}\,{\rm eV}$ [78].[15]

Finally, DM is believed to have been produced in the early universe, as must be the case if it is the seed of large-scale structure. At the time at which galactic-size perturbations entered the horizon ($T \sim$ keV), the dominant component of DM is thought to have been non-relativistic, and is thus classified as cold. As DM is still abundant today, it is clear that it must be either stable or have a lifetime much greater than the age of the universe. It is observed to be gravitationally attractive. However, there is currently no evidence that it is charged under the other three fundamental forces [114].

Dark Energy

The observable universe has been shown to have an accelerating expansion, as opposed to merely slowing down as was originally thought for a universe containing only baryonic matter and cold DM. This acceleration is easily accommodated within the

[14] An alternative explanation for the flattening of the velocity curves is a modification to Newton's laws at galactic scales [108]. This MOdified Newtonian Dynamics (MOND) model works well at the scale of galaxies, without any need for DM, but it fails at larger scales [52], including cosmological scales [128], without the inclusion of DM. A potential covariant generalisation of MOND, the Tensor-Vector-Scalar (TeVeS) model [16], also fails without the inclusion of DM [52].

[15] If the DM is fermionic in nature, this leads to a much higher lower bound of $m_{\rm fermion} \gtrsim 0.7\,{\rm keV}$ [77].

framework of GR, either by a geometric cosmological constant or a component of the energy similar to a vacuum energy, which does not become more diffuse as the universe accelerates.[16] The origins of either, or both, of these is, however, a mystery. The measured energy density associated to this accelerated expansion is of order $(10^{-3}\,\mathrm{eV})^4$, whereas contributions from the SM are calculated to be at least $(\mathrm{GeV})^4$.

The Matter-Anti-Matter Asymmetry

It is now incontrovertible that, at least in our patch of the universe, there is an overabundance of matter over anti-matter. The evidence for this is simply that we do not see a proliferation of annihilation events when matter comes into contact with its anti-matter counterparts, and the fact that matter structures were able to form in the early universe at all. In order for a mechanism to produce an overabundance of matter over anti-matter, it must adhere to the Sakharov conditions [125]:[17]

1. furnish a departure from thermal equilibrium;
2. have sufficient C and CP violation;
3. violate the U(1) charge conservation.

The early universe could provide the conditions for these. However, it is not known if the early universe ever departed far enough from equilibrium and whether it was even hot enough for effective B and L number violation – in the SM, for example, there is not enough B and L violation. Thus, this remains an open question.

1.4.2 Theoretical Concerns

In this subsection, we describe a subset of the theoretical concerns with the structure of the SM.

The Hierarchy Problem

The hierarchy problem finds its origin in the question "why is gravity so much weaker than the other forces?", but is often formulated as "why is the Higgs so light?" As shown above, the Higgs couples to all states with a fundamental mass in the SM. If there exists BSM physics at a higher energy scale, presumably this will couple new

[16] This additional energy makes up the remaining energy budget of the universe not already taken by ordinary matter and DM.

[17] This is not limited to baryon number. Any overabundance of charge associated to a global $U(1)$ symmetry must follow these conditions.

mass states to the Higgs. These new mass states will introduce inescapable one-loop corrections to the Higgs mass squared that are proportional to the mass squared of the new states. If the new scale is particularly heavy, this will pull the Higgs mass up towards it. One could counter this argument by merely positing that no new physics exists at a higher energy scale – the "desert" hypothesis. However, the Planck scale represents the energy where GR breaks down, as we will discuss below. Given that a new theory must take over, why isn't the Higgs mass pulled up towards this scale?

It is helpful to think of the hierarchy problem in a different way, in terms of a fine-tuning problem. A hierarchy problem exists only in theories with at least two distinct physical scales. The renormalisation group connects the physics at these different scales, offering a phase space of flows (trajectories) between various fixed points. If we consider a flow from a theory in the UV to an IR scale, the trajectory linking the SM to the UV theory is not generic. The Higgs mass operator itself perturbs the location of the SM theory away from an IR fixed point representing a (conformal) theory with the SM gauge group, where the masses and couplings are set to zero. This perturbation pushes the flow towards another fixed point of a theory characterised by the $SU(3) \times U(1)$ gauge group, i.e., with $SU(2)$ broken. For a flow to represent the symmetry breaking pattern observed in the SM, it must spend most of its time in the vicinity of first fixed point before heading towards the second. That a generic flow from the UV passes through the SM is thus unlikely, and the true trajectory seen in nature is thus finely-tuned. It would be more likely – less fine-tuning – if the SM were at a scale closer to the UV scale. The hierarchy problem is thus defined as the question: what allows the separation of the UV scale and the SM, given that the trajectory linking them both is fine-tuned?

Proposed solutions to the hierarchy problem often come with new dynamics at around the weak scale. It should be noted, however, that these new dynamics have yet to be discovered.

The Coleman-Mandula Theorem

The Coleman-Mandula theorem [33] is a no-go theorem that effectively states that there is no Lie group symmetry that combines the internal symmetries of the SM, together with the Poincaré group of spacetime isometries, that is anything other than a product group of the two sets of symmetries. Thus, it is impossible to unify internal symmetries with spacetime symmetries using the established structures. However, the theorem contains a loophole, namely that the unified group of symmetries need

not be associated to a Lie algebra, but can in fact be associated to a Lie superalgebra, whereby the algebra is defined by anti-commutators alongside the familiar commutators. This framework is referred to as supersymmetry (SUSY).

SUSY relates the bosonic and fermionic states of the Poincaré group and therefore generically includes "superpartners" to the states of the SM. These are identical to the original states except that they differ in fundamental spin by half a unit and, in particular, the matter fermions have associated scalar superpartners. Clearly, supersymmetry is not a symmetry of our world as we do not observe these superpartners at the same mass scales as those in the SM. Thus, if it is to exist, it must be broken at some scale. If this scale of breaking occurs at around the weak scale, this offers a solution to the hierarchy problem mentioned above by cancelling the quantum corrections to the Higgs, and even includes candidates for DM via the superpartners. However, this is yet to be observed.

The Flavour Puzzle

In the SM, the Yukawa couplings, and associated CKM matrices, are free parameters to be measured by experiment. However, these are vastly different in value, as can be seen in the hierarchy of masses of SM particles. For example, the top quark has a mass of 173 GeV, whereas the electron has a mass of 511 keV. The question, therefore, is is there an origin for this hierarchy of masses given that there is no reason for it to exist in the first place? A closely related question is why are there three generations of fermion families?

The Strong-CP Problem

A term consistent with all SM symmetries is the "theta-term",

$$\mathcal{L} = \frac{\theta}{32\pi^2}\epsilon_{\mu\nu\rho\lambda}G^{\mu\nu}G^{\rho\lambda}. \tag{1.35}$$

This term arises from the QCD vacuum structure and so we cannot just omit it from the SM structure. It also violates CP in the strong sector of the SM. Through measurements of the electric dipole moment of the neutron, the parameter θ is bound to be smaller than 10^{-9}. The strong-CP problem is then the question, why is this parameter so small?[18] Many solutions to this problem exist which predominantly introduce new symmetries (including the theory of the axion). However, no experimental evidence yet exists to solve this problem.

[18] One can be more general in including the weak interactions here. Diagonalising the quark mass matrix involves adding an extra term to the theta parameter. Thus, the question is then why is a parameter with origins in the strong and weak sectors so small?

Grand Unified Theories

Is the SM a small part of a larger symmetry structure? A Grand Unified Theory (GUT) is defined as a renormalisable, quantum field theory in four dimensions, invariant under a gauge group, G, such that

$$SU(3) \times SU(2) \times U(1) \subset G. \tag{1.36}$$

As such, the gauge groups of the SM are unified into a single gauge group. Furthermore, it is also required that the representations of G, which house the matter states, contain the degrees of freedom of the SM. Finally, it is also required that some Higgs-like mechanism exists which breaks the larger symmetry group, G, down to the SM gauge group. The smallest group that can consistently house the SM gauge group is $SU(5)$ [65], but other gauge groups have been considered. Ubiquitously in these models, the proton is found to decay. Thus far, no evidence has been found of this. Conversely, these theories offer up explanations for experimental parameters in the SM, most notably the Weinberg angle. Moreover, the addition of supersymmetry to GUT theories introduces an additional (light) Higgs state, which in turn lowers the mass of the broken bosons which has the effect of improving the prediction of the Weinberg angle [48, 49].

A tantalising prospect of these models comes from considering the running of the SM couplings. If we consider the $SU(5)$ GUT,[19] together with weak-scale supersymmetry, then the gauge couplings unify at a scale of $\sim 10^{16}\,\text{GeV}$. This is theoretically satisfying, as instead of the GUT gauge group just taking over at the relevant energy scale, the gauge couplings tend towards the same unified value, after which the GUT takes over. This effect has been shown for other GUT groups, however, without the inclusion of supersymmetry, only two of the three coupling constants unify. Thus, supersymmetry seems to be a necessary component to this unification.

Quantum Gravity

GR is a classical theory that identifies as equivalent all observers linked by the Poincaré group of local transformations. That it also be a theory that describes the gravitational interaction – by noting the equivalence of gravitational and inertial mass – is the key genius of its creator, Einstein. Gravitational energy, and thus, information, is now known to be transported via gravitational waves [3]. These tensor modes would quantum mechanically be described by a spin-2 state. Given this,

[19] Specifying the GUT is necessary as it sets the normalisation of hypercharge which, due to its Abelian nature, is not intrinsically normalisable.

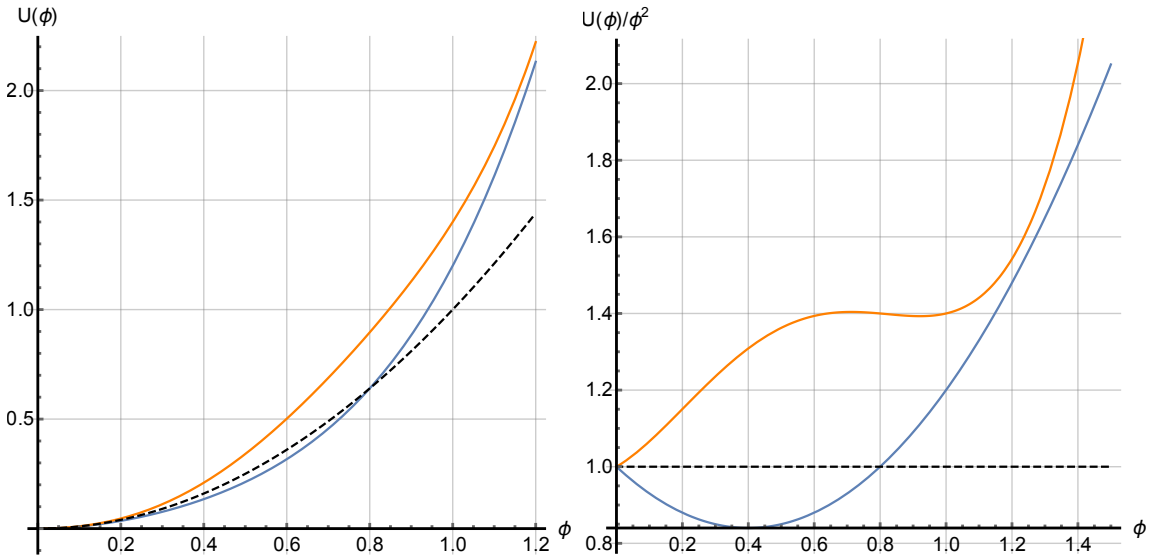

Figure 1.1: Examples of a 2-D slice of two potentials, $U(\phi)$, where ϕ represents the magnitude of Φ, and the corresponding function U/ϕ^2. The dotted line on the left-hand side represents $U = \phi^2$, whereas the dotted line on the right-hand side represents $U/\phi^2 = 1$, where we have set $m^2 = 1$ in both instances. Both potentials have a corresponding minimum in the associated function $U(\phi)/\phi^2$. However, the potential in blue is the only one to admit Q-ball solutions.

one might naively expect that it would therefore be simple to write down the quantum field theory associated to this state, which has GR as its limit. However, this leads to a theory with an infinite number of higher-dimensional terms and so is non-renormalisable. GR is therefore only considered an effective field theory, valid up to some scale – the Planck scale, $M_{\rm Pl} \sim 1.6 \times 10^{19}\,\text{GeV}$ – above which quantum effects can no longer be ignored. Furthermore, the SM, in the absence of any gauge unification, is also believed to only be valid up to this scale, above which gravitational effects cannot be ignored from its structure. It is believed that there exists some new framework – some theory of quantum gravity, or even a "theory of everything" – that will supersede the current paradigm. Though many attempts exist at constructing this framework, there is, as of yet, no experimental evidence for any of them.

1.5 Q-balls

With the discovery of a fundamental scalar in the Higgs boson, it is reasonable to ask whether any other fundamental scalars exist in nature, alongside their composite

cousins in the meson sector. Given that many extensions to the SM contain scalar states, it is important to understand the structures that can form in such a sector.

Stable soliton-like solutions exist in a wide variety of quantum field theories in $3+1$, and other, spacetime dimensions. Broadly speaking, solitons may be characterised as either *topological* or *non-topological* solitons. Topological solitons have their stability guaranteed by the conservation of a suitable topological 'charge' or winding number. For example, 't Hooft-Polyakov monopoles in spontaneously broken non-Abelian (3+1)-dimensional gauge theories are characterised by the second homotopy group of the vacuum manifold and the associated winding numbers. Alternatively, for non-topological-solitons stability is commonly ensured by other means (see, for example, [98] and references therein).

Q-balls [31] are examples of non-topological solitons which are comprised exclusively of scalars.[20] These spherically symmetric, extended states arise when a symmetry preserving potential admits stable mass states, whose masses (for a given charge) are smaller than the total mass of the individual quanta. We can thus think of Q-balls as the most energy-efficient method for a scalar theory to store charge. Canonically, these Q-balls have been analytically studied in two limits: spatially-large "thin-walled" Q-balls, appropriate for objects with large charge and whose interior is homogeneous and referred to as "Q-matter"; and spatially small, "thick-walled" Q-balls, appropriate for objects with small charge. More recently, work has been done to extend the thin-wall analysis to smaller charges [75], which is particularly useful in theories that possess no thick-wall limit and, thus, no small charge limit.

The simplest theory that admits Q-ball solutions is a U(1)-invariant theory of a complex scalar field

$$\mathcal{L} = \partial_\mu \Phi^* \partial^\mu \Phi - U\left(\Phi^*, \Phi\right), \tag{1.37}$$

where $U\left(\Phi^*, \Phi\right)$ is a U(1)-invariant potential, where it is assumed that the leading order term is quadratic in the field Φ, i.e., there are no linear or inverse powers of Φ, and that the potential vanishes for vanishing field – we will analyse this theory in detail for Q-ball solutions in Chapter 2, but give a heuristic discussion here. Mass terms in Lagrangians are quadratic in the fields. If the potential is to be symmetry-preserving, the mass term must go like $\sim |\Phi|^2$. We thus find that the mass of the excitations found by perturbing about the origin are

$$\mu^2 \equiv \left.\frac{\partial^2 U}{\partial \Phi^* \partial \Phi}\right|_{\Phi=0} = \left.\frac{U}{|\Phi|^2}\right|_{\Phi=0}. \tag{1.38}$$

[20] Though Q-balls are formed from scalar states, analogous objects could be formed from vector states.

We will show in the technical introduction to Q-balls – Chapter 2 – that the function on the right-hand side can possess a minimum away from $\Phi = 0$ that is deeper than μ^2,

$$\min_{\Phi \neq 0} \left[\frac{U}{|\Phi|^2} \right] < \mu^2. \tag{1.39}$$

The solutions to this condition are Q-balls, and these have a lower mass (for a given charge) than for the individual quanta of mass μ. In Fig. 1.1, we plot two examples of potentials: one which satisfies this condition and admits Q-ball solutions, and a second which does not. This function on the left-hand side may have many local minima, each of which satisfy the above condition. In this thesis, we usually assume that only one such minimum exists and thus the Q-ball solution is unique.

The only renormalisable potential, which is left invariant by the U(1) symmetry, we can write down for this system is

$$U\left(\Phi^*, \Phi\right) = a\left(\Phi^*\Phi\right) + b\left(\Phi^*\Phi\right)^2. \tag{1.40}$$

This potential will not admit Q-ball solutions, as b must be non-negative to ensure a stable theory. We are left with three options:

1. we have a non-analytic term, such as $c\left(\Phi^*\Phi\right)^{3/2}$;

2. we consider higher-dimensional terms, such as with an effective theory;

3. we consider a more complex system, such as with multiple scalar fields.

In this thesis, we'll first consider a system of a single scalar field, before generalising to multiple fields. We will find, in the case of single-field thick-wall Q-balls, that non-analytic terms are a necessity for their stability.

The canonical Q-ball analysis has been extended to accommodate a number of contexts including: Abelian [31] and non-Abelian [122, 123] global symmetries; and multi-field contexts including coupling the charged scalars to uncharged scalars [57], supersymmetric theories [13, 90], and mirror-world like models [18, 19].[21] They have also been studied in theories of higher dimensions: if the dimensions are non-compact, the analysis simply generalises by virtue of using the Laplacian and integration measure appropriate for the given dimension [107, 136]; in theories where the extra dimensions are compact, the Q-balls form an infinite tower of states [4, 40].

[21] One could extend these ideas to other BSM scenarios in which the SM Higgs is realised as a pNGB.

The stabilising symmetry can be gauged [74, 96]. These Q-balls are stable when the electrostatic energy of the Q-ball is smaller than the other energies of the Q-ball, that is, if the electrostatic cost of bringing together a charge Q – in units where the gauge coupling has been factored out – over an extended object is smaller than the reduction of energy from arranging the quanta into a Q-ball. The repulsive nature of the Coulombic force sets an upper bound on the charge, and thus, the size of the Q-ball. The component of the mass due to surface effects of a Q-ball are more important for smaller Q, and thus the binding energy of small Q-balls is consequently lower. As such, the addition of a Coulombic component can render smaller Q-balls unstable. Since the surface effects become more negligible with increasing Q, this implies a lower bound on the charge. If $Q_{\max} < Q_{\min}$, no stable gauged Q-balls exist. For Q-balls that are large compared to the Compton wavelength of the gauge field, the charge is pushed to the surface of the Q-ball. It resides in a shell with a thickness of order the size of the Compton wavelength of the gauge field. In this way, the Q-ball acts as a U(1) superconductor.

The analysis has been extended to even more exotic objects. In higher dimensions, "Q-branes" have been theorised, in which a brane is stabilised by a combination of energy and Noether charge [4]. Q-balls with an extra topological charge, referred to as Q-lumps, have also been studied [99, 113]. It has also been shown that potentials that admit Q-balls also admit diffuse, spherically symmetric configurations, without well-defined edges, referred to as Q-clouds [8]. These Q-clouds have a total mass smaller than a configuration of the quanta of the theory, but are unstable. In the gauged case, the resulting radial profile need not be that of a ball, and can in fact take the form of a thin shell [12, 76, 116, 135].

Q-balls are kept stable by conservation of charge and energy. The stability of ordinary matter relies on conservation of particle number. Here, the charge Q plays that role. As the Q-ball solution minimises $U/|\Phi|^2$ for a given Q, it is impossible for the Q-ball to decay to other particles by conservation of energy and charge. One could could also consider quantum tunnelling: treating the Q-matter as a false vacuum, quantum fluctuations can produce a bubble of true vacuum, by tunnelling through the potential, which then classically grows. This is referred to as "spontaneous cavitation", but it is not possible as quantum tunnelling conserves both E and Q. Thus, in the simplest scenario, the Q-ball is absolutely stable. There are, however, ways to render Q-balls unstable. If the constituent quanta of the Q-ball have decay channels, this can lead to decay of the Q-ball [29]. In particular, if the channel is to fermions, as is the case in supersymmetric theories, then the decay is surface area limited –

the Q-balls can be said to "evaporate". This has its origins in the exclusion principle – spontaneous cavitation within the bulk of the Q-ball cannot happen if the decay mode is to fermions, as they saturate the states allowed within the cavity by the exclusion principle. If the decay channel is bosonic, however, then the decay happens throughout the bulk as no such problem exists with the exclusion principle. Further instances that may destabilise a Q-ball include gravitational effects and the collapse into black holes [124, 133, 134], thermal effects in the early universe [95], or symmetry breaking effects [85].

Q-balls that are absolutely stable, or quasi-stable with cosmological lifetimes, have been studied as a potential candidate for DM [68, 93, 94]. In order for Q-balls to be a major component of DM, they must have been produced in high abundance in the early universe. The Affleck-Dine mechanism [6] has long been studied as a possible source for baryogenesis in the early universe. This mechanism exploits baryon-number-violating flat-directions – directions in field space which grow no faster than quadratically – usually in supersymmetric extensions of the SM [42, 43], during an inflationary phase in the early universe to produce a net baryon number. This is a highly efficient process which can give an $\mathcal{O}(1)$ asymmetry in baryon number. The Affleck-Dine mechanism may also be used to create any net U(1) charge by exploiting any symmetry-violating[22] flat direction, and hence Q-balls. In this case, a Q-condensate is formed when the flat direction is lifted and the underlying field, displaced from its minimum during the inflationary phase, coherently oscillates as it returns to equilibrium. This condensate later fragments into Q-balls [50, 93] as it is unstable due to quantum fluctuations during inflation leading to non-uniformities. Other production methods in the early universe include "solitogenesis" [47, 58, 70], whereby Q-balls are formed in a phase transition in the early universe, and "solitosynthesis" [59, 69, 88], whereby Q-balls are formed through fusion, but these seem unlikely to be able to produce Q-balls with a large enough charge to survive to the present day in the most conventional supersymmetric models. Given work on Hawking radiation of extended objects in Ref. [82], one could conceive of a situation whereby an initial population of black holes in the early universe could seed an abundance of Q-balls, similarly to the mechanism discussed in Refs. [9, 103] for particle-like DM. However, it seems that the rate of emission of Q-balls – or other extended objects – of size $\gtrsim$ fm, i.e., greater than the size of nucleons, would be highly suppressed [73], and so the resulting Q-balls will not be distinguishable from existing particle-like states in direct detection experiments.

[22] This symmetry violation could, for example, come from an underlying UV theory.

There are a number of existing experiments which can be used to detect Q-balls as DM, such as Super Kamiokande [11, 91, 132], by using proton absorption, or MACRO [10, 91], which can directly detect charged Q-balls. DM direct detection experiments can also be used if the Q-balls interact with the SM, as extended DM states can leave an explicit signature [62]. Specifically, the extended nature of the Q-ball allows it to coherently scatter with the particles in the detector, which introduces a form factor that is strongly peaked at low energies, i.e., towards the lower energy threshold of the experiment. One could also envisage detecting gravitational waves from the fragmentation of an early universe Affleck-Dine Q-condensate [92]. There has also been work on utilising laser interferometers as detectors for (heavy) extended states [71]. Atomic clocks can also be used to study DM which is formed of an extended object [41].

1.6 The Rest of This Thesis

This thesis represents a study on the formal properties of field theories to determine which class of theories admit Q-ball solutions. Consequently, its goals are two-fold:

- To constrain the theories that possess stable Q-ball states by: (i) determining the differential equations that govern the VEV of the constituent scalar in the thin-wall limit, together with the physical properties of the resulting Q-ball; (ii) constraining the small-field expansions that lead to stable thick-wall Q-balls by demanding that the minimum of energy be classically stable against decay to the underlying quanta of the scalar field;

- To determine whether stable Q-balls, in both the thick- and thin-wall limit, can form from scalar mesons arising from the breaking of an approximate chiral symmetry in the SM and in a specific BSM theory.

We will not discuss the phenomenology of these theories in this thesis.

The content of this thesis is laid out in three parts. Part I is concerned with Q-balls in theories possessing only one scalar field, and comprises Chapters 2 and 3, whereas Part II is concerned with theories with multiple scalar fields, and comprises Chapters 4-6. Finally, Part III analyses theories when the underlying scalars of the theory are pNGBs arising from the breaking of an approximate chiral symmetry, as in the SM – this final part comprises Chapters 7 and 8. We outline the content of each individual chapter below.

In Chapter 2, we reproduce the classic mathematical analyses of theories for Q-ball solutions, introducing the formal theory of Q-balls as we go. Specifically, we study a class of theories of a single, complex scalar field, invariant under a single $U(1)$ symmetry, with potentials that are only composed of terms that are each power laws of the field. We refer to these as "canonical Q-ball solutions". We focus on the analytic limits of the theory, that is, the thin- and thick-wall limits of the Q-ball solutions. This is reproduced from the existing literature, most notably from Coleman's classic thin-wall analysis in Ref. [31] and Kusenko's thick-wall analysis in Ref. [89]. We show that there is an additional restriction on theories that possess an energetically stable thick-wall limit that doesn't also apply to the thin-wall limit. This is a result known in the literature, and can be found in Refs. [115,119]. We prove this result in a novel way, and this will be the basis of much of the following chapters. This original work, performed solely by the author, can be found in Ref. [101].

With the basic Q-ball analysis established in Chapter 2, we then seek to modify the underlying theory in the following chapters, with each chapter introducing a separate modification. In Chapter 3, we modify the theory by allowing the potential to contain terms that couple to the derivatives of the field. More precisely, only terms containing two derivatives of the field will be studied. We find that a thin-wall limit exists in these theories, and that the thick-wall limit is similarly restricted as in the canonical case. This latter result is particularly interesting since the functional dependence on the variables of the theory are fundamentally different to the canonical case. This original work, performed solely by the author, can be found in Ref. [101].

In Chapter 4, we return to the canonical theory and modify it to include more than one field, but still only a single symmetry, and no terms that couple the field to its derivatives. The thin-wall analysis of this class of theory can be found in the literature in Refs. [57, 90]. Due to the added complexity caused by the additional fields, it is not possible to proceed in the thick-wall limit analytically without some further simplification – we assume that the fields have the same shape of spatial profile inside the Q-balls, as was assumed in Refs. [18, 119]. With this assumption, we find a set of sufficient conditions on the existence of stable thick-wall Q-balls in certain situations, notably in the case that all additional fields are uncharged. Furthermore, in the case that the additional fields are massive, the thick-wall Q-balls are only energetically stable if enough charge has built up. The thick-wall analysis of theories possessing one charged field and an arbitrary number of uncharged fields is original work, performed solely by the author, and can be found in Ref. [100]. The remaining original work, performed solely by the author, remains unpublished.

We modify the multi-field theory of the previous chapter to include multiple symmetries in order to study multi-charged Q-balls in Chapter 5. Specifically, we consider the special case where each scalar field in the theory transforms under its own $U(1)$. As in the previous chapter, we perform the thin- and thick-wall analyses. We find, in the thin-wall case, that the scalar field takes on a charge-dependent value inside the Q-ball, which is in contrast to all previous cases in which it is charge-independent. With the same assumption on the spatial profiles of the fields as in the previous chapter, we also find that the theories that allow energetically stable thick-wall Q-balls to form are always restricted as in Chapters 2 and 3. This original work, performed solely by the author, can be found in Ref [102].

In Chapter 6, we introduce a new type of object: a cored Q-ball. The example given is from a theory with multiple fields and multiple symmetries. Thin-wall Q-balls are characterised by an approximately homogeneous core, and so provide a homogeneous background for any object travelling through it. If the object passing through is another scalar that couples to the background field, it is reasonable to ask whether the trapped scalar can form a small Q-ball that settles in the core (by the symmetry of object), and whether this total object is energetically stable. We determine the conditions for this stability. This original work, performed solely by the author, can be found in Ref. [102].

In Chapter 7, we explore the SM for Q-ball solutions. As the Higgs potential will not allow for Q-balls, we focus on the only remaining scalars in the theory, namely the light mesons. These pseudoscalars are the pNGBs associated to the breaking of the approximate chiral symmetry in the quark sector of the SM. They are mathematically described by the chiral Lagrangian. To leading order, this was already studied for thin-wall Q-balls in Ref. [44]. We present an original thick-wall analysis, which is adapted from the appendix given in Ref. [18], performed by the author alongside Bishara, Johnson, and March-Russell. Our analysis suggests that no Q-ball states are allowed in the leading order chiral Lagrangian.

Given that no Q-balls can exist in the leading order chiral Lagrangian as it is in the SM, we investigate a hidden sector with slightly modified dynamics in Chapter 8. We assume that we have an almost exact copy of the SM in some hidden sector that only interacts with our world via a portal coupling with the Higgs boson. The light bosons of the theory are the pseudoscalar mesons of the hidden sector and the Higgs boson. Together, these form stable Q-balls and we investigate the thin- and thick-wall sectors of the theory. This original work by the author was published in a paper,

written with Bishara, Johnson, and March-Russell, in Ref. [18], and another with Bishara in Ref. [19].

Finally, we note that one other paper was written by the author, together with collaborators, during the writing of this thesis in Ref. [103]. However, we do not include this as it is not the focus of this thesis.

Part I

Single-Field Q-balls

Chapter 2

The Canonical Q-ball Solutions

2.1 Introduction

Q-balls are objects that can exist within scalar field theories that are invariant under a group of transformations. For a scalar field whose quanta possess unit charge, a Q-ball represents a semi-classical, coherent state of Q quanta – in some sense, these can be thought of as a bound state of these particles.[1] These objects are the state within the theory that minimises the energy for a given charge, i.e., they are the most energy efficient way for a scalar theory to store charge. However, finding the extremum of the energy is not analytically tractable in the most general of scenarios, but analytic limits do exists. Specifically, these are referred to as the thin- and thick-wall limits, valid in the limit of large and small charge, respectively. More recently, work has been done in Ref. [75] to analytically extend the thin-wall limit in theories that possess no thick-wall limit, but we shall not comment on this work further.

This chapter acts as a technical introduction to the formal theory of Q-balls. In particular, we review what we call the "canonical" Q-ball solutions. These represent the Q-balls, in the thin- and thick-wall limits, found in theories of a single, complex scalar field, invariant under a group of $U(1)$ transformations, whose potential is only a function of powers of the scalar field, and *not* its derivatives. These represent the classic works of Coleman [31] and Kusenko [89].

Specifically, in Section 2.2, we set out the procedure for determining the solution that minimises the energy for a fixed charge. This involves introducing a Lagrange

[1] Though the underlying states of the theory are quantum mechanical – i.e., bosonic (spin-one) particles of unit charge – we will describe their collective phenomena as solutions of a classical field theory. This is valid when enough of the quanta accumulate such that quantum fluctuations are "small" in some sense – we briefly discuss this at the end of this chapter. Though a description of the quantum nature of Q-balls is desirable – as it is for any fundamental understand of a physical object – quantum mechanics is a theory of *point-particles*, and so a quantum description is lacking.

multiplier, as in Ref. [90], to set the fixed charge constraint. Moreover, we show that this Lagrange multiplier can be interpreted as a chemical potential for the Q-balls. The resulting functional cannot be minimised analytically. In Section 2.3, we review the thin-wall limit, showing that the physical properties of the Q-ball are well-described by those of its homogeneous core. We derive the differential equation governing the VEV of the scalar field inside the core and solve it for a specific class of potential. We then derive the physical properties of a Q-ball in the case that the energy of the core vanishes, as in the case of certain special potentials. In Section 2.4, we review the case of thick-wall Q-balls. A theory that possesses a thin-wall limit does not generically possess a stable thick-wall limit. We, thus, constrain the theories that admit stable thick-wall Q-balls by demanding that the minimum of the energy be classically stable against decay to individual quanta of the field.

The bulk of this chapter is a review of the background literature on canonical Q-ball solutions. However, the proof that stable thick-wall Q-balls only exist in specific theories – namely, those with a potential whose small-field expansion is given by

$$U(\Phi^*, \Phi) \approx m^2 \Phi^* \Phi - \frac{c_p}{\Lambda^{p-4}} \left(\Phi^* \Phi\right)^{p/2}, \tag{2.1}$$

where $2 < p < 10/3$, $c_p, \Lambda > 0$ – is original. However, the result was already known, and proven via other means, in the literature [115, 119]. We give this here as it will be the basis of many studies throughout this thesis.

2.2 Minimising the Energy in a Sector of Fixed Charge

Q-balls represent the state in a scalar field theory that minimises the energy for a given Noether charge. In this section, we outline the specific class of theory we study in this chapter, and the minimisation procedure for determining the Q-ball solutions in that theory.

2.2.1 The Minimisation Procedure

We will consider the theory of a single complex scalar field, $\Phi(\vec{x}, t)$, and its complex conjugate, governed by the Lagrangian density

$$\mathcal{L} = \partial_\mu \Phi^* \partial^\mu \Phi - U(\Phi^*, \Phi). \tag{2.2}$$

The function $U(\Phi^*, \Phi)$ is a potential that we leave generic for the time being – we only stipulate that it is a function of the fields Φ^* and Φ only, and not their derivatives,

and, without loss of generality, that the zero of the potential occurs with vanishing field. We further assume that the leading order term in the potential is quadratic in the fields, i.e., there are no terms linear or inverse in powers of the fields. The Euler-Lagrange equation for this theory is given by

$$\partial_\mu \partial^\mu \Phi + \frac{\partial U}{\partial \Phi^*} = 0, \tag{2.3}$$

with a similar equation governing the evolution of Φ^*.

We require that this theory be invariant under some global $U(1)$ symmetry, made manifest by the invariance of the Lagrangian under the transformation

$$\Phi \to e^{i\alpha}\Phi, \quad \alpha \in \mathbb{R}, \tag{2.4}$$

with the transformation for the complex conjugate field being the complex conjugate of this transformation. Due to the Abelian nature of this global symmetry, we are free to normalise charges as we please – we have implicitly set the charges of individual quanta of the field Φ to be unity, with the complex conjugate field being assigned the same charge with opposite sign. To this invariance is associated a conserved Noether current density,

$$\begin{aligned} j^\mu &= \lim_{\alpha\to 0}\left(\frac{\partial \mathcal{L}}{\partial(\partial_\mu \Phi)}\frac{\delta\Phi}{\alpha} + \frac{\partial \mathcal{L}}{\partial(\partial_\mu \Phi^*)}\frac{\delta\Phi^*}{\alpha}\right) \\ &= i\left(\Phi\partial^\mu\Phi^* - \Phi^*\partial^\mu\Phi\right), \end{aligned} \tag{2.5}$$

which satisfies

$$\partial_\mu j^\mu = 0, \tag{2.6}$$

by application of the Euler Lagrange equations given in Eq. (2.3). This symmetry fixes the potential to be a function of the product of the fields only,

$$U(\Phi^*, \Phi) = U(\Phi^*\Phi). \tag{2.7}$$

We wish to analyse this theory for Q-ball solutions. These are the states that minimise the energy per unit Noether charge. The Hamiltonian, coincident with the energy, for this theory is

$$\begin{aligned} H &= \int \mathrm{d}^3x \left[\frac{\partial \mathcal{L}}{\partial \dot{\Phi}}\dot{\Phi} + \frac{\partial \mathcal{L}}{\partial \dot{\Phi}^*}\dot{\Phi}^* - \mathcal{L}\right] \\ &= \int \mathrm{d}^3x \left[\dot{\Phi}^*\dot{\Phi} + \vec{\nabla}\Phi^* \cdot \vec{\nabla}\Phi + U(\Phi^*\Phi)\right]. \end{aligned} \tag{2.8}$$

To determine the states with the lowest energy for a given charge, we employ the method of Ref. [90]. We introduce a Lagrange multiplier, ω, and minimise the functional given by

$$\mathcal{E}_\omega = H + \omega \left(Q - \int \mathrm{d}^3x \, j^0 \right), \tag{2.9}$$

where j^0 is the zero-component of the Noether current density. Note that minimisation of this functional with respect to the Lagrange multiplier yields the charge of the configuration. In our theory, this functional evaluates to

$$\mathcal{E}_\omega = \omega Q + \int \mathrm{d}^3x \left[\left| \dot{\Phi} - i\omega\Phi \right|^2 - \omega^2 \Phi^* \Phi + \vec{\nabla}\Phi^* \cdot \vec{\nabla}\Phi + U(\Phi^*\Phi) \right], \tag{2.10}$$

where we have completed the square on the terms with explicit time-dependence. The solution $\Phi = 0$ corresponds to a configuration with $Q = 0$, and so we infer that a configuration with finite charge must have a profile that differs from zero over some finite domain.

The first term under the integral is positive semi-definite and is minimised when it vanishes, i.e., if

$$\dot{\Phi} - i\omega\Phi = 0. \tag{2.11}$$

This can be readily solved to give

$$\Phi(\vec{x}, t) = e^{i\omega t}\phi(\vec{x}), \tag{2.12}$$

where $\phi(\vec{x})$ is, without loss of generality, a real-valued function of the spatial coordinates. This functional form is generic to Q-ball solutions: they are said to rotate in field space with an angular velocity ω. Given this prescription, the Euler-Lagrange equation governing the shape of the spatial potential, derived from Eq. (2.3), is thus

$$\nabla^2\phi = \frac{1}{2}\frac{\mathrm{d}}{\mathrm{d}\phi}\left(U(\phi) - \omega^2\phi^2 \right), \tag{2.13}$$

where $U(\phi)$ is the potential derived from $U(\Phi^*\Phi)$ where $\Phi^*\Phi \to \phi^2$. Notice, the full function in brackets defines a new effective potential function under which ϕ is determined. This differential equation is the well-studied bounce equation associated to the creation of bubbles of true vacua in the early universe [22, 30, 32] for the potential given in brackets on the right-hand side. This differential equation is not possible to solve in general. However, analytic expressions can be found in certain limits:

- Q is very large, and the energy is dominated by the volume: these are the thin-wall Q-balls attributed to Ref. [31];[2]

- Q is small, and surface effects are an important energy contribution: these are the thick-wall Q-balls first appearing in Ref. [89].

These will be the subject of Section 2.3 and Section 2.4 of this chapter, respectively. What is known, however, is that the lowest energy configuraton is always spherically symmetric [32], i.e.,

$$\phi(\vec{x}) = \phi(r). \tag{2.14}$$

This differential equation is then solved with the following boundary conditions:

$$\lim_{r\to 0}\phi = \phi_0, \quad \lim_{r\to 0}\frac{\mathrm{d}\phi}{\mathrm{d}r} = 0, \quad \lim_{r\to\infty}\phi = 0, \quad \lim_{r\to\infty}\frac{\mathrm{d}\phi}{\mathrm{d}r} = 0, \tag{2.15}$$

where $\phi_0 \in \mathbb{R}$ is some constant. These boundary conditions will ensure that the configuration does indeed differ from zero over some finite range, and that the energy remains finite.

Given the spherical symmetry of the Q-ball, we may now readily write the Euler-Lagrange equation for the spatial profile as

$$\frac{1}{r^2}\frac{\mathrm{d}}{\mathrm{d}r}\left(r^2\frac{\mathrm{d}\phi}{\mathrm{d}r}\right) = \frac{1}{2}\frac{\mathrm{d}U}{\mathrm{d}\phi} - \omega^2\phi. \tag{2.16}$$

The charge of this configuration is given by

$$Q = 8\pi\omega\int \mathrm{d}r\, r^2\phi^2, \tag{2.17}$$

and the energy is similarly found to be

$$\begin{aligned} E &= 4\pi\int \mathrm{d}r\, r^2\left[\omega^2\phi^2 + \left(\frac{\mathrm{d}\phi}{\mathrm{d}r}\right)^2 + U\right] \\ &= \omega Q + 4\pi\int \mathrm{d}r\, r^2\left[\left(\frac{\mathrm{d}\phi}{\mathrm{d}r}\right)^2 - \omega^2\phi^2 + U\right], \end{aligned} \tag{2.18}$$

where we have used Eq. (2.17) in determining the final line. We will use these expressions to derive two results below.

[2] As Coleman himself noted in the added proof of his paper, there was already some literature on Q-balls and Q-ball-like solutions found in Refs. [97, 109, 110, 120, 142].

2.2.2 The Lagrange Multiplier as a Chemical Potential

Before we discuss the two analytic limits mentioned above, we first explore two general implications of Eq. (2.12). For this subsection, we follow a presentation similar to that found in Ref. [75]. Firstly, we show that the Lagrange multiplier can be interpreted as a chemical potential for the Q-ball [57]. Taking a derivative of the energy given in Eq. (2.18) with respect to the Lagrange multiplier ω yields

$$\frac{\mathrm{d}E}{\mathrm{d}\omega} = \omega\frac{\mathrm{d}Q}{\mathrm{d}\omega} + Q + 8\pi\int \mathrm{d}r\, r^2 \left[\frac{\mathrm{d}\phi}{\mathrm{d}r}\frac{\mathrm{d}}{\mathrm{d}\omega}\left(\frac{\mathrm{d}\phi}{\mathrm{d}r}\right) - \omega\phi^2 + \left(\frac{1}{2}\frac{\mathrm{d}U}{\mathrm{d}\phi} - \omega^2\phi\right)\frac{\mathrm{d}\phi}{\mathrm{d}\omega}\right]. \quad (2.19)$$

We recognise the second integrated term as $-Q$, and so this cancels. We perform an integration by parts on the first term under the integral, ignoring a surface term by the boundary conditions stipulated above, to give

$$\frac{\mathrm{d}E}{\mathrm{d}\omega} = \omega\frac{\mathrm{d}Q}{\mathrm{d}\omega} + 4\pi\int \mathrm{d}r\, r^2 \left[-\frac{\mathrm{d}}{\mathrm{d}r}\left(r^2\frac{\mathrm{d}\phi}{\mathrm{d}r}\right) + \frac{1}{2}\frac{\mathrm{d}U}{\mathrm{d}\phi} - \omega^2\phi\right]\frac{\mathrm{d}\phi}{\mathrm{d}\omega}. \quad (2.20)$$

The term in the square brackets vanishes by the Euler-Lagrange equation for the spatial profile given in Eq. (2.16), so we are left with the result

$$\frac{\mathrm{d}E}{\mathrm{d}\omega} = \omega\frac{\mathrm{d}Q}{\mathrm{d}\omega}. \quad (2.21)$$

This result is universal and holds for all Q-balls. Furthermore, for a non-vanishing derivative of Q with respect to ω, we note that

$$\frac{\mathrm{d}E}{\mathrm{d}Q} = \omega. \quad (2.22)$$

Recall, for field quanta of unit charge, Q also indexes the number of constituent scalars forming the Q-ball. Thus, not only can we interpret the Lagrange multiplier as an angular velocity in field space, but here it takes the form of a chemical potential:

- If $\mathrm{d}Q/\mathrm{d}\omega > 0$, it is energetically favourable for the Q-ball to decrease in size via ejection of quanta;
- If $\mathrm{d}Q/\mathrm{d}\omega < 0$, it is energetically favourable for the Q-ball to increase in size via absorption of quanta;

We now show that we may rewrite the energy of a Q-ball that makes manifest the energy of the bulk volume and the surface of a Q-ball [96]. Consider the Lagrangian of the system in light of Eqs. (2.12) and (2.14),

$$L = 4\pi\int \mathrm{d}r\, r^2 \left[-\left(\frac{\mathrm{d}\phi}{\mathrm{d}r}\right)^2 + \omega^2\phi^2 - U(\phi)\right]. \quad (2.23)$$

We make a change of variables of $r \to \chi\rho$, so

$$L = 4\pi \int \mathrm{d}\rho\, \rho^2 \left[-\chi \left(\frac{\mathrm{d}\phi}{\mathrm{d}\rho} \right)^2 + \chi^3 \omega^2 \phi^2 - \chi^3 U(\phi) \right]. \tag{2.24}$$

We now consider variations of this Lagrangian with respect to χ, noting that there is explicit dependence on χ and implicit dependence through $\phi(r) \to \phi(\chi\rho)$,

$$\delta L = \delta L_{\text{implicit}} + \delta L_{\text{explicit}}. \tag{2.25}$$

First, we analyse the implicit variation, which evaluates to

$$\delta L_{\text{implicit}} = 8\phi \int \mathrm{d}\rho\, \rho^3 \frac{\mathrm{d}\phi}{\mathrm{d}\rho} \left[-\frac{1}{\rho^2} \frac{\mathrm{d}}{\mathrm{d}\rho} \left(\rho^2 \frac{\mathrm{d}\phi}{\mathrm{d}\rho} \right) - \frac{1}{2} \frac{\mathrm{d}U}{\mathrm{d}\phi} + \omega^2 \phi \right] \delta\chi. \tag{2.26}$$

When $\chi \to 1$, i.e., $\rho \to r$, the term in brackets vanishes by Eq. (2.16). We must similarly demand that the explicit variation vanish in this same limit. This implies that

$$4\pi \int \mathrm{d}r\, r^2 \left[-\omega^2 \phi^2 + U(\phi) \right] = -\frac{4\pi}{3} \int \mathrm{d}r\, r^2 \left(\frac{\mathrm{d}\phi}{\mathrm{d}r} \right)^2. \tag{2.27}$$

This allows us to rewrite Eq. (2.18) as

$$E = \omega Q + \frac{8\pi}{3} \int \mathrm{d}r\, r^2 \left(\frac{\mathrm{d}\phi}{\mathrm{d}r} \right)^2. \tag{2.28}$$

We can loosely interpret the first term as the energy of the bulk volume, and the second term as the energy of the surface: this assignment becomes exact in the thin-wall case explored below.

2.3 Thin-Wall Q-balls

In this section, we review the thin-wall Q-ball solution from Coleman's classic paper on the subject.

2.3.1 Coleman's Q-balls

Thin-wall Q-balls correspond to the large volume limit, whereby the energy of the Q-ball is dominated by a large, homogeneous core of "Q-matter",[3] and a spatially

[3] Q-matter is so named due to the scaling of the mass, derived soon, of the Q-ball with Q. This is similar to nuclear matter, which scales approximately with N. It should be further noted that Q-matter represents a state that spontaneously breaks the global symmetry which stabilises the Q-ball, in a manner similar to superfluids. The resulting NGB modes – phonons – are massless in the infinite volume limit, but pick up a mass in the finite volume limit, and represent the lightest excitation modes of the Q-ball.

thin wall that interpolates between the VEV in the core, ϕ_0, and the vacuum of the theory, $\phi = 0$. This approximation scheme was first studied in Ref. [31]. In this limit, we approximate the spatial profile by

$$\phi(r) \approx \phi_0 \Theta(R - r), \tag{2.29}$$

where $\phi_0 \in \mathbb{R}$ and R is the radius of the core. This ansatz is consistent with the boundary conditions given in Eq. (2.15). As the core is homogeneous, we infer from Eq. (2.28) that

$$E = \omega_0 Q, \tag{2.30}$$

as the derivatives only contribute over the thin-wall of the Q-ball. We will show below that this latter term is indeed subdominant in this case.

To determine an expression for ω_0, we reconsider the functional given in Eq. (2.10), which in this limit becomes

$$\mathcal{E}_\omega \approx \omega_0 Q + V\left[-\omega_0^2 \phi_0^2 + U(\phi_0)\right], \tag{2.31}$$

where

$$V = \frac{4\pi}{3} R^3, \tag{2.32}$$

is the volume of the core of the Q-ball. This function must be minimised with respect to ω_0, V and ϕ_0. For stability, the value at the minimum must be less than Qm_ϕ, as otherwise it would be energetically favourable for the Q-ball to classically decay to Q quanta of the scalar field. Minimisation with respect to ω_0 yields

$$Q = 2\omega_0 \phi_0^2 V, \tag{2.33}$$

which is expected – this is precisely Eq. (2.17) in the thin-wall limit. The Lagrange multiplier was, after all, initially introduced in order to fix the charge of the Q-ball. Reinserting this, we obtain the energy of the core of the Q-ball

$$E = \frac{Q^2}{4\phi_0^2 V} + U(\phi_0) V. \tag{2.34}$$

To determine the volume of the core, we minimise this expression with respect to the volume to obtain

$$V^2 = \frac{Q^2}{4\phi_0^2 U(\phi_0)}. \tag{2.35}$$

Once more, reinserting yields the rest mass of the Q-ball

$$m_Q = Q\sqrt{\frac{U(\phi_0)}{\phi_0^2}}, \tag{2.36}$$

where we read off

$$\omega_0 = \sqrt{\frac{U(\phi_0)}{\phi_0^2}}. \tag{2.37}$$

This is not an unexpected result – this expression for ω_0 inside the core of the thin-wall Q-ball is consistent with Eq. (2.16) governing the spatial profile of ϕ when the profile is constant.

Finally, the energy must be minimised with respect the to field value, subject to the constraint $\omega_0 < m_\phi$ for classical stability. This yields

$$\frac{\mathrm{d}U(\phi_0)}{\mathrm{d}\phi_0} = 2\frac{U(\phi_0)}{\phi_0}. \tag{2.38}$$

This constrains the potentials that can admit Q-ball solutions. We will consider an example of a potential that admits Q-ball solutions below. However, we must first show that the energy of the surface is indeed subdominant and can be safely ignored.

In determining the contribution to the Q-ball rest mass due to the surface energy, we approximate $\omega = \omega_0$ throughout. The energy due to the volume is given by

$$E_{\text{volume}} = \omega_0 Q = 8\pi\omega_0^2 \int \mathrm{d}r\, r^2\phi^2 = \frac{8\pi}{3}\omega_0^2\phi_0^2 R^3. \tag{2.39}$$

The final equality implicitly defines the radius of the Q-ball, which is somewhat arbitrary due to the fuzziness of the surface. The energy due to the surface, using Eq. (2.28), is then given by

$$E_{\text{surface}} = \frac{8\pi}{3}\int \mathrm{d}r\, r^2 \left(\frac{\mathrm{d}\phi}{\mathrm{d}r}\right)^2. \tag{2.40}$$

In the case of a thin-wall Q-ball, in which the field only varies through a thin-shell, this integral will be tightly peaked at the surface, so we approximate this as

$$\int \mathrm{d}r\, r^2 \left(\frac{\mathrm{d}\phi}{\mathrm{d}r}\right)^2 \approx R^2 \int \mathrm{d}r \left(\frac{\mathrm{d}\phi}{\mathrm{d}r}\right)^2. \tag{2.41}$$

We wish to rewrite this integral without explicit dependence on the r-coordinate such that we may associate it with the surface tension of the Q-ball.

Consider now the bounce equation as given in Eq. (2.16). In the large volume limit, we drop the term proportional to $1/r$ in the vicinity of the surface, such that

$$\frac{\mathrm{d}^2\phi}{\mathrm{d}r^2} = \frac{1}{2}\frac{\mathrm{d}}{\mathrm{d}\phi}\left(U(\phi) - \omega_0^2\phi^2\right). \tag{2.42}$$

We may integrate this over ϕ,

$$\int_0^\phi \mathrm{d}\phi \frac{\mathrm{d}^2\phi}{\mathrm{d}r^2} = \int_0^\phi \mathrm{d}\phi \frac{1}{2}\frac{\mathrm{d}}{\mathrm{d}\phi}\left(U(\phi) - \omega_0^2\phi^2\right). \tag{2.43}$$

Integrating the term on the left-hand side by parts, and applying the boundary conditions for the Q-ball solution, yields

$$\left(\frac{\mathrm{d}\phi}{\mathrm{d}r}\right)^2 = U(\phi) - \omega_0^2\phi^2. \tag{2.44}$$

We finally find that

$$E_{\text{surface}} = \frac{8\pi}{3}R^2 \int \mathrm{d}\phi \sqrt{U(\phi) - \omega_0^2\phi^2}. \tag{2.45}$$

We can now associate this integral to a surface tension that does not explicitly depend on the radial coordinate. Thus, we see that, in the large-volume limit, the surface energy is indeed subdominant to the energy contained within the core due to its scaling with a lower power than for the volume energy.

Upon including gravity, thin-wall Q-balls may not have arbitrarily large charge. One can see above that the radius grows more slowly with charge than the mass. As such, there will come a charge when the radius becomes smaller than the Schwarzschild radius of the Q-ball, and it will thus collapse into a black hole [124, 133, 134]. Demanding that $R_Q < 2m_Q/M_{\text{Pl}}^2$ sets an upper bound on the charge,

$$Q < \sqrt{\frac{3}{8\pi}}\frac{\phi_0}{U(\phi_0)}M_{\text{Pl}}^3. \tag{2.46}$$

This is turn sets an upper bound on the mass,

$$m_Q < \sqrt{\frac{3}{8\pi}}\frac{M_{\text{Pl}}^3}{\sqrt{U(\phi_0)}}, \tag{2.47}$$

and radius of a thin-wall Q-ball to be

$$R < \frac{1}{4^{1/3}}\sqrt{\frac{3}{2\pi}}\frac{M_{\text{Pl}}}{\sqrt{U(\phi_0)}}. \tag{2.48}$$

These quantities are clearly theory-dependent.

The most straightforward example of a classical potential that admits thin-wall Q-balls is

$$U(\Phi^*, \Phi) = m_\phi^2\Phi^*\Phi - \frac{c_p}{\Lambda^{p-4}}(\Phi^*\Phi)^{p/2} + \frac{c_q}{\Lambda^{q-4}}(\Phi^*\Phi)^{q/2}, \tag{2.49}$$

where $c_p, c_q > 0$ are constant coefficients, Λ is some mass scale, and $q > p > 2$. Upon insertion of the Q-ball ansatz in Eq. (2.12), and taking the thin-wall limit, this becomes

$$U(\phi_0) = m_\phi^2\phi_0^2 - \frac{c_p}{\Lambda^{p-4}}\phi_0^p + \frac{c_q}{\Lambda^{q-4}}\phi_0^q, \tag{2.50}$$

The condition given in Eq. (2.38) tells us that

$$\phi_0^{q-p} = \left(\frac{p-2}{q-2}\right)\frac{c_p}{c_q}\Lambda^{q-p}. \tag{2.51}$$

The volume of the resultant Q-ball is given by

$$V = \frac{1}{2\Lambda^2 m_\phi}\left(\frac{q-2}{p-2}\frac{c_q}{c_p}\right)^{2/(q-p)}\left[1 - c_p\left(\frac{p-2}{q-2}\frac{c_p}{c_q}\right)^{(p-2)/(q-p)}\left(\frac{q-p}{q-2}\right)\frac{\Lambda^2}{m_\phi^2}\right]^{-1/2} \tag{2.52}$$

and the rest mass is

$$m_Q = Qm_\phi\left[1 - c_p\left(\frac{p-2}{q-2}\frac{c_p}{c_q}\right)^{(p-2)/(q-p)}\left(\frac{q-p}{q-2}\right)\frac{\Lambda^2}{m_\phi^2}\right]^{1/2}. \tag{2.53}$$

This is less than Qm_ϕ for all $q, p \in \mathbb{R}$ such that $q > p > 2$, and so the resultant Q-balls are classically stable against decay into Q quanta of the field Φ.[4]

2.3.2 Surface-Dominated Thin-Wall Q-balls

Notice, there is a special case in Eq. (2.53). If

$$c_p\left(\frac{p-2}{q-2}\frac{c_p}{c_q}\right)^{(p-2)/(q-p)}\left(\frac{q-p}{q-2}\right)\frac{\Lambda^2}{m_\phi^2} = 1, \tag{2.54}$$

the energy apparently vanishes, and the volume diverges. This is the case where the potential has two minima such that $U(\phi) = 0$, and so the vacuum of the theory is degenerate. This theory can still produce Q-balls, but the core does not contribute to the overall mass of the Q-ball. The surface, however, still does. This is the example of thin-wall Q-balls that are surface energy dominated, as studied in Ref. [130]. We summarise this here.

We note that the energy of a Q-ball configuration may be written

$$E = \frac{Q^2}{16\pi\int \mathrm{d}r\, r^2\phi^2} + 4\pi\int \mathrm{d}r\, r^2\left[\left(\frac{\mathrm{d}\phi}{\mathrm{d}r}\right)^2 + U(\phi)\right]. \tag{2.55}$$

[4]In Coleman's original paper, given in Ref. [31], a stronger statement was proven in that if the potential satisfies some technical conditions, then stable Q-balls that minimise the energy exist, i.e., that the infimum of the energy (rest mass) are at a given charge are Q-balls that satisfy: $m_Q < m_\phi Q$. Here, we have just shown that the energy of the objects derived satisfy the condition given, and not that this is associated to the infimum of the energies of all objects with this charge. Thus, what we give here is not a statement of stability in the mathematical sense, but is sufficient for our purposes in physics.

We define ϕ_0 as the location in field space of the minimum of $U(\phi)$ degenerate with $U(0) = 0$. We define, implicitly, the radius of the Q-ball through

$$\frac{4\pi}{3} R^3 \phi_0^2 = 4\pi \int \mathrm{d}r\, r^2 \phi^2, \tag{2.56}$$

thus allowing us to write the energy of the configuration as

$$E = \frac{3Q^2}{16\pi R^3 \phi_0^2} + 4\pi \int \mathrm{d}r\, r^2 \left[\left(\frac{\mathrm{d}\phi}{\mathrm{d}r} \right)^2 + U(\phi) \right]. \tag{2.57}$$

The integral in this expression will only contribute over the surface. It is impossible to solve, but we can approximate our ignorance by considering the average quantities over the surface. We define the thickness of the surface as δ, and introduce two dimensionless parameters, α and β, such that

$$\left(\frac{\mathrm{d}\phi}{\mathrm{d}r} \right)^2 \sim \alpha \left(\frac{\phi_0}{\delta} \right)^2 \quad \text{and} \quad U(\phi) \sim \beta m_\phi^2 \phi_0^2. \tag{2.58}$$

The energy is thus

$$E = \frac{3Q^2}{16\pi R^3 \phi_0^2} + \left(4\pi R^2 \delta\right) \left[\alpha \left(\frac{\phi_0}{\delta} \right)^2 + \beta m_\phi^2 \phi_0^2 \right]. \tag{2.59}$$

This is expression must be separately minimised with respect to δ and R. This gives us that

$$\delta = \frac{1}{m_\phi} \sqrt{\frac{\alpha}{\beta}} \quad \text{and} \quad R = \left(\frac{9Q^2}{256\pi^2} \frac{1}{\phi_0^4} \frac{1}{m_\phi (\alpha\beta)^{1/2}} \right)^{1/5}. \tag{2.60}$$

From this, we can calculate two quantities of interest. Firstly, the ratio of the wall thickness to the radius is

$$\frac{\delta}{R} \sim \left(\frac{256\pi^2}{9} \frac{\alpha^3}{\beta^2} \right)^{1/5} \left(\frac{\phi_0}{m_\phi} \right)^{4/5} \frac{1}{Q^{2/5}}. \tag{2.61}$$

We see that the limit $\delta \ll R$, i.e., the thin-wall limit, corresponds to the large Q limit.[5] The mass of the resultant Q-ball is

$$m_Q = 5 \left(\frac{\pi}{6} \right)^{1/5} (\alpha\beta)^{3/10} \phi_0^{2/5} m_\phi^{3/5} Q^{4/5}. \tag{2.62}$$

The energy here scales differently compared to the standard thin-wall limit, when the rest mass is dominated by the volume. We thus see that this class of Q-balls is not composed of Q-matter.

[5]This is not strictly true. We could have that $\phi_0 \ll m_\phi$, but this corresponds to a very specific potential shape, and so is not a generic statement.

Finally, we note that

$$\frac{m_Q}{m_\phi Q} \propto \left(\frac{\delta}{R}\right)^{1/2}. \tag{2.63}$$

In the thin-wall limit, therefore, these Q-balls are classically stable against decay into the constituent scalar particles. It should be noted that these results generalise to the case where we have almost degenerate minima in $U(\phi)$, such that the contribution of the volume to the rest mass of the thin-wall Q-balls is dominated by the surface effects.

2.4 Thick-Wall Q-balls

We found in the previous section that for large Q, Q-balls are well-described by the thin-wall limit. In this section, we review the opposite limit, i.e., Q-balls for small Q, otherwise known as thick-wall Q-balls.

2.4.1 The Bounce Potential

We now seek other analytic Q-ball solutions. To find these, it is illuminating to take a step back and analyse the form of the bounce potential and subsequent solutions to the bounce equation for different values of ω – see Fig. 2.1 for examples. The forthcoming discussion is based on that given in Ref. [89].

When viewed from the point of view of a Euclidean bounce, the bounce action describes the tunnelling of a field from a metastable vacuum to one of greater (or equal) stability. This tunnelling process can only occur if there exists two minima in the bounce potential, such that the minimum for $\phi > 0$ satisfies $U(\phi) \leq U(0)$, and if there is a potential barrier separating both minima from each other.

At the conclusion of this tunnelling process, the field will exit the barrier with a value ϕ_{exit} that is the smallest non-zero solution of

$$U(\phi_{\text{exit}}) = U(0) = 0. \tag{2.64}$$

In the language of Q-balls, this value of the field denotes the characteristic VEV of the field inside the Q-ball. The further away from $\phi = 0$ the exit point of the bounce potential lies, the larger the values in field space the Q-ball probes.

The bounce potential is of the form

$$U_\omega(\phi) = U(\phi) - \omega^2\phi^2. \tag{2.65}$$

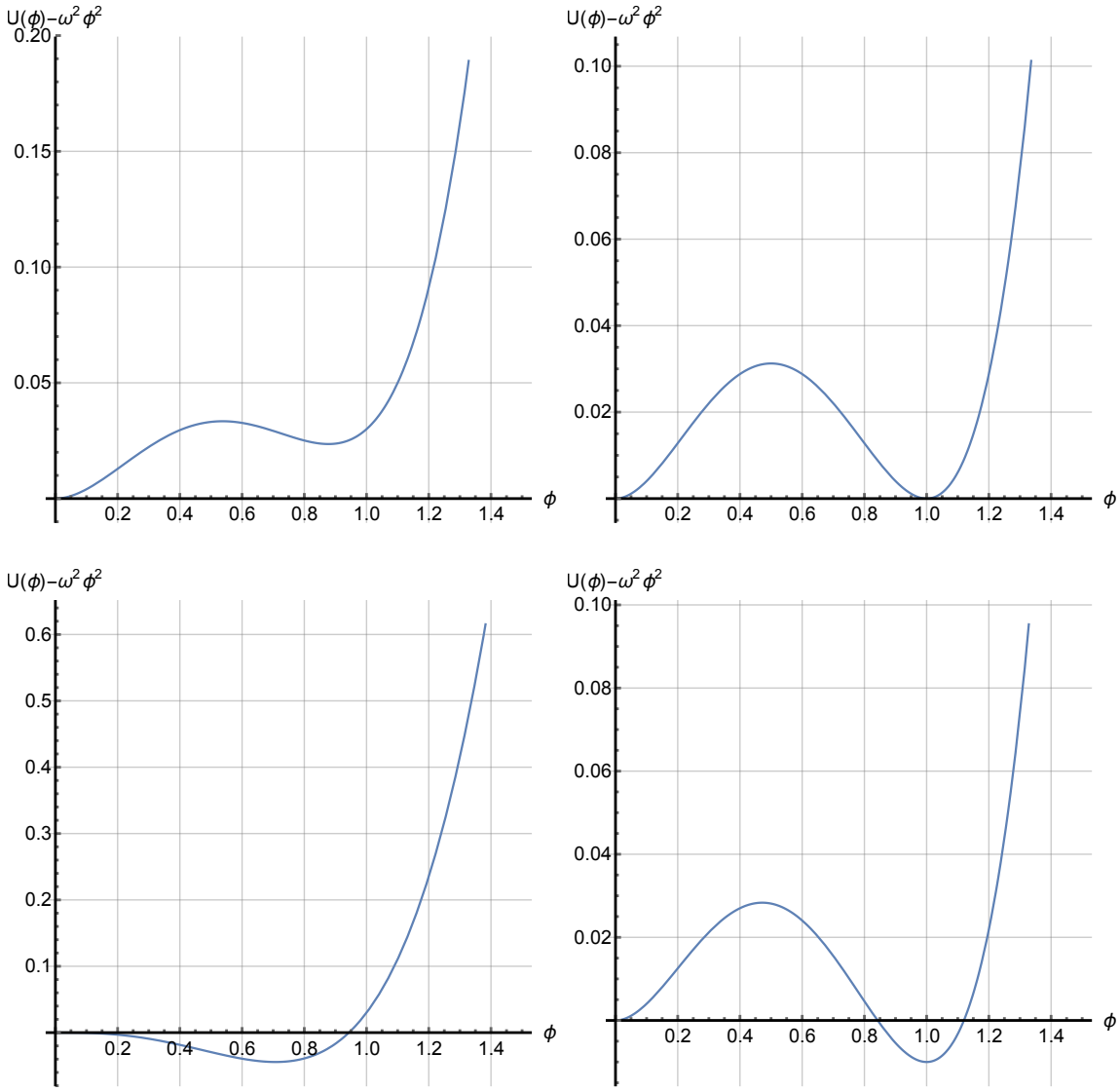

Figure 2.1: Examples of the bounce potential for different values of ω. Here, we consider the potential $U(\phi) = m^2\phi^2 - A\phi^p + \lambda\phi^q$, where $q > p > 2$. Clockwise from the top left: (i) the case $\omega < \omega_0$ – the second minimum of the bounce potential, away from $\phi = 0$, is not more stable than the origin, and so no tunnelling occurs; (ii) the thin-wall case $\omega = \omega_0$ – the two minimum are equally stable; (iii) the thick-wall case $\omega_0 < \omega < m_\phi$ – the second minimum of the bounce potential, away from $\phi = 0$, is more stable than the origin, and tunnelling occurs to $\phi = \phi_{\text{exit}}$; (iv) the case $\omega \geq m_\phi$ – there exists no barrier in the bounce potential, and so no tunnelling occurs.

As stated above, it is key for the existence of Q-ball solutions that $U(\phi)$ contain terms to form a second minimum in the bounce potential, and to stabilise the potential at large field value. There also necessarily must be a barrier in this potential. At quadratic order in the bounce potential, only the mass term and the term proportional to ω^2 appear. If this term is overall negative – i.e., if $m \leq \omega$ – then there exists no potential barrier between the origin and the rest of field space. Therefore, the barrier in this function only exists if, at quadratic order in the bounce potential,

$$m^2\phi^2 - \omega^2\phi^2 > 0, \tag{2.66}$$

or if $\omega < m_\phi$. To reiterate, if $\omega \geq m_\phi$, we have no barrier in the bounce potential, and thus no Q-ball solution. Similarly, there is no exit point for the tunnelling trajectory if

$$U(\phi) - \omega^2\phi^2 > 0, \tag{2.67}$$

for all values of $\phi > 0$, i.e., if

$$\omega^2 < \frac{U(\phi)}{\phi^2}. \tag{2.68}$$

Thus, we see that in order to have solutions to the bounce equation valid for Q-balls, we require that, for some ϕ,

$$\frac{U(\phi)}{\phi^2} \leq \omega < m_\phi. \tag{2.69}$$

Notice, the limiting case in the lower bound is precisely the thin-wall limit discussed in the previous section. This occurs when the bounce potential has degenerate minima, such that the exit point after the barrier occurs at the minimum away from zero field.

We now consider the other limiting case of this bound on ω, namely $\omega \to m_\phi^-$, first studied in Ref. [89]. As ω tends to this bound from below, the barrier in the bounce potential becomes smaller such that the exit point post-barrier is at relatively small field value. Thus, this limit is equivalent to the limit of small field excursion – as it is mathematically the opposite limit to the thin-wall approximation, and surface effects are taken into account, the resulting Q-balls are often referred to as "thick-wall" Q-balls.[6]

[6]One might wonder what happens when we remove the barrier by setting $\omega = m_\phi$. This is equivalent to setting $Q = 0$, i.e., no stable Q-ball exists. In this limit, the Q-balls completely dissolve into their respective quanta. In practice, one wouldn't even use a Q-ball description when very close to this limit – when the charge of the Q-ball is small, the quantum fluctuations are such that a semi-classical description is no longer appropriate, and a quantum mechanical description of the quanta and their interactions would be more so.

2.4.2 Q-balls in the Small-Field Limit

As we are working in the small-field limit, we approximate the bounce potential by an expansion in its lowest order terms, i.e., those that are most relevant,

$$U_\omega(\phi) \approx \left(m_\phi^2 - \omega^2\right)\phi^2 - \frac{c_p}{\Lambda^{p-4}}\phi^p + \frac{c_q}{\Lambda^{q-4}}\phi^q, \tag{2.70}$$

where $c_p, c_q > 0$ are constant coefficients, Λ is some mass scale, and $q > p > 2$. The signs in this potential are fixed in order to allow for a Q-ball solution to exist – the negative sign on the second term allows for the second minimum in the bounce potential to exist, and the positive sign on the final term lifts and stabilises the potential. We will ignore the final term for now in our analysis, but will return to it later. For now, we assume that the quadratic and next-to-quadratic terms are of roughly equal importance within the Q-ball, i.e., that the VEV is such that they are approximately equal – this sets the VEV to be precisely the exit point of the bounce potential when all higher order terms are negligible.

Before we proceed, notice that this small-field expansion corresponds exactly to a theory with a potential defined by Eq. (2.50). We found above that this potential generically allows for stable thin-wall Q-balls to exist within its spectrum of states. It is therefore interesting to know whether this potential allows stable Q-balls with a small charge to form. We consider this below.

To find stable Q-ball solutions, we once more study the functional given in Eq. (2.10), i.e.,

$$\mathcal{E}_\omega = \omega Q + \int \mathrm{d}^3x \left[\vec{\nabla}\phi\cdot\vec{\nabla}\phi + (m_\phi^2 - \omega^2)\phi^2 - \frac{c_p}{\Lambda^{p-4}}\phi^p\right]. \tag{2.71}$$

In what follows, we will constrain the value of p that allows for stable Q-balls of this type to exist. The result can be found in the literature in Refs. [115, 119], but we prove it in a novel way – this new proof can be found in Ref. [101]. In what follows, we prove this result in $3+1$-dimensions. Defining the dimensionless variables,

$$\varphi \equiv \left[\frac{c_p}{\Lambda^{p-4}}\right]^{1/(p-2)} \frac{\phi}{(m_\phi^2 - \omega^2)^{1/(p-2)}} \quad \text{and} \quad \xi_i \equiv (m_\phi^2 - \omega^2)^{1/2} x_i, \tag{2.72}$$

leads to

$$\mathcal{E}_\omega = \omega Q + (m_\phi^2 - \omega^2)^{(6-p)/(2p-4)} \left[\frac{\Lambda^{p-4}}{c_p}\right]^{2/(p-2)} S_\varphi, \tag{2.73}$$

where S_φ is the dimensionless integral

$$S_\varphi = \int \mathrm{d}^3\xi \left[\vec{\nabla}_\xi\varphi\cdot\vec{\nabla}_\xi\varphi + \varphi^2 - \varphi^p\right], \tag{2.74}$$

whose precise value will not concern us here – for numerical values of this integral for different values of p, see Ref. [104], with the general trend being that the value is positive and increases for increasing p. It should be noted that for $p \geq 6$, this cannot be extremised and so the thick-wall limit is not a good approximation [115]. However, we keep p general for now for, as we will see, $p \geq 6$ fails for other reasons. Minimisation with respect to ω yields

$$\epsilon = \Omega \left(1 - \Omega^2\right)^{(10-3p)/(2p-4)}, \tag{2.75}$$

where $\Omega \equiv \omega/m_\phi$ is a dimensionless parameter and

$$\epsilon \equiv \frac{Q m_\phi^{(2p-8)/(p-2)}}{S_\varphi} \left[\frac{p-2}{6-p}\right] \left[\frac{c_p}{\Lambda^{p-4}}\right]^{2/(p-2)} \tag{2.76}$$

is a dimensionless number. In principle, this expression can give Ω in terms of ϵ. Notice, since $\Omega < 1$, we must have that $\epsilon > 0$ in order for a valid solution to exist. Thus, for $p > 6$, we must have that $S_\varphi < 0$ to maintain this sign assignment. However, this would seem to contravene the general trend of Ref. [104] for which $S_\varphi > 0$ – it should be noted, however, that the case for $p = 6$ has not been determined. We, thus, will simply ignore $p > 6$ here, though it will turn out to not matter below. Recognise also that we have implicitly assumed that $p \neq 6$ – in this case, the Q-balls would need to have zero charge and thus cannot exist.

Instead of solving this for Ω in terms of ϵ, we reinsert the expression into $\mathcal{E}_\omega$ to give

$$\mathcal{E}_\omega = mQ \left[\Omega + \left[\frac{p-2}{6-p}\right] \frac{(1-\Omega^2)}{\Omega}\right]. \tag{2.77}$$

For stable Q-balls to exist, we necessarily require that this expression be less than $m_\phi Q$, or that

$$\Omega + \left[\frac{p-2}{6-p}\right] \frac{(1-\Omega^2)}{\Omega} < 1, \tag{2.78}$$

which can be rewritten as

$$\frac{2(4-p)}{6-p}\Omega^2 - \Omega + \frac{p-2}{6-p} < 0. \tag{2.79}$$

Notice already that $p = 4$ implies that $\Omega > 1$, which is in contradiction with our starting assumption that $\Omega < 1$. Assume now that $p \neq 4$ such that our requirement is given by

$$(\Omega - 1)\left(\Omega - \frac{p-2}{2(4-p)}\right) < 0. \tag{2.80}$$

We thus see that this is only satisfied if Ω lies between the two roots of the equation. However, recognise that if $p > 10/3$, the second root is greater than unity, and so Ω lies outside of its assumed range, with the limiting case of $p = 10/3$ leading to $\Omega = 1$, which is also forbidden. We conclude that stable Q-balls may only be formed in potentials where $2 < p < 10/3$, and so the only integer p that allows for thick-wall Q-balls is $p = 3$, i.e., the case of study in Ref. [89].

2.4.3 A Worked Example: $p = 3$

Setting $p = 3$, we see that our expressions above become

$$\mathcal{E}_\omega = \Omega m_\phi Q + \frac{m_\phi^3 S_\varphi}{A^2}(1-\Omega^2)^{3/2}, \tag{2.81}$$

where we have defined $A = c_p \Lambda$, and S_φ is numerically minimised to be approximately 38.8 [104]. A first derivative of $\mathcal{E}_\omega$, and requiring it vanish for an extremum, yields the condition

$$\epsilon = \Omega(1-\Omega^2)^{1/2}, \tag{2.82}$$

where

$$\epsilon \equiv \frac{QA^2}{3S_\varphi m_\phi^2}. \tag{2.83}$$

We may solve this equation to give

$$\Omega^2 = \frac{1 \pm \sqrt{1-4\epsilon^2}}{2}. \tag{2.84}$$

As Ω is constrained to be real, we require that $\epsilon \leq 1/2$. A second derivative of $\mathcal{E}_\omega$, and requiring that it be positive for a minimum, yields the condition

$$-3S_\varphi m_\phi \frac{1-2\Omega^2}{(1-\Omega^2)^{1/2}} > 0, \tag{2.85}$$

which sets the sign in the solution for Ω^2 to be positive, and also that $\epsilon < 1/2$.

Given Ω, we may now expand $\mathcal{E}_\omega$ in powers of ϵ to give the mass of the Q-ball,

$$m_Q = m_\phi Q \left(1 - \frac{1}{6}\epsilon^2 - \mathcal{O}\left(\epsilon^4\right)\right). \tag{2.86}$$

As expected, we see that $m_Q < m_\phi Q$, and so the resulting Q-ball is indeed stable to decay to quanta of the field Φ. To determine the characteristic radius, R, and VEV of the field, $\langle\phi\rangle$, we note that these are given when $\xi \sim 1$ and $\varphi \sim 1$, and so

$$R^{-1} \sim \epsilon m_\phi \left(1 + \mathcal{O}\left(\epsilon^2\right)\right) \quad \text{and} \quad \langle\phi\rangle \sim \frac{\epsilon^2 m_\phi^2}{A}\left(1 + \mathcal{O}\left(\epsilon^2\right)\right). \tag{2.87}$$

We thus see that this Q-balls are large compared to the Compton wavelength of the constituent scalars, and that the field inside the Q-ball is indeed small in some sense.

This analysis rested on two assumptions, namely, that the higher order term that stabilises the potential be small in comparison to the cubic and quadratic terms inside the Q-ball, and that $\mathcal{E}_\omega$ has a minimum in the range $0 < \omega < m_\phi$. These conditions lead to constraints on the allowed charge of the thick-wall Q-ball solution. Using the characteristic VEV given above, we demand that

$$A\langle\phi\rangle^3 \gg \frac{c_q}{\Lambda^{q-4}}\langle\phi\rangle^q, \tag{2.88}$$

which leads to the constraint on Q,

$$Q \ll 116.4 m_\phi \left[\frac{\Lambda^{q-4}A^{10-3q}}{c_q}\right]^{1/(2q-6)}. \tag{2.89}$$

Demanding this for the quadratic term leads to the same constraint. The second condition on Q arises from rearranging the condition $\epsilon < 1/2$,

$$Q < 58.2\frac{m_\phi^2}{A^2}. \tag{2.90}$$

The fact that these constraints place an upper bound on the charge of these Q-balls shows us that this is the appropriate description for Q-balls with small charge. If both of these conditions are strongly violated, then the thin-wall approximation should be used.

There is no classical lower bound on the charge, but this is a semi-classical object: for the description to be appropriate, quantum effects cannot be large. The fractional fluctuation of the field ϕ will go like $1/\sqrt{N}$, where N is the number of ϕ quanta within a volume λ^3. Here, λ represents how extended the wavefunctions of the ϕ quanta are within the Q-ball, with a maximum size being that of the Q-ball itself. When this number, N, is much greater than unity, the quantum fluctuations remain small in some sense. For $N \gtrsim 10$, this should be fine – the choice is predominantly down to taste.

2.5 Summary

In this chapter, we have reviewed the so-called "canonical" Q-ball analysis, that is, we have derived the physical properties of thin- and thick-wall Q-balls in theories of a single, complex scalar field, invariant under a group of $U(1)$ symmetries whose

potential is a function of powers of the field. In the thick-wall case, by arguing that the minimal energy solution be classically stable against decay into the individual quanta of the field, we constrained the theories that possess a thick-wall limit to those whose small-field expansion is given by

$$U(\Phi^*, \Phi) \approx m^2 \Phi^* \Phi - \frac{c_p}{\Lambda^{p-4}} \left(\Phi^* \Phi\right)^{p/2}, \tag{2.91}$$

where $2 < p < 10/3$ and $c_p, \Lambda > 0$.

This analysis shows that for theories in which $p > 10/3$, that possess a thin-wall limit, there is a minimum amount of charge that must aggregate before the resulting Q-ball is classically stable. The value of this minimum charge in general theories is a topic for future research. This has further important phenomenological consequences in the scenario that real-world Q-balls are formed via solitosynthesis, i.e., through fusion of the underlying quanta in the early universe. In this case, the timescale of formation must be much less than the timescale of dissolution. Whether these theories can produce Q-balls in this scenario is a topic for future research.

We use this analysis as the basis of the work presented in the rest of this thesis. Each chapter will bring a different modification to the canonical analysis, namely: theories with non-canonical kinetic terms; multiple fields, both charged and uncharged; multiple independent symmetries; and Q-balls expanded in the background of another field.

Chapter 3

Q-balls in Theories with Non-Canonical Kinetic Terms

3.1 Introduction

In the last chapter, we considered the Q-ball solutions arising in theories with canonical kinetic terms and potentials containing only terms that are powers of the complex scalar field. Though this covers a multitude of theories, it is not the general case. Theories, particularly effective field theories such as chiral perturbation theory, can have more complex structures that couple the field to its derivatives.[1]

In this chapter, we seek to perform the same analysis as before – for theories of a single, complex scalar field invariant under the group of $U(1)$ transformations – but with terms that couple the field to its derivative. We will consider terms with two derivatives only – one could extend the analysis to even higher derivatives. The addition of these non-canonical kinetic terms fundamentally changes the dependence of the resulting expressions on the Lagrange multiplier, ω, and so warrants study. Work has been performed before on examples of such theories, primarily in chiral perturbation theory, but this is done in an ad-hoc manner [18, 19, 44]. We seek, at least in the single-field case, to study this class of theory in general.

Specifically, in Section 3.2 we introduce the class of model of study. We begin the minimisation procedure as in the previous chapter. We note here that the spatial profile obeys a differential equation that differs from a bounce. However, the offending terms are subleading in the thin- and thick-wall limits and so we progress as usual. In Section 3.3, we perform the thin-wall analysis, deriving the differential equation

[1] It should be noted that chiral perturbation theory is a *multi-field* theory with non-canonical kinetic terms, and so this analysis does not strictly cover that model. We return to this issue in Chapters 7 and 8.

governing the VEV of the scalar field inside the Q-ball as well as the resultant physical parameters of the Q-ball. In Section 3.4, we perform the thick-wall analysis, noting that if all terms containing a derivative are subleading to those without, we recover the analysis in the previous chapter. We determine the subclass of theories that admit a thick-wall state by demanding that the minimum of energy be classically stable against decay into the quanta of the field.

The work contained within this chapter is original and can be found in Ref. [101].[2]

3.2 Minimising the Energy in a Sector of Fixed Charge

We consider a theory modified from the one of the previous chapter. We now incorporate a coupling between the field and its derivative,

$$\mathcal{L} = \left(1 + f(\Phi^*, \Phi)\right) \partial_\mu \Phi^* \partial^\mu \Phi - U(\Phi^*, \Phi). \tag{3.1}$$

The function $U(\Phi^*, \Phi)$ is once more a potential, and $f(\Phi^*, \Phi)$ is a function that denotes the coupling between the field and its derivative. Note, as f modifies the time derivative – the kinetic energy – terms in the Lagrangian density, this furnishes a non-canonical kinetic term. We leave both of these functions generic for the time being, demanding only that both be functions of the fields only, and not their derivatives, and that, for simplicity, they vanish for vanishing field.[3] The Euler-Lagrange equation for this theory is given by

$$(1 + f)\partial_\mu \partial^\mu \Phi + \left(\partial_\mu \Phi \partial^\mu \Phi\right) \frac{\partial f}{\partial \Phi} + \frac{\partial U}{\partial \Phi^*} = 0, \tag{3.2}$$

with an analogous equation governing the behaviour of Φ^*.

We require that this theory be invariant under some $U(1)$ symmetry, in the same way as in Eq. (2.4). We once more set the charges of the quanta of the field Φ to be unity. The Noether current density associated to the $U(1)$ symmetry in this theory is then

$$j^\mu = i(1 + f)\left(\Phi \partial^\mu \Phi^* - \Phi^* \partial^\mu \Phi\right). \tag{3.3}$$

[2]After this thesis was submitted to the examiners, Ref. [106] appeared which also studied these non-canonical Q-balls in the thin-wall limit in an inflationary scenario. The corresponding expressions between both works completely agree.

[3]Generally, f would tend to some constant as $\phi \to 0$. However, with field redefinitions, we can make sure that the coefficient of the kinetic term is still unity in this limit. We thus assume, for simplicity, that this has already been done.

This symmetry also fixes the potential and coupling function to be functions of the product of the fields,

$$U(\Phi^*, \Phi) = U(\Phi^*\Phi) \quad \text{and} \quad f(\Phi^*, \Phi) = f(\Phi^*\Phi). \tag{3.4}$$

The Hamiltonian for this theory is given by

$$H = \int \mathrm{d}^3x \left[(1+f) \left(\dot{\Phi}^* \dot{\Phi} + \vec{\nabla}\Phi^* \cdot \vec{\nabla}\Phi \right) + U(\Phi^*\Phi) \right]. \tag{3.5}$$

We seek Q-ball solutions, which are the configurations of the field that minimise the energy for a fixed charge. We once more introduce a Lagrange multiplier, ω, to fix the charge of the configuration, and analyse the functional

$$\mathcal{E}_\omega = \omega Q + \int \mathrm{d}^3x \left[(1+f) \left(\left| \dot{\Phi} - i\omega\Phi \right|^2 - \omega^2 \Phi^*\Phi + \vec{\nabla}\Phi^* \cdot \vec{\nabla}\Phi \right) + U(\Phi^*\Phi) \right]. \tag{3.6}$$

We note that, for this theory to not contain tachyons or negative probability states, the function f cannot change the sign on the kinetic terms. We thus demand that $f > -1$. We see that, as in the canonical case, the term that contains explicit time-dependence is positive semi-definite and is minimised if

$$\Phi(\vec{x}, t) = e^{i\omega t}\phi(\vec{x}), \tag{3.7}$$

where $\phi(\vec{x})$ is some real-valued function of the spatial coordinates. Recall, in the last chapter, we showed that the Euler-Lagrange equation governing $\phi(\vec{x})$ was a bounce equation. However, in this case, the Euler-Lagrange equation in this theory is now

$$(1+f)\nabla^2\phi + \frac{1}{2}\frac{\mathrm{d}f}{\mathrm{d}\phi}(\vec{\nabla}\phi \cdot \vec{\nabla}\phi) = \frac{1}{2}\frac{\mathrm{d}}{\mathrm{d}\phi}\left(U - \omega^2(1+f)\phi^2\right). \tag{3.8}$$

This equation is not in the form of a bounce equation, and so we cannot state that, in general, the lowest energy configuration of the field is spherically symmetric. However, consider the offending terms

$$f\,\nabla^2\phi \quad \text{and} \quad \frac{1}{2}\frac{\mathrm{d}f}{\mathrm{d}\phi}(\vec{\nabla}\phi \cdot \vec{\nabla}\phi). \tag{3.9}$$

We note that the function $f(\phi)$ must be dimensionless, and thus must be suppressed by some mass scale. Furthermore, these terms will be subleading to all other terms in the regime where ϕ is slowly varying. Recall, the thin-wall limit is characterised by a core of constant field; the thick-wall limit describes small Q-balls in which the "wall" is a large component of their size. We thus posit that we can treat this equation as

a bounce equation in these limits and solve it with the boundary conditions given in Eq. (2.15) to give the properties of a spherically symmetric solution. Of course, in the thick-wall case in particular, it will need to be checked that this assumption holds *a posteriori* in any specific theory. Since we will be speaking in general terms, we will forthwith assume that this holds – when we study a particular theory with non-canonical kinetic terms in Chapter 8, we will check this assumption.

The structure of the bounce potential is analogous to that of Eq. (2.65), and so our analysis in Sec. 2.4.1 holds. Specifically, the bounce potential in the thin- and thick-wall limits is given by

$$U_\omega(\phi) = U - \omega^2(1+f)\phi^2. \tag{3.10}$$

We earlier stated, for simplicity, that $f \to 0$ when $\phi \to 0$, and so the bounce potential vanishes at zero field. We find, therefore, that we still seek Q-ball solutions in the range $\omega_0 \lesssim \omega < m_\phi$, where the thin-wall case is given by $\omega = \omega_0$ and the thick-wall case corresponds to $\omega \to m_\phi^-$.

3.3 The Thin-Wall Limit

We assume once more that the Q-ball rest mass is dominated by a spherical, homogeneous core of volume V. The value of the field inside the core is given by ϕ_0. We thus find that

$$\mathcal{E}_\omega \approx \omega Q + V\left[-\left(1+f(\phi_0)\right)\omega_0^2\phi_0^2 + U(\phi_0)\right]. \tag{3.11}$$

This function must be minimised with respect to the Lagrange multiplier, volume and field such that the resulting rest mass be less than Qm_ϕ to ensure classical stability against decay to quanta of the field. Minimisation with respect to ω_0 yields

$$Q = 2\left(1+f(\phi_0)\right)\omega_0\phi_0^2 V, \tag{3.12}$$

as expected from Eq. (3.3). Eliminating ω_0 and subsequently minimising with respect to the volume yields

$$V^2 = \frac{Q^2}{4\left(1+f(\phi_0)\right)\phi_0^2 U(\phi_0)}. \tag{3.13}$$

Reinserting this expression finally gives us an expression for the rest mass,

$$m_Q = Q\sqrt{\frac{U(\phi_0)}{\left(1+f(\phi_0)\right)\phi_0^2}}. \tag{3.14}$$

Notice that this expression is expected from the structure of the bounce potential given in Eq. (3.8) since, for thin-wall Q-balls, $m_Q = Q\omega_0$. Furthermore, we see that $f(\phi_0) > -1$ is a necessary condition for the existence of these Q-balls. However, this was also a necessary condition for our theory, and so this is automatically satisfied.

To determine the value of the field inside the Q-ball, we minimise the rest mass with respect to the field to give

$$\big(1 + f(\phi_0)\big)\,\frac{\mathrm{d}U(\phi_0)}{\mathrm{d}\phi_0} = 2\frac{U(\phi_0)}{\phi_0}\,\big(1 + f(\phi_0)\big) + U(\phi_0)\frac{\mathrm{d}f(\phi_0)}{\mathrm{d}\phi_0}. \tag{3.15}$$

This constrains the forms of $f(\phi_0)$ and $U(\phi_0)$.

Consider the following example. Let $U(\phi_0) = m_\phi^2\phi_0^2$. This is a potential that clearly does not allow Q-ball solutions in the canonical case given in Chapter 2. However, in the case presented here, Q-ball solutions exist for a $\phi_0 \neq 0$ if

$$\frac{\mathrm{d}f(\phi_0)}{\mathrm{d}\phi_0} = 0. \tag{3.16}$$

The rest mass of these Q-balls are then given by

$$m_Q = Qm_\phi\frac{1}{\sqrt{1 + f(\phi_0)}}, \tag{3.17}$$

which is less than Qm_ϕ if $f(\phi_0) > 0$. We thus see that terms coupling the field to its derivatives can allow for Q-ball solutions to exist even when the potential without these couplings does not.

3.4 The Thick-Wall Limit

As discussed in Chapter 2, the properties of thick-wall Q-balls are determined in the small field-limit. The bounce potential in this scenario contains two separate functions of ϕ,

$$U_\omega(\phi) = U(\phi) - \big(1 + f(\phi)\big)\,\omega^2\phi^2 \tag{3.18}$$

Expanding each function to its lowest order term after the quadratic gives

$$U_\omega(\phi) \approx \left(m_\phi^2\phi^2 - \frac{c_p}{\Lambda^{p-4}}\phi^p\right) - \left(1 + \frac{c_q}{\Lambda^q}\phi^q\right)\omega^2\phi^2, \tag{3.19}$$

where $c_p, c_q \in \mathbb{R}$, $p > 2$ and $q > 0$ and Λ is some mass scale. As ever, we assume that there is some higher order term that stabilises the potential at large ϕ. There exists three regimes we can study:

- Case One: $p < q+2$, and so the term coming from the function $f(\phi)$ is irrelevant in the small field limit. The appropriate analysis is that found in the canonical case in Chapter 2, provided that $c_p > 0$, otherwise no thick-wall Q-balls can exist in this potential.

- Case Two: $p > q + 2$, and so the term coming from the potential $U(\phi)$ is irrelevant in the small field limit. It is plausible that Q-balls can exist provided that $c_q > 0$; if $c_q < 0$, then the bounce potential doesn't contain a barrier, and thus no Q-ball solution exists.

- Case Three: $p = q + 2$, and so both terms are of the same order in ϕ. However, this is only the case if
$$\frac{c_p}{c_p} \sim \left(\frac{\omega}{\Lambda}\right)^2 \sim \left(\frac{m_\phi}{\Lambda}\right)^2, \tag{3.20}$$
where we have used the fact the $\omega \to m_\phi^-$ in the thick-wall limit in the final approximation. If this is not true, then either Case One or Case Two is a more appropriate description for any resulting objects. Stable Q-balls are a possibility if
$$c_p\Lambda^2 + c_q\omega^2 > 0, \tag{3.21}$$
as otherwise no barrier exists in the bounce potential. Since, in the thick-wall limit, $\omega \to m_\phi^-$, we can rewrite this inequality as
$$c_p\Lambda^2 + c_q m_\phi^2 > 0, \tag{3.22}$$
where the signs of c_p and c_q are not set, apart from the fact that they cannot both be negative.

We study both Case Two and Case Three below, noting that Case Three is equivalent to Case Two in the limit $c_p \to 0$ and $c_q > 0$. The bounce potential is thus given by
$$U_\Omega(\phi) \approx m_\phi^2(1-\Omega^2)\phi^2 - \frac{m_\phi^2}{\Lambda^{p-2}}\left(\lambda + c_q\Omega^2\right)\phi^p, \tag{3.23}$$
where, for notational convenience, we have defined $\Omega \equiv \omega/m_\phi$ and $\lambda \equiv c_p\Lambda^2/m_\phi^2$. The functional we wish to study for thick-wall Q-balls is then
$$\mathcal{E}_\omega = m_\phi Q\Omega + \int \mathrm{d}^3x \left[\vec{\nabla}\phi\cdot\vec{\nabla}\phi + m_\phi^2(1-\Omega^2)\phi^2 - \frac{m_\phi^2}{\Lambda^{p-2}}\left(\lambda + c_q\Omega^2\right)\phi^p\right]. \tag{3.24}$$

We may render the integral dimensionless by introducing the dimensionless variables

$$\varphi = \left[\frac{\lambda + c_q\Omega^2}{1-\Omega^2}\right]^{1/(p-2)} \frac{\phi}{\Lambda} \quad \text{and} \quad \xi_i = m_\phi (1-\Omega^2)^{1/2} x_i, \tag{3.25}$$

such that

$$\mathcal{E}_\omega = m_\phi Q\Omega + \frac{\Lambda^2}{m_\phi} \frac{(1-\Omega^2)^{(6-p)/(2p-4)}}{\left(\lambda + c_q\Omega^2\right)^{2/(p-2)}} S_\varphi, \tag{3.26}$$

where

$$S_\varphi = \int \mathrm{d}^3\xi \left[\vec{\nabla}_\xi\varphi \cdot \vec{\nabla}_\xi\varphi + \varphi^2 - \varphi^p\right] \tag{3.27}$$

is a dimensionless integral, whose precise value is irrelevant for the current discussion – this integral has been calculated for some values of p in Ref. [104], and, for those calculated, been found to be positive and increasing in value for increasing p.

Minimisation of this expression with respect to Ω yields the condition

$$\epsilon = \Omega \frac{(1-\Omega^2)^{(10-3p)/(2p-4)}}{\left(\lambda + c_q\Omega^2\right)^{p/(p-2)}} \left(c_q + \frac{6-p}{4}\lambda - c_q\frac{p-2}{4}\Omega^2\right), \tag{3.28}$$

where

$$\epsilon \equiv \frac{p-2}{4}\frac{Q}{S_\varphi}\frac{m_\phi^2}{\Lambda^2}. \tag{3.29}$$

Note, as $p > 2$, we see that $\epsilon > 0$. In Eq. (3.28), the term in brackets could plausibly be negative for certain values of p. For now, we take this term to be positive and return to this point later. We cannot solve this expression for Ω as a function of ϵ for any $p > 2$. However, we can find values of p that plausibly lead to Q-balls.

Reinserting this expression into Eq. (3.26) yields

$$\mathcal{E}_\omega = m_\phi Q \left[\Omega + \frac{p-2}{4}\frac{1}{\Omega}\frac{(1-\Omega^2)\left(\lambda + c_q\Omega^2\right)}{c_q + \frac{6-p}{4}\lambda - c_q\frac{p-2}{4}\Omega^2}\right]. \tag{3.30}$$

In order for Q-balls to form that are classically stable against decay into the quanta of the scalar field, we require the term in brackets to be less than unity. This translates into the condition

$$(1-\Omega)\left[c_q\left(\frac{p-2}{2}\right)\Omega^3 + c_q\left(\frac{p-2}{4}\right)\Omega^2 + \Omega\left(\frac{p-4}{2}\lambda - c_q\right) + \frac{p-2}{4}\lambda\right] < 0. \tag{3.31}$$

The first term in brackets is always positive for $0 < \Omega < 1$. The term in square brackets is a cubic polynomial in Ω whose shape is defined by the parameters c_q, λ and $p > 2$.

Notice, for $\Omega = 0$, the final term is only negative if $\lambda < 0$. However, this is perfectly allowed for all λ and c_q – the true lower bound on Ω is Ω_0, as found in the thin-wall case. In order to constrain p, we thus only need to show that this expression is negative for $\Omega \to 1^-$, as this is the vicinity in which thick-wall Q-ball solutions lie. The constraint then reduces to

$$\left(\lambda + c_q\right)\left(\frac{3p-10}{4}\right) < 0. \tag{3.32}$$

By the assumption given in Eq. (3.22), the first term in brackets is always positive. So we are left with the requirement $2 < p < 10/3$, which is exactly the same as in the case for theories that do not couple the field to its derivative. Notice, for Case Two, where $\lambda \to 0$ and $c_q > 0$, we have the exact same condition arising.

Focussing now on the case $p = 3$, our minimisation condition given in Eq. (3.28) becomes

$$\epsilon = \Omega \frac{(1-\Omega^2)^{1/2}}{\left(\lambda + c_q\Omega^2\right)^3}\left(c_q + \frac{3}{4}\lambda - \frac{c_q}{4}\Omega^2\right), \tag{3.33}$$

where

$$\epsilon = \frac{1}{4}\frac{Q}{S_\varphi}\frac{m_\phi^2}{\Lambda^2}. \tag{3.34}$$

Recall above that we required that the term in the bracket be positive in order for this condition to be valid. We may rewrite this condition as

$$c_q(4-\Omega^2) + 3\lambda > 0 \tag{3.35}$$

If both $c_q > 0$ and $\lambda > 0$, this is certainly true. For $c_q = -|c_q| < 0$ and $\lambda > 0$, we find that

$$\Omega^2 > 4\left(1 - \frac{3}{4}\frac{\lambda}{|c_q|}\right). \tag{3.36}$$

Note, if $\lambda \to 0$, this condition fails, as we would expect in this scenario. We require that $\lambda > |c_q|$ by Eq. (3.22) in this case. However, this is not enough to make the right-hand side negative, such that this condition would hold generically. Thus, this is a condition on these theories and sets a lower bound on Ω. However, from the analysis above, we noted that $\Omega > \Omega_0$, where Ω_0 is found from the thin-wall analysis, and so this condition is only relevant if

$$4\left(1 - \frac{3}{4}\frac{\lambda}{|c_q|}\right) > \Omega_0^2. \tag{3.37}$$

For $\lambda = -|\lambda| < 0$ and $c_q > 0$, we find that

$$\Omega^2 < 4\left(1 - \frac{3}{4}\frac{|\lambda|}{c_q}\right). \tag{3.38}$$

Note, if $c_q \to 0$, this condition fails, as we would expect in this scenario. We know that $\Omega < 1$. The right-hand side of this condition is greater than unity if $c_q > |\lambda|$. However, this is required by Eq. (3.22), and so this condition holds generically in this case.

Though the function given in Eq. (3.33) is unbound in the range $0 < \Omega < 1$, it is bound in the range $\Omega_0 < \Omega < 1$, where Ω_0 is found from considering the thin-wall limit. When $\Omega = 1$, $\epsilon = 0$ and thus $Q = 0$, i.e., no Q-ball forms, which is expected. The upper bound on ϵ is found when $\Omega = \Omega_0$, though one would expect a thick-wall description to break down before that bound is reached. Denoting the upper bound in ϵ to be ϵ_0, we can conservatively state that this description is valid for

$$Q \ll 155.2\left(\frac{\Lambda}{m_\phi}\right)^2 \epsilon_0, \tag{3.39}$$

where we have used that $S_\varphi \approx 38.8$ for the case $q + 2 = 3$ [104]. It should be noted that this upper bound is model-dependent.

3.5 Summary

In this chapter, we have studied a class of theory with terms coupling the field to its derivative – specifically those that couple the field to two derivatives of said field – for Q-ball solutions. We have determined the physical properties of the Q-balls in the thin-wall limit. By demanding that the minimum of the energy be energetically stable against decay to the quanta of the field, we determine the subclass of theories possessing Q-balls in the thick-wall limit. It is interesting that, despite the difference in functional form with respect to ω, the bounce potential still has the same requirements with regards to allowed terms that lead to stable thick-wall Q-balls. To reiterate, for a theory of a single, complex scalar field, thick-wall Q-balls can only exist if the bounce potential, in the limit of small field, has the form

$$U_\omega(\phi) = (m_\phi^2 - \omega^2)\phi^2 - \left(c_p\Lambda^2 + c_q\omega^2\right)\frac{\phi^p}{\Lambda^{p-2}}, \tag{3.40}$$

where $2 < p < 10/3$, and $c_p, c_q \in \mathbb{R}$ and $c_p\Lambda^2 + c_q\omega^2 > 0$. If both c_p and c_q are negative semi-definite, Q-balls cannot form in the low Q limit. This has ramifications for production mechanisms in real-world scenarios, particularly for solitosynthesis.

We have only studied a subclass of single-field theories that possess terms coupling the field to its derivative. It would be interesting to repeat the above analysis for theories that couple the field to a higher number of derivatives. At least in the thick-wall case, it would reduce to our analysis given in this chapter if the terms with two derivatives are present in the theory, since terms with higher derivatives will likely be further suppressed by some higher mass scale.

Part II

Multi-Field Q-balls

Chapter 4

Canonical Q-balls in the Multi-Field Case

4.1 Introduction

In the previous part of this thesis, we studied theories containing only a single, complex scalar. We now consider theories containing a multitude of scalar fields. Specifically, in this chapter we study the case of multiple scalar fields, both real and complex, under one stabilising symmetry – this is the multi-field version of the canonical case. We perform a similar analysis as in both previous chapters – we seek the physical properties of the thin-wall case, and constrain the theories that allow a stable thick-wall limit.

In Section 4.2, we perform the minimisation procedure appropriate for the multi-field case. In Section 4.3, we unify the works of Ref. [90] and Ref. [57], which considered thin-wall Q-balls of multiple charged scalars, and one charged scalar with a real scalar, respectively, into one framework. Note, real scalars do not carry charge. However, a Q-ball may contain uncharged fields if the overall mass-to-charge ratio of the configuration is less than that of the individual quanta of the charged scalar. In this section, we determine the differential equations that govern the VEV of the complex and real scalars within the resulting thin-wall Q-balls, together with their physical properties of mass and volume. In Section 4.4, we analyse the thick-wall limit in the approximation scheme that the fields all have the same spatial profile up to a positive normalisation – this is a necessity to make analytic progress. In reality, the spatial profiles of the fields might differ, but this extra freedom in the minimisation process can only further lower the Q-ball energy. Thus, any constraints found under this approximation scheme are sufficient to show the existence of thick-wall Q-balls, but are not strictly necessary, as in the previous chapters. With this in mind, we show the

existence of thick-wall Q-balls in a class of theories by demanding that the minimum be energetically stable against classical decay into the quanta of the charged scalar fields. We fully solve a special case – one complex scalar with an arbitrary number of massless (or very light) scalars. Work with this assumption on the spatial profiles has been done in an ad-hoc manner in Refs. [18, 119].

This chapter is largely a review of existing literature, albeit presented slightly differently. However, much of Section 4.4, aside from the assumption on the spatial profile of the fields, is original. The work on theories containing a single charged scalar and an arbitrary number of uncharged scalars can be found in Ref. [100], with the rest of the original work of this chapter remaining unpublished.

4.2 Minimising the Energy in a Sector of Fixed Charge

We consider a theory of N complex scalars, $\Phi_i(\vec{x}, t)$, and M real scalars, $\Psi_j(\vec{x}, t)$. The Lagrangian density we consider is

$$\mathcal{L} = \sum_i^N \partial_\mu \Phi_i \partial^\mu \Phi_i^* + \frac{1}{2} \sum_j^M \partial_\mu \Psi_j \partial^\mu \Psi_j - U(\Phi_i, \Phi_i^*, \Psi_j), \tag{4.1}$$

where $U(\Phi_i, \Phi_i^*, \Psi_j)$ is some potential that we leave generic for now, stipulating only that it be a function of the fields, and not their derivatives, and that it vanish for vanishing field. The Euler-Lagrange equations for this theory are

$$\partial_\mu \partial^\mu \Phi_i + \frac{\partial U}{\partial \Phi_i^*} = 0 \quad \text{and} \quad \partial_\mu \partial^\mu \Psi_j + \frac{\partial U}{\partial \Psi_j} = 0, \tag{4.2}$$

with a similar equation governing the dynamics of Φ_i^*.

We demand that the theory be invariant with respect to a single global $U(1)$ group of transformations defined through

$$\Phi_i \to e^{iq_i\alpha} \Phi_i \quad \text{and} \quad \Psi_j \to \Psi_j, \tag{4.3}$$

where $\alpha \in \mathbb{R}$ and the charges of the individual complex scalars are given by q_i, with the real scalars uncharged. Associated to this symmetry is a Noether current density given by

$$j^\mu = i \sum_i^N q_i \left(\Phi_i \partial^\mu \Phi_i^* - \Phi_i^* \partial^\mu \Phi_i \right). \tag{4.4}$$

This symmetry doesn't place any further functional constraints on the potential as in the single-field case, beyond demanding that it be invariant overall. The case that

the potential be a function of the absolute value of the complex fields is only true when we have one complex scalar and an arbitrary number of real scalars.

A Q-ball is the state in a theory which minimises the energy for a fixed, non-zero Noether charge. The Hamiltonian for this theory is

$$H = \int \mathrm{d}^3x \left[\sum_i^N \left(\dot{\Phi}_i \dot{\Phi}_i^* + \vec{\nabla}\Phi_i \cdot \vec{\nabla}\Phi_i^* \right) + \frac{1}{2} \sum_j^M (\dot{\Psi}_j \dot{\Psi}_j + \vec{\nabla}\Psi_j \cdot \vec{\nabla}\Psi_j) + U(\Phi_i, \Phi_i^*, \Psi_j) \right]. \tag{4.5}$$

To determine if this system admits Q-ball solutions, we introduce a Lagrange multiplier ω, as in Ref. [90], that enforces charge conservation upon minimisation with respect to it:

$$\mathcal{E}_\omega = H + \omega \left(Q - \int \mathrm{d}^3x j^0 \right), \tag{4.6}$$

where j^0 is the zeroth component of the Noether current density given in Eq. (4.4). Thus, the functional we wish to analyse is given by

$$\mathcal{E}_\omega = \omega Q + \int \mathrm{d}^3x \left[\sum_i^N \left(\dot{\Phi}_i \dot{\Phi}_i^* - i q_i \omega \dot{\Phi}_i^* \Phi_i + i q_i \omega \Phi_i^* \dot{\Phi}_i + \vec{\nabla}\Phi_i \cdot \vec{\nabla}\Phi_i^* \right) + \frac{1}{2} \sum_j^M (\dot{\Psi}_j \dot{\Psi}_j + \vec{\nabla}\Psi_j \cdot \vec{\nabla}\Psi_j) + U(\Phi_i, \Phi_i^*, \Psi_j) \right]. \tag{4.7}$$

We may complete the square on the first term to give

$$\mathcal{E}_\omega = \omega Q + \int \mathrm{d}^3x \left[\sum_i^N \left(\left| \dot{\Phi}_i - i q_i \omega \Phi_i \right|^2 - \omega^2 q_i^2 \Phi_i^* \Phi_i + \vec{\nabla}\Phi_i \cdot \vec{\nabla}\Phi_i^* \right) + \frac{1}{2} \sum_j^M (\dot{\Psi}_j \dot{\Psi}_j + \vec{\nabla}\Psi_j \cdot \vec{\nabla}\Psi_j) + U(\Phi_i, \Phi_i^*, \Psi_j) \right]. \tag{4.8}$$

The terms containing derivatives with respect to time are the only terms with explicit time dependence. These are positive semi-definite and are minimised if they vanish. Thus, we require that

$$\Phi_i(\vec{x}, t) = e^{i q_i \omega t} \phi_i(\vec{x}) \quad \text{and} \quad \Psi_j(\vec{x}, t) = \psi_j(\vec{x}), \tag{4.9}$$

where $\phi_i(\vec{x})$ and $\psi_j(\vec{x})$ are functions purely of the spatial coordinate which we take, without loss of generality, to be real-valued. The energy functional is then

$$\mathcal{E}_\omega = \omega Q + \int \mathrm{d}^3x \left[\sum_i^N \left(\vec{\nabla}\phi_i \cdot \vec{\nabla}\phi_i - \omega^2 q_i^2 \phi_i^2 \right) + \frac{1}{2} \sum_j^M (\vec{\nabla}\psi_j \cdot \vec{\nabla}\psi_j) + U(\phi_i, \psi_j) \right]. \tag{4.10}$$

Notice that spatial profiles for the fields ϕ_i that vanish everywhere lead to a configuration of zero charge. Thus, a configuration of non-zero charge must have spatial profiles for the charged fields that differs from zero in some finite domain – this is not the case for the uncharged fields, which can be vanishing inside a multi-field Q-ball. The spatial profiles satisfy the equations

$$\nabla^2\phi_i = \frac{1}{2}\frac{\partial}{\partial\phi_i}\left(U(\phi_i,\psi_j) - \omega^2 q_i^2\phi_i^2\right), \quad \nabla^2\psi_j = \frac{\partial U(\phi_i,\psi_j)}{\partial\psi_j}. \tag{4.11}$$

These differential equations take the form of a bounce equation [22, 30, 32], with bounce potentials defined by $U(\phi_i, \psi_i) - \omega^2 q_i^2 \phi_i^2$ and $U(\phi_i, \psi_i)$, respectively. The lowest energy configurations are known to be spherically symmetric [32], under the boundary conditions of the field vanishing at spatial infinity, and being constant at the coordinate origin, and the first derivative vanishing at spatial infinity and the coordinate origin.

These highly-coupled differential equations cannot in general be solved analytically. However, under certain assumptions, analytic progress can be made.

4.3 Thin-Wall Q-balls

The thin-wall limit for multi-field Q-balls was first considered in Ref. [90] for the case of multiple charged scalars and in Ref. [57] for the case of one complex scalar and one real scalar. In this limit, the properties of the Q-ball are well-approximated by the properties of a spherical core of homogeneous Q-matter. We have that

$$\mathcal{E}_\omega \approx \omega Q + V\left[U(\phi_i,\psi_j) - \omega^2 \sum_i^N q_i^2\phi_i^2\right], \tag{4.12}$$

where V is the volume of the spherical core of the Q-ball. Minimisation with respect to the Lagrange multiplier yields

$$Q = 2\omega V \sum_i^N q_i^2\phi_i^2, \tag{4.13}$$

as we would expect from the Noether current density given in Eq. (4.4). Eliminating ω from $\mathcal{E}_\omega$ yields

$$E = \frac{Q^2}{4V}\left[\sum_i^N q_i^2\phi_i^2\right]^{-1} + U(\phi_i,\psi_j)V. \tag{4.14}$$

Minimising with respect to the volume gives us

$$V^2 = \frac{Q^2}{4U(\phi_i,\psi_j)}\left[\sum_i^N q_i^2\phi_i^2\right]^{-1}, \tag{4.15}$$

which, when eliminated, finally gives us an expression for the rest mass of a multi-field Q-ball:

$$m_Q = Q\sqrt{U(\phi_i,\psi_j)\left[\sum_i^N q_i^2\phi_i^2\right]^{-1}}. \tag{4.16}$$

This expression must be minimised such that the resulting Q-ball is stable against decay to the quanta of any of the fields ϕ_i, i.e., that

$$\frac{m_Q}{Q} < \frac{m_i}{q_i} \tag{4.17}$$

where m_i is the mass of the quanta of the field ϕ_i. This condition must be separately satisfied for each field. The minimisation procedure with respect to the field content leads to the conditions on the potentials that

$$\frac{\partial U(\phi_i,\psi_j)}{\partial\phi_k} = 2q_k^2\phi_k\left[\sum_i^N q_i^2\phi_i^2\right]^{-1}U(\phi_i,\psi_j) \quad \text{and} \quad \frac{\partial U(\phi_i,\psi_j)}{\partial\psi_k} = 0. \tag{4.18}$$

A straightforward example of a potential that allows for multi-field Q-balls is the following:

$$U(\Phi^*,\Phi,\Psi) = m^2\Phi^*\Phi - A\Psi\Phi^*\Phi + \lambda(\Phi^*\Phi)^2 + \lambda'\Psi^4, \tag{4.19}$$

where Φ is a massive, charged field (with charge set to unity) and Ψ is a massless, uncharged field. The coefficients, m^2, A, λ, λ', are all taken positive, such that the sign assignment of each term is explicit. The Q-ball ansatz, given in Eq. (4.9), means that we can rewrite this as

$$U(\phi,\psi) = m^2\phi^2 - A\psi\phi^2 + \lambda\phi^4 + \lambda'\psi^4. \tag{4.20}$$

The thin-wall conditions above yield the field values

$$\phi = \frac{1}{4}\frac{A}{(\lambda^3\lambda')^{1/4}} \quad \text{and} \quad \psi = \frac{1}{4}\frac{A}{(\lambda\lambda')^{1/2}}. \tag{4.21}$$

The resulting Q-ball has a mass given by

$$m_Q = Q\sqrt{m^2 - \frac{1}{8}\frac{A^2}{(\lambda\lambda')^{1/2}}}, \tag{4.22}$$

which is clearly smaller than Q amounts of the mass of the charged scalar, m. Thus, this theory allows for stable, multi-field Q-balls. As in the single-field case, there is special point where

$$\frac{1}{8}\frac{A^2}{(\lambda\lambda')^{1/2}} = m^2. \tag{4.23}$$

As before, the core of the thin-wall Q-ball does not contribute to the overall mass of the object – it will all come from the wall.

4.4 Thick-Wall Q-balls

We now analyse multi-field Q-balls in the thick-wall limit. In order to analytically progress further, we must make an assumption about the spatial profile of the fields. Armed with this, we can begin to constrain the theory space to those which plausibly allow Q-balls to exist.

4.4.1 The Spatial Profile Problem

Though the small-field limit offers up the simplification that only the next-to-quadratic order in the potential is relevant, this is not enough to make analytic progress. The complication is purely due to the number of fields.

In Refs. [18, 119], this was circumvented by assuming that all spatial profiles of the fields were the same up to a positive semi-definite normalisation constant for each field, with the resulting expressions minimised with respect to these normalisation constants.[1] The purpose of this ansatz is to provide sufficient conditions for the existence of thick-wall Q-balls in a class of multi-field theories, as well as to provide approximate values for the Q-ball properties. In reality, the spatial profiles of the fields might differ, but this extra freedom in the minimisation process can only further lower the Q-ball energy. To provide necessary conditions for a thick-wall limit, we must pursue a dedicated numerical analysis of the true spatial profiles of all individual fields, and this is the topic of future work. This would also allow us to see how accurate the analytic Q-ball properties are. Moreover, given that we have effectively

[1] In some sense, this is borrowing from the thin-wall analysis, whereby the field profiles are ignored apart from their homogeneous core values which differ only by a positive normalisation constant.

reduced our multi-field system into one of a single-field, we expect to find results similar to those in Section 2.4.

In the previous section, we found that thin-wall Q-balls were stable if $\omega < m_i/q_i$ for all species of complex scalar. In the set of these ratios, $\{m_i/q_i\}$, there is a minimum value. We let this minimum value be associated to the field ϕ_1, and it is this field that we take to be the reference field. By our assumption, we may write

$$\phi_i = \alpha_i \phi_1, \quad \psi_j = \beta_j \phi_1, \tag{4.24}$$

where $\alpha_1 = 1$, by definition. The equations governing the spatial profiles are now given by

$$\alpha_i \nabla^2 \phi_1 = \frac{1}{2}\frac{\partial U}{\partial \phi_i} - \omega^2 q_i^2 \alpha_i \phi_1, \quad \beta_j \nabla^2 \phi_1 = \frac{\partial U}{\partial \psi_j}. \tag{4.25}$$

Whether or not these equations are satisfied in general, and what it means for the properties of the Q-ball calculated, is the subject of future work. Nevertheless, we progress.

4.4.2 The Thick-Wall Analysis

The full bounce potential can now be written as

$$U_\omega(\phi_1, \alpha_i, \beta_j) \approx \left[\sum_i^N \left(m_i^2 - q_i^2\omega^2\right)\alpha_i^2 + \frac{1}{2}\sum_j^M m_j^2 \beta_j^2\right]\phi_1^2 - g(\alpha_i, \beta_j)\phi^p. \tag{4.26}$$

The coefficient of the quadratic term is clearly positive for $\omega < m_i/q_i$. The function $g(\alpha_i, \beta_j)$ is model-dependent and so is left general for now, but it is assumed that it is positive definite, as otherwise there would be no Q-ball solution. The energy in Eq. (4.10) is then

$$\begin{aligned}\mathcal{E}_\omega = \omega Q + \int \mathrm{d}^3x \Bigg[&\left(\sum_i^N \alpha_i^2 + \frac{1}{2}\sum_j^M \beta_j^2\right)\vec{\nabla}\phi_1 \cdot \vec{\nabla}\phi_1 \\ &+ \left[\sum_i^N \left(m_i^2 - q_i^2\omega^2\right)\alpha_i^2 + \frac{1}{2}\sum_j^M m_j^2\beta_j^2\right]\phi_1^2 - g(\alpha_i, \beta_j)\phi_1^p\Bigg].\end{aligned} \tag{4.27}$$

Consider the substitutions

$$\xi_i = \left(\frac{\sum_i^N \left(m_i^2 - q_i^2 \omega^2 \right) \alpha_i^2 + \frac{1}{2} \sum_j^M m_j^2 \beta_j^2}{\sum_i^N \alpha_i^2 + \frac{1}{2} \sum_j^M \beta_j^2} \right)^{1/2} x_i,$$
$$\varphi = \left(\frac{g(\alpha_i, \beta_j)}{\sum_i^N \left(m_i^2 - q_i^2 \omega^2 \right) \alpha_i^2 + \frac{1}{2} \sum_j^M m_j^2 \beta_j^2} \right)^{1/(p-2)} \phi_1. \tag{4.28}$$

Then,

$$\mathcal{E}_\omega = \omega Q + \frac{\left(\sum_i^N \alpha_i^2 + \frac{1}{2} \sum_j^M \beta_j^2 \right)^{3/2} \left[\sum_i^N \left(m_i^2 - q_i^2 \omega^2 \right) \alpha_i^2 + \frac{1}{2} \sum_j^M m_j^2 \beta_j^2 \right]^{(6-p)/(2p-4)}}{g(\alpha_i, \beta_j)^{2/(p-2)}} S_\varphi, \tag{4.29}$$

where S_φ is a dimensionless integral given by

$$S_\varphi = \int \mathrm{d}^3 \xi \left[\vec{\nabla}_\xi \varphi \cdot \vec{\nabla}_\xi \varphi + \varphi^2 - \varphi^p \right]. \tag{4.30}$$

For different values of p, this has been numerically minimised in Ref. [104], with the general trend being that S_φ increases for increasing p. Our expression for the energy must be minimised with respect to α_i, β_j and ω. To proceed further, we must specify the theory and therefore $g(\alpha_i, \beta_j)$. However, we can restrict the types of theories that could plausibly lead to stable thick-wall Q-balls.

Consider the first derivative with respect to ω. Requiring that this vanishes leads to the condition

$$\epsilon = \Omega \left[\sum_i^N \left(\mu_i^2 - q_i^2 \Omega^2 \right) \alpha_i^2 + \frac{1}{2} \sum_j^M \beta_j^2 \mu_j^2 \right]^{(10-3p)/(2p-4)}, \tag{4.31}$$

where we have assumed that $p \neq 6$, since this leads to a Q-ball with vanishing charge, and

$$\epsilon \equiv \frac{Q}{S_\varphi} \left[\frac{p-2}{6-p} \right] \frac{g(\alpha_i, \beta_j)^{2/(p-2)}}{\left[\sum_i^N \alpha_i^2 + \frac{1}{2} \sum_j^M \beta_j^2 \right]^{3/2} \left[\sum_i^N q_i^2 \alpha_i^2 \right]} \left(\frac{m_1}{q_1} \right)^{(2p-8)/(p-2)}, \tag{4.32}$$

and we define the dimensionless parameters,

$$\mu_i \equiv \frac{q_1}{m_1} m_i \quad \text{and} \quad \Omega \equiv \frac{q_1}{m_1} \omega, \tag{4.33}$$

and similarly for the masses of the real scalars, which are denoted by the index j. Note, $0 < \Omega < 1$, as $\omega < m_1/q_1$, by definition. Also, notice that is $p > 6$ then $\epsilon < 0$. However, ϵ is strictly positive and so this cannot be true. Thus, $p < 6$.[2] From this condition, we can rewrite $\mathcal{E}_\omega$ as

$$\mathcal{E}_\omega = Q\frac{m_1}{q_1}\left[\Omega + \frac{1}{\Omega}\left(\frac{p-2}{6-p}\right)\left(\kappa - \Omega^2\right)\right], \tag{4.34}$$

where

$$\kappa = \frac{\sum_i^N \mu_i^2\alpha_i^2 + \frac{1}{2}\sum_j^M \beta_j^2\mu_j^2}{\sum_i^N q_i^2\alpha_i^2}. \tag{4.35}$$

Note, $\kappa > 0$ and is related to the mass to charge ratio of the configuration. We will find that its size denotes regimes for which we can constrain the theories with a thick-wall limit. We can see that in the single-field limit, $\kappa = 1$, and so we would expect this value to have a similar condition as found in previous chapters. This will be the limiting value that splits parameter space.

For stable Q-balls to form, we require that $\mathcal{E}_\omega < Qm_1/q_1$. Thus,

$$\Omega + \frac{1}{\Omega}\left(\frac{p-2}{6-p}\right)\left(\kappa - \Omega^2\right) < 1, \tag{4.36}$$

which can be rewritten as

$$\frac{2(4-p)}{6-p}\Omega^2 - \Omega + \frac{p-2}{6-p}\kappa < 0. \tag{4.37}$$

Notice, if $\Omega \to 0$, this condition is violated for $2 < p < 6$ and $\kappa > 0$. However, since $\omega_0 < \omega < m_1/q_1$, this is acceptable. Notice, if $\kappa = 1$ this reduces to

$$(\Omega - 1)\left(\frac{2(4-p)}{6-p}\Omega - \frac{p-2}{6-p}\right) < 0, \tag{4.38}$$

which is precisely the condition for single-field Q-balls, i.e., that $0 < p < 10/3$. As stated above, the single-field case is an example of a theory for which $\kappa = 1$, and so this was expected. We must therefore now consider theories for which $\kappa \neq 1$.

For $\kappa \neq 1$ and $\Omega \to 1^-$, the condition given in Eq. (4.37) must be satisfied. Considering $\Omega = 1$, this leads to

$$\frac{p-2}{6-p}(\kappa - 1) < 0. \tag{4.39}$$

[2]It was shown in Ref. [115] that, at least in the single-field case, that Q-balls cannot exist in theories that $p \geq 6$ as S_φ cannot be extremised, so this is consistent.

We thus see that for any $\kappa < 1$, we have classical stability for all $Q > 0$ when $2 < p < 6$. This is therefore a model-dependent condition that depends on the minimisation with respect to α_i and β_j.

We now consider the case of $\kappa > 1$. Our requirement is broken at both $\Omega \to 0$ and $\Omega \to 1$. As such, if any stable Q-balls were to form, there would be a minimum charge required to reach stability. In order to determine if this can be the case, we require that both the roots of the quadratic given in Eq. (4.37) lie in the range $0 < \Omega < 1$. The roots of this polynomial are

$$\Omega_{\pm} = \frac{6-p}{4(4-p)} \pm \frac{6-p}{4(4-p)} \sqrt{1 - 8\frac{(4-p)(p-2)}{(6-p)^2}\kappa}. \tag{4.40}$$

For $\Omega \in (0,1)$, it is a necessary requirement that the first term on the right-hand side be in the range $(0,1)$, which leads to the condition

$$2 < p < 10/3. \tag{4.41}$$

Requiring that the roots exist at all – the term under the square root be positive – leads to a κ-dependent condition for p,

$$1 - 8\frac{(4-p)(p-2)}{(6-p)^2}\kappa > 0. \tag{4.42}$$

The function on the left-hand side is a monotonically decreasing function of κ if $2 < p < 10/3$. Taking, therefore, the limit $\kappa \to \infty$ shows us that both roots always exist. Furthermore, the larger κ is, the smaller the difference between the roots, and so the smaller the range of values which allow for a stable Q-ball.

To understand these requirements, consider a theory with a single complex scalar and an arbitrary number of real scalars. We find that

$$\kappa = 1 + \frac{1}{2}\sum_{j}^{M} \beta_j^2 \frac{m_j^2}{m_1^2} \geq 1, \tag{4.43}$$

with equality only coming when either $m_j = 0$ or $\beta_j = 0$. Thus, we cannot form a stable Q-ball for all $Q > 0$ unless the j-th species is either massless (or very light) or $\beta_j = 0$ for the species. We study a theory of this type ($\kappa = 1$) in Chapter 8 – which was also the subject of Ref. [18] – whereby one real scalar is taken to be effectively massless, and the other has $\beta = 0$.

In the case that $\kappa > 1$, we find that we have a lower bound on the charge of these Q-balls for them to be stable. This makes sense here – the real scalars increase the mass

of the Q-ball without increasing the charge of the Q-ball. Classical stability requires that the mass to charge ratio of the Q-balls be less than that of the constituent scalars. Thus, in the presence of real scalars, the Q-ball must accumulate enough charge to offset this increase in mass. This is therefore the origin of the requirements given above: as κ gets larger, more charge must be accumulated.

4.4.3 A Worked Example: Arbitrary Number of Massless Real Scalars

As stated above, the minimisation with respect to the α_i and β_j is model-dependent and cannot be completed in general. As an example that can be fully worked out analytically, consider a simple theory of one complex scalar Φ with unit charge and M massless scalars Ψ_j defined through the Lagrangian

$$\begin{aligned}\mathcal{L} = \partial_\mu \Phi \partial^\mu \Phi^* + \frac{1}{2}\sum_j^M \partial_\mu \Psi_j \partial^\mu \Psi_j \\ - \left(m^2 - \sum_j^M A_j \Psi_j\right) \Phi^* \Phi - \mathcal{O}\left(\Psi^4, (\Phi^*\Phi)^2, \Phi^*\Phi\Psi^2\right).\end{aligned} \tag{4.44}$$

Notice, we have taken the leading order interaction between the real and complex scalars to be cubic[3] – this is because we are in the regime where $\kappa = 1$, and so $2 < p < 10/3$. We seek stable thick-wall Q-balls, and assume that all spatial profiles are, up to some positive semi-definite normalisation, the same. The functional in Eq. (4.29) is then given by

$$\mathcal{E}_\omega = \Omega m Q + m^3 \frac{\left(1 + \frac{1}{2}\sum_j^M \beta_j^2\right)^{3/2}\left(1-\Omega^2\right)^{3/2}}{\left(\sum_j^M A_j \beta_j\right)^2} S_\varphi, \tag{4.45}$$

where $S_\varphi \approx 38.8$ after numerical minimisation [104]. This expression must be minimised with respect to all β_j and Ω. First, we minimise with respect to all β_j. This process leads to the condition

$$\frac{3}{4}\beta_k = A_k \frac{\left(1 + \frac{1}{2}\sum_j^M \beta_j^2\right)}{\left(\sum_j^M A_j \beta_j\right)}. \tag{4.46}$$

[3]Note, we could have also written down a term cubic in only the real scalars as it is not forbidden by the $U(1)$ symmetry. This class of term will only render the Q-ball more unstable as it will increase the energy (rest mass) of the configuration without increasing the charge. We omit this for simplicity here, but it is important to note.

If the k-th species of real scalar does not have a coupling to the complex scalar that is cubic in the fields, it does not contribute to the Q-ball.[4] Taking A_k to therefore be non-vanishing, we find

$$\frac{\beta_k}{A_k} = \frac{4}{3}\frac{\left(1+\frac{1}{2}\sum_j^M \beta_j^2\right)}{\left(\sum_j^M A_j\beta_j\right)}. \tag{4.47}$$

This expression holds for each species of real scalar, but the right-hand side is a constant for each species, and so we can we can then relate all species through

$$\frac{\beta_k}{A_k} = \frac{\beta_l}{A_l}. \tag{4.48}$$

We can use this to eliminate all but a single β from the above condition since

$$\sum_j^M \beta_j^2 = \left(\frac{\beta_l}{A_l}\right)^2 \sum_j^M A_j^2 \quad \text{and} \quad \sum_j^M A_j\beta_j = \frac{\beta_l}{A_l}\sum_j^M A_j^2. \tag{4.49}$$

We then find that

$$\beta_l = \frac{2A_l}{\left(\sum_j^M A_j^2\right)^{1/2}}. \tag{4.50}$$

Minimisation with respect to Ω yields

$$\epsilon = \Omega(1-\Omega^2)^{1/2}, \tag{4.51}$$

where

$$\epsilon = \frac{4Q}{3^{5/2}S_\varphi m^2}\sum_j^M A_j^2, \tag{4.52}$$

where we have eliminated all the β_i by invoking the above condition. Notice, this has the same functional form as the single-field case given in Section 2.4. Thus, we may simply read off the solution that

$$\Omega^2 = \frac{1+\sqrt{1-4\epsilon^2}}{2}, \tag{4.53}$$

where $\epsilon < 1/2$. Given this, we may now expand $\mathcal{E}_\omega$ in powers of ϵ to give the mass of the Q-ball,

$$m_Q = m_\phi Q\left(1-\frac{1}{6}\epsilon^2 - \mathcal{O}\left(\epsilon^4\right)\right). \tag{4.54}$$

[4]If a real scalar has a coupling to the complex scalar that is greater than cubic in the fields, it should contribute. However, this contribution to the properties of the Q-ball would be subleading to those calculated from only considering from the cubic coupling.

We see that $m_Q < m_\phi Q$, and so the resulting Q-ball is indeed classically stable against decay to quanta of the field Φ. The characteristic radius, R, and VEV of the field, $\langle\phi\rangle$, are given when $\xi \sim 1$ and $\varphi \sim 1$, and so

$$R^{-1} \sim \frac{\epsilon m_\phi}{\sqrt{3}} \left(1 + \mathcal{O}\left(\epsilon^2\right)\right) \quad \text{and} \quad \langle\phi\rangle \sim \frac{\epsilon^2 m_\phi^2}{2\left(\sum_j^M A_j^2\right)^{1/2}} \left(1 + \mathcal{O}\left(\epsilon^2\right)\right). \tag{4.55}$$

We thus see that these Q-balls are large compared to the Compton wavelength of the constituent complex scalars, and that the field inside the Q-ball is indeed small in some sense.

This analysis rested on two assumptions, namely, that the higher order term that stabilises the potential be small in comparison to the cubic and quadratic terms inside the Q-ball, and that $\mathcal{E}_\omega$ has a minimum in the range $0 < \omega < m_\phi$. These conditions lead to constraints on the allowed charge of the thick-wall Q-ball solution. Assuming that this stabilising term comes in at order q (as opposed to the minimal 4 given in the Lagrangian for this theory) and using the characteristic VEV given above, we demand that

$$\left(\sum_j^M A_j \beta_j\right) \langle\phi\rangle^3 \gg \frac{c_q}{\Lambda^{q-4}} \langle\phi\rangle^q, \tag{4.56}$$

which leads to the constraint on Q,

$$Q \ll 604.8 m_\phi \left[\frac{\Lambda^{q-4}}{c_q}\right]^{1/(2q-6)} \left[2\left(\sum_j^M A_j^2\right)^{1/2}\right]^{(10-3q)/(2q-6)}. \tag{4.57}$$

Demanding this for the quadratic term leads to the same constraint. The second condition on Q arises from rearranging the condition $\epsilon < 1/2$,

$$Q < 151.2 \frac{m_\phi^2}{\sum_j^M A_j^2}. \tag{4.58}$$

Again, as in the single-field case, the upper bounds on the charge of these object imply that these are small Q-balls.

4.5 Summary

In this chapter, we reviewed canonical Q-ball solutions in the multi-field case, with only one stabilising symmetry. We found the physical parameters associated with the thin-wall Q-balls in this class of theory. For the thick-wall limit, we presented

a sufficient constraint for the existence of thick-wall Q-balls by assuming that all spatial profiles of the fields are the same up to a positive semi-definite normalisation constant. To reiterate, a sufficient condition on the existence of stable thick-wall Q-balls is governed by a positive definite parameter κ, defined in Eq. (4.35) – in summary:

- $0 < \kappa < 1$ – then $2 < p < 6$;
- $\kappa \geq 1$ – then $2 < p < 10/3$,

where p denotes the index of the next-to-quadratic term.

The key part of the thick-wall analysis was the assumption that all fields have the same spatial shape. However, as we noted in the main text, this isn't necessarily valid from the point of view of the field equations. It is expected that the additional freedom afforded by the multitude of spatial profiles would allow for a lower energy solution to exist, and this is the fundamental reason for our work to represent sufficient, but not necessary, conditions. This assumption must be checked and verified numerically, with the necessary conditions for a stable thick-wall limit derived – this will be the subject of future work.

Chapter 5

Multi-Charged Q-balls

5.1 Introduction

In all that we have done so far, we have only considered a single stabilising symmetry in our Lagrangian density. As such, the resulting Q-balls have only been labelled by a single charge and the corresponding analysis only involves a single constraint to fix this charge. We now generalise to the case of multiple symmetries and, as such, multiple constraints to be satisfied. This introduces many Lagrange multipliers into the analysis and this extra complexity is worthy of study.

In Section 5.2, we outline the class of theory of study. The most straightforward example is a multi-field theory in which each scalar transforms non-trivially under its own symmetry, and is a singlet under all others – in some sense, this is similar to multiple copies of a single-field theory. The key to this analysis is then the requirement that the potential associated to a single field does not admit Q-ball solutions, and that stability is only achieved due to the couplings between the fields. We then perform the minimisation procedure analogously to the previous chapters. In Section 5.3, we perform the thin-wall analysis. We determine the differential equation governing the value of the VEV of the fields inside the resultant Q-ball. Contrary to each of the previous chapters, we find that this condition is dependent on the total number of each of the quanta that comprise the Q-ball – previously, these equations have been charge-independent. In Section 5.4, we perform the thick-wall analysis, once again making use of the assumption that all fields have the same spatial profile up to a positive semi-definite normalisation constant. Under this assumption, we produce sufficient constraints on the theories that may possess a thick-wall limit. Interestingly, despite the added complexity in the analysis, we again find the same result – that the next-to-quadratic term must have have an index p such that $2 < p < 10/3$. This

result certainly adds to the idea that this scenario is similar to multiple copies of a single field theory.

The work presented in this chapter is original and can be found in Ref. [102].

5.2 Minimising the Energy in a Sector of Fixed Charge

We consider a theory of N complex scalars, $\Phi_i(\vec{x}, t)$. The Lagrangian density describing the theory is given by

$$\mathcal{L} = \sum_i^N \partial_\mu \Phi_i \partial^\mu \Phi_i^* - U(\Phi_i, \Phi_i^*), \tag{5.1}$$

where $U(\Phi_i, \Phi_i^*)$ is some generic potential that is a function of the fields only, and not their derivatives, and vanishes for vanishing field. The Euler-Lagrange equations for this theory are

$$\partial_\mu \partial^\mu \Phi_i + \frac{\partial U}{\partial \Phi_i^*} = 0, \tag{5.2}$$

with a similar equation governing the dynamics of Φ_i^*.

We demand that the theory be invariant under an N-fold global symmetry,

$$U(1)^N = U(1)_1 \times U(1)_2 \times \cdots \times U(1)_N, \tag{5.3}$$

that is, N independent $U(1)$ symmetries. We consider here the special case that each field Φ_i is charged under its own independent $U(1)$ symmetry and is uncharged under all other $U(1)$ symmetries. For each $U(1)$, its corresponding field transforms as

$$\Phi_i \to e^{iq_i\alpha}\Phi_i, \tag{5.4}$$

where $\alpha \in \mathbb{R}$ and q_i is the charge of the i-th species of complex scalar under the i-th $U(1)$ symmetry. Associated to each $U(1)$ symmetry is a Noether current density given by

$$j_i^\mu = iq_i \left(\Phi_i \partial^\mu \Phi_i^* - \Phi_i^* \partial^\mu \Phi_i\right). \tag{5.5}$$

This symmetry places the constraint on the potential that it be a function of the absolute value of the individual fields,

$$U(\Phi_i, \Phi_i^*) = U(\Phi_i^* \Phi_i). \tag{5.6}$$

We further demand that potential does not support Q-balls if all but one of the fields vanish: otherwise, this system reduces to that of the single-field case discussed

in Chapter 2.[1] We thus assume that the field content is the minimal set of fields, greater than a single field, required to support a Q-ball state.

A Q-ball is the state in a theory which minimises the energy per unit charge. The Hamiltonian for this theory is

$$H = \int \mathrm{d}^3x \left[\sum_i^N \left(\dot{\Phi}_i \dot{\Phi}_i^* + \vec{\nabla}\Phi_i \cdot \vec{\nabla}\Phi_i^* \right) + U(\Phi_i, \Phi_i^*) \right]. \tag{5.7}$$

To determine if this system admits Q-ball solutions, we introduce a set of Lagrange multipliers, $\{\omega_k\}$, similar to Ref. [90], that each enforce charge conservation upon minimisation with respect to them:

$$\mathcal{E}_\omega = H + \sum_k^K \omega_k \left(Q_k - \int \mathrm{d}^3x j_k^0 \right), \tag{5.8}$$

where j_k^0 is the zeroth component of the Noether current density associated to the k-th $U(1)$ symmetry given in Eq. (5.5), and Q_k is the total charge associated to the configuration of the field Φ_k. Thus, the functional we wish to analyse is given by

$$\begin{aligned} \mathcal{E}_\omega =& \sum_i^N \omega_i Q_i \\ &+ \int \mathrm{d}^3x \left[\sum_i^N \left(\dot{\Phi}_i \dot{\Phi}_i^* - i\omega_i q_i \left(\Phi_i \dot{\Phi}_i^* - \Phi_i^* \dot{\Phi}_i \right) + \vec{\nabla}\Phi_i \cdot \vec{\nabla}\Phi_i^* \right) + U(\Phi_i, \Phi_i^*) \right]. \end{aligned} \tag{5.9}$$

We may complete the square on the first two terms under the integral to give

$$\begin{aligned} \mathcal{E}_\omega =& \sum_i^N \omega_i Q_i \\ &+ \int \mathrm{d}^3x \left[\sum_i^N \left(\left| \dot{\Phi}_i - i\omega_i q_i \Phi_i \right|^2 + \vec{\nabla}\Phi_i \cdot \vec{\nabla}\Phi_i^* - \omega_i^2 q_i^2 \Phi_i^* \Phi_i \right) + U(\Phi_i, \Phi_i^*) \right]. \end{aligned} \tag{5.10}$$

The terms containing derivatives with respect to time are the only terms with explicit time dependence. These are positive semi-definite and are minimised if they vanish. Thus, we require, for each species of scalar, that

$$\Phi_i(\vec{x}, t) = e^{i\omega_i q_i t} \phi_i(\vec{x}), \tag{5.11}$$

[1] The additional charged fields could in principle pick up expectation values of their own and thus lower the energy of the Q-ball in that way. We discuss the case of a Q-ball in the background of another field in the next chapter.

where $\phi_i(\vec{x})$ are functions purely of the spatial coordinate which we take, without loss of generality, to be real-valued. The energy functional is then

$$\mathcal{E}_\omega = \sum_i^N \omega_i Q_i + \int \mathrm{d}^3x \left[\sum_i^N \left(\vec{\nabla}\phi_i \cdot \vec{\nabla}\phi_i - \omega_i^2 q_i^2 \phi_i^2 \right) + U(\phi_i) \right]. \tag{5.12}$$

Notice that spatial profiles for the ϕ_i that vanish everywhere lead to a configuration of zero charge. Thus, a configuration of non-zero charge must have spatial profiles for the charged fields that differs from zero in some finite domain. The spatial profiles satisfy the equations

$$\nabla^2 \phi_i = \frac{1}{2} \frac{\partial}{\partial \phi_i} \left(U(\phi_i) - \omega_i^2 q_i^2 \phi_i^2 \right). \tag{5.13}$$

These differential equations take the form of a bounce equation [22,30,32], under the potentials given by $U(\phi_i, \psi_i) - \omega^2 q_i^2 \phi_i^2$. The lowest energy configurations are known to be spherically symmetric [32], under the boundary conditions of the field vanishing at spatial infinity, and being constant at the coordinate origin, and the first derivative vanishing at spatial infinity and the coordinate origin.

These coupled differential equations cannot in general be solved analytically. However, under certain assumptions, analytic progress can be made.

5.3 Thin-Wall Q-balls

Q-balls in the thin-wall limit are characterised by a spherical core of homogeneous Q-matter and a thin-shell through which the field returns to its vacuum value. The Q-ball properties are then well-approximated by those of the core. However, each field does not need to have a core of the same size *a priori*. In principle, therefore, we need to introduce a different volume for each field, V_i, and must assume a hierarchy of sizes in order to progress mathematically. However, this calculation is rather cumbersome in general. We thus first assume that all volumes correspond to the same volume, V. We then present the result for a two-field system where $V_1 > V_2$.

In the thin-wall regime where each field is contained within a coincident volume V, we have that

$$\mathcal{E}_\omega \approx \sum_i^N \omega_i Q_i + V \left[U(\phi_i) - \sum_i^N \omega_i^2 q_i^2 \phi_i^2 \right]. \tag{5.14}$$

Minimisation of this expression with respect to each of the ω_k yields

$$Q_k = 2\omega_k V q_k^2 \phi_k^2, \tag{5.15}$$

as would be expected from the Noether current density given in Eq. (5.5). Eliminating the Lagrange multipliers from the energy yields

$$E = \frac{1}{4V}\sum_{i}^{N}\frac{Q_i^2}{q_i^2\phi_i^2} + U(\phi_i)V. \tag{5.16}$$

Minimisation with respect to the volume gives us that

$$V^2 = \frac{1}{4U(\phi_i)}\sum_{i}^{N}\frac{Q_i^2}{q_i^2\phi_i^2}, \tag{5.17}$$

which, upon substitution, finally gives us that

$$m_Q = \sqrt{U(\phi_i)\sum_{i}^{N}\frac{Q_i^2}{q_i^2\phi_i^2}}. \tag{5.18}$$

This expression must be minimised with respect to the field content subject to the condition

$$m_Q < \sum_{i}^{N}\frac{Q_i}{q_i}m_i, \tag{5.19}$$

where m_i are the masses of the quanta associated to the field ϕ_i. This ensures that these Q-balls are classically stable against evaporation into the field content. The result of this minimisation is the constraint on the potential:

$$\frac{\partial U(\phi_i)}{\partial\phi_k}\sum_{i}^{N}\frac{Q_i^2}{q_i^2\phi_i^2} = 2\frac{Q_k^2}{q_k^2\phi_k^3}U(\phi_i). \tag{5.20}$$

Since this must be true for all k, we therefore find that

$$\frac{\partial U(\phi_i)}{\partial\phi_j}\frac{q_j^2\phi_j^3}{Q_j^2} = \frac{\partial U(\phi_i)}{\partial\phi_k}\frac{q_k^2\phi_k^3}{Q_k^2} \tag{5.21}$$

Unlike in all cases thus far, the VEV of the fields inside of a thin-wall Q-ball in this theory depend on the charge of the Q-ball, or, the total number of quanta that are part of the Q-ball structure (as $N_i = Q_i/q_i$). However, we must see if this is merely an artefact of our earlier assumption.

Consider now a two-field system with potential

$$U(\phi_1, \phi_2) = f(\phi_1) + g(\phi_2) + h(\phi_1, \phi_2). \tag{5.22}$$

We assume that the field ϕ_1 is contained within a volume V_1, and the field ϕ_2 is contained within a volume V_2. For definiteness, and without loss of generality, we

further assume that $V_1 > V_2$. Then, following the same procedure as before, we find that

$$V_1^2 = \frac{Q_1}{4q_1^2\phi_1^2 f(\phi_1)} \quad \text{and} \quad V_2^2 = \frac{Q_2}{4q_2^2\phi_2^2[g(\phi_2) + h(\phi_1, \phi_2)]}, \tag{5.23}$$

and that rest mass of the configuration is

$$m_Q = Q_1\sqrt{\frac{f(\phi_1)}{q_1^2\phi_1^2}} + Q_2\sqrt{\frac{g(\phi_2) + h(\phi_1, \phi_2)}{q_2^2\phi_2^2}}. \tag{5.24}$$

Thus far, this looks a lot like two copies of the single-field case. However, though the VEV of the second field obeys a differential equation much like the single field case,

$$\frac{\partial}{\partial\phi_2}\left[g(\phi_2) + h(\phi_1, \phi_2)\right] = \frac{2}{\phi_2}\left[g(\phi_2) + h(\phi_1, \phi_2)\right], \tag{5.25}$$

the VEV of the first field obeys a more complex differential equation,

$$\frac{Q_1}{f(\phi_1)q_1^2\phi_1^2}\left[\frac{\partial f(\phi_1)}{\partial\phi_1} - 2\frac{f(\phi_1)}{\phi_1}\right] + \frac{Q_2}{[g(\phi_2) + h(\phi_1, \phi_2)]q_2^2\phi_2^2}\frac{\partial h(\phi_1, \phi_2)}{\partial\phi_1} = 0. \tag{5.26}$$

We thus see that the VEV of the field in the larger volume obeys a differential equation that is dependent on the charges of both fields. If the roles were reversed and $V_2 > V_1$, then the field ϕ_2 would be the one dependent on the charges of both fields. Thus, the situation in which both fields are contained within exactly the same volume is indeed special – it is where *all* fields have a VEV dependent on the total charge of the configuration.

Intriguingly, this seems that suggest that theories with multiple charges and scalars can possess Q-balls with cores. This, in part, motivates the heuristic discussion of the next chapter, though the scenario will be different to the one given above.

5.4 Thick-Wall Q-balls

We now consider the thick-wall limit of this theory. As in the multi-field case with only a single symmetry, this theory suffers from the fact that it is not analytically tractable due to the number of fields. As before, this problem must be circumvented by assuming that all the spatial profiles of the fields are the same up to some positive-definite normalisation constant – we must then minimise the energy with respect to each of these normalisation constants. We thus write that

$$\phi_i = \alpha_i\phi, \tag{5.27}$$

where $\phi \in \{\phi_i\}$ is some reference field – it does not affect the analysis in this case which field is used. Given this, the full bounce potential can be written in the small field limit as

$$U_\omega(\phi, \alpha_i) \approx \left[\sum_i^N \alpha_i^2 m_i^2 (1 - \Omega_i^2)\right] \phi^2 - g(\alpha_i)\phi^p, \tag{5.28}$$

where $p > 2$ and, as usual, we have defined

$$\Omega_i \equiv \frac{q_i \omega_i}{m_i}, \tag{5.29}$$

with $\Omega_i \in (0, 1)$, such that the coefficient of the quadratic term is always positive. The function $g(\alpha_i)$ is model-dependent and we leave it general apart from the fact that it must be positive definite for the potential to allow Q-ball solutions. We have omitted the next term in the series, but it is assumed that it is positive definite and stabilises the potential at high field values. The energy in Eq. (5.12) is then

$$\mathcal{E}_\omega = \sum_i^N m_i \Omega_i \frac{Q_i}{q_i} + \int \mathrm{d}^3x \left[\sum_i^N \alpha_i^2 \left(\vec{\nabla}\phi \cdot \vec{\nabla}\phi + m_i^2(1 - \Omega_i^2)\phi^2\right) - g(\alpha_i)\phi^p\right]. \tag{5.30}$$

We wish to render the integral dimensionless. To do so, we define the dimensionless variables

$$\varphi \equiv \phi \left[\frac{g(\alpha_i)}{\sum_i^N \alpha_i^2 m_i^2 (1 - \Omega_i^2)}\right]^{1/(p-2)} \quad \text{and} \quad \xi_i \equiv x_i \left[\frac{\sum_i^N \alpha_i^2 m_i^2 (1 - \Omega_i^2)}{\sum_i^N \alpha_i^2}\right]^{1/2}. \tag{5.31}$$

The functional of study is then given by

$$\mathcal{E}_\omega = \sum_i^N m_i \Omega_i \frac{Q_i}{q_i} + \frac{S_\varphi}{g(\alpha_i)^{2/(p-2)}} \left[\sum_i^N \alpha_i^2\right]^{3/2} \left[\sum_i^N \alpha_i^2 m_i^2 (1 - \Omega_i^2)\right]^{(6-p)/(2p-4)}, \tag{5.32}$$

where S_φ is a dimensionless integral, defined as

$$S_\varphi = \int \mathrm{d}^3\xi \left[\vec{\nabla}_\xi \varphi \cdot \vec{\nabla}_\xi \varphi + \varphi^2 - \varphi^p\right]. \tag{5.33}$$

For different values of p, this has been numerically minimised in Ref. [104], with the general trend being that S_φ increases for increasing p. This expression must be minimised with respect to the $\{\Omega_i\}$ and $\{\alpha_i\}$. Without specifying the model, it is difficult to make progress. However, as in previous chapters, we can place limits on the theories that can house Q-ball states.

We minimise the above function in Eq. (5.32) with respect to some Ω_k. This yields the condition

$$\frac{Q_k}{q_k\alpha_k^2 m_k\Omega_k} = \frac{S_\varphi}{g(\alpha_i)^{2/(p-2)}}\left[\frac{6-p}{p-2}\right]\left[\sum_i^N \alpha_i^2\right]^{3/2}\left[\sum_i^N \alpha_i^2 m_i^2(1-\Omega_i^2)\right]^{(10-3p)/(2p-4)}. \tag{5.34}$$

Notice, the left hand-side is k-dependent, but the right-hand side is not. Since this condition holds for all k, we can readily write

$$\frac{Q_k}{q_k\alpha_k^2 m_k\Omega_k} = \frac{Q_i}{q_i\alpha_i^2 m_i\Omega_i} \tag{5.35}$$

for all $k, i \in \{1, \cdots, N\}$. Given that $\alpha = 1$ for, say, the field ϕ_1, we can readily write

$$\alpha_k^2 = \frac{q_1}{Q_1}\frac{Q_k}{q_k}\frac{m_1}{m_k}\frac{\Omega_1}{\Omega_k}, \tag{5.36}$$

and so α is now defined for all fields in the theory.

Using our above condition for minimisation, we can rewrite Eq. (5.32) as

$$\mathcal{E}_\omega = \sum_i^N m_i\Omega_i\frac{Q_i}{q_i} + \frac{Q_k}{q_k\alpha_k^2 m_k\Omega_k}\left[\frac{p-2}{6-p}\right]\left[\sum_i^N \alpha_i^2\right]^{3/2}\left[\sum_i^N \alpha_i^2 m_i^2(1-\Omega_i^2)\right]. \tag{5.37}$$

At its minimum, this expression must satisfy

$$\mathcal{E}_\omega < \sum_i^N \frac{Q_i}{q_i}m_i \tag{5.38}$$

in order for the resulting Q-balls to be classically stable against decay to the constituent quanta of the complex scalar fields. From Eq. (5.35), we see that we can write

$$\sum_i^N m_i\Omega_i\frac{Q_i}{q_i} = \frac{Q_k}{q_k\alpha_k^2 m_k\Omega_k}\sum_i^N \alpha_i^2 m_i^2\Omega_i^2, \tag{5.39}$$

and

$$\sum_i^N \frac{Q_i}{q_i}m_i = \frac{Q_k}{q_k\alpha_k^2 m_k\Omega_k}\sum_i^N \alpha_i^2 m_i^2\Omega_i. \tag{5.40}$$

Thus, our condition on the minimum becomes

$$\sum_i^N \alpha_i^2 m_i^2\left[\Omega_i^2 + \left(\frac{p-2}{6-p}\right)(1-\Omega_i^2) - \Omega_i\right] < 0. \tag{5.41}$$

For this condition to hold, we necessarily require that that term in brackets be negative for some i in the range $\Omega \in (0,1)$. However, this is nothing more than the same requirement on the canonical single-field case found in Section 2.4. We thus infer that, for stable thick-wall Q-balls to form in this theory, we must have that $2 < p < 10/3$.

5.5 Summary

In this chapter, we studied a subclass of multi-field and multi-symmetry theories for Q-ball solutions. Specifically, we consider a theory of N complex scalar fields, each charged under their own $U(1)$ symmetry. Thus, the stabilising symmetry is an N-fold $U(1)$ symmetry. In this scheme, we studied both the thin- and thick-wall limits, using the standard multi-field approximation of similar spatial profiles in order to progress analytically.

In the thin-wall case, we determined the physical properties of the Q-ball, together with the differential equation that governs the VEV of the fields inside the Q-ball. In sharp contrast to all previous studies, we have found that the VEVs depend upon the charge of the Q-ball itself. The differential equation must then be solved for each charge configuration, independently. It would be interesting to solve this in future work in, say, the "doubly-charged" case.

In the thick-wall case, we performed a similar analysis to all previous chapters. By demanding that the minimum of energy be classically stable against decay into constituent quanta of the fields, we gave sufficient constraints on the theories that possess a thick-wall limit. The general set up of the theory was such that we had, in some sense, N copies of the single-field case, and so it comes to no surprise that the restriction of theories is the same as in previous chapters, namely, that $2 < p < 10/3$, where p denotes the index of the next-to-quadratic term in the bounce potential.

Chapter 6

Cored Q-balls

6.1 Introduction

We close out this part of the thesis with a predominantly heuristic discussion of a new structure within multi-field theories: a cored Q-ball. We envisage a thin-wall Q-ball in one field which possesses a core composed of a thick-wall Q-ball of another field that is stabilised precisely in the homogeneous VEV of the larger Q-ball.[1][2] Each field is stabilised by its own global $U(1)$ symmetry, and so this structure is in principle stable.

In Section 6.2, we first consider the scenario whereby one field exists in the background VEV of another. We seek Q-ball solutions that are stabilised precisely due to this background VEV. We perform both the thick- and thin-wall analyses in this scenario, but we note that the calculation proceeds precisely as it would for the single-field case. We merely include these calculations here for completeness and for introducing the notation in the rest of the chapter. In Section 6.3, we consider the case when the background VEV is provided by a large, thin-wall Q-ball. We then merely seek to see whether a cored Q-ball is a stable structure. This leads to two inequalities to be satisfied: the first arises from the requirement that the Q-ball be stable against decay into the individual quanta of both fields; the second arises from the

[1] In principle, these objects are a subclass of "speckled" Q-balls, whereby the larger Q-ball is populated by many smaller ones throughout its core – this is beyond this thesis, but is an interesting avenue of research for the future. This is an interesting addition to the consideration of Q-balls that interact with other fields. This line of thinking has obvious similarities to theories with multiple vacua in the early universe such that the vacuum bubbles develop "barnacles" of other vacua – see Refs. [14, 38, 126]. Moreover, non-spherically symmetric, composite Q-balls, referred to as "charge swapping Q-balls", also possess core-like structures, as discussed in Refs. [35, 143].

[2] In principle, the core could be composed of a thin-wall Q-ball. However, presumably, the larger VEVs in the core would then have a larger knock on effect on the VEVs in the Q-ball that houses it. We therefore stick with the simpler, heuristic example of the thick-wall core in this chapter.

demand that the core be smaller than the Q-ball that houses it. These requirements are model-dependent.

This chapter represents original work and can be found in Ref. [102].

6.2 Q-balls in the Background of Another Field

A key component of this chapter is the idea of a Q-ball stabilised in the background of another field. In this section, we formulate this idea for a background VEV extending over all space.

6.2.1 The Minimisation Procedure

We consider a theory of two complex scalars, $\Phi_1(\vec{x},t)$ and $\Phi_2(\vec{x},t)$. Let each of these scalars be charged under their own global $U(1)$ symmetry, which we label $U(1)_1$ and $U(1)_2$, respectively. The symmetry is realised by the invariance of the Lagrangian describing the theory under the independent transformations

$$\Phi_1 \to e^{iq_1\alpha}\Phi_1 \quad \text{and} \quad \Phi_2 \to e^{iq_2\beta}\Phi_2, \tag{6.1}$$

where $\alpha,\beta \in \mathbb{R}$, and q_1 denotes the charge of Φ_1 under the $U(1)_1$ symmetry, and similarly for q_2. It is understood that Φ_1 is uncharged under $U(1)_2$, and similarly for Φ_2 under $U(1)_1$. We will consider the following Lagrangian,

$$\mathcal{L} = \partial_\mu\Phi_1\partial^\mu\Phi_1^* + \partial_\mu\Phi_2\partial^\mu\Phi_2^* + U(\Phi_1,\Phi_2), \tag{6.2}$$

where $U(\Phi_1,\Phi_2)$ is some potential invariant under $U(1)_1 \times U(1)_2$. We write this potential as

$$U(\Phi_1,\Phi_2) = f(\Phi_1) + g(\Phi_2) + h(\Phi_1,\Phi_2), \tag{6.3}$$

where it is understood that h contains all terms that couple the two fields together. Without loss of generality, we take $U(0,0) = 0$.

We assume that the field Φ_1 acquires some constant VEV – in this section, we leave the method of acquisition of this VEV open, but in the next section, we will assume that it comes after the formation of a thin-wall Q-ball. We thus seek Q-ball solutions for the field Φ_2 in this constant background. Furthermore, this constant background will merely change the coefficients of the field Φ_2 by constant amounts, and so this analysis will proceed exactly as for a single-field system. Despite the repetition of previous chapters, we perform the analysis below.

The energy of a configuration of Φ_2 in the background of $\bar{\phi}_1$ is

$$H = \int \mathrm{d}^3x \left[\dot{\Phi}_2 \dot{\Phi}_2^* + \vec{\nabla}\Phi_2 \cdot \vec{\nabla}\Phi_2^* + g(\Phi_2) + h(\bar{\phi}_1, \Phi_2) \right]. \tag{6.4}$$

A Q-ball is a state that minimises the energy for a given charge and so we introduce a Lagrange multiplier, ω_2, that ensures charge conservation upon minimisation with respect to it. The functional we wish to analyse is then

$$\mathcal{E}_\omega = H + \omega_2 \left(Q_2 - \int \mathrm{d}^3x j_2^0 \right), \tag{6.5}$$

where j_2^0 is the zeroth component of the Noether current density associated to the $U(1)_2$ symmetry,

$$j_2^0 = iq_2 \left(\dot{\Phi}_2^* \Phi_2 - \Phi_2^* \dot{\Phi}_2 \right). \tag{6.6}$$

We may thus rewrite our functional of study as

$$\mathcal{E}_\omega = \int \mathrm{d}^3x \left[\left| \dot{\Phi}_2 - i\omega_2 q_2 \Phi_2 \right|^2 + \vec{\nabla}\Phi_2 \cdot \vec{\nabla}\Phi_2^* + g(\Phi_2) + h(\bar{\phi}_1, \Phi_2) - \omega_2^2 q_2^2 \Phi_2^* \Phi_2 \right] + \omega_2 Q_2. \tag{6.7}$$

Note, the term containing explicit time-dependence is positive semi-definite. This is therefore minimised when it vanishes, i.e., if

$$\Phi_2(\vec{x}, t) = e^{i\omega_2 q_2 t} \phi_2(\vec{x}), \tag{6.8}$$

where we take the spatial profile to be real-valued, without loss of generality. Reinsertion of this into the functional of study leads to

$$\mathcal{E}_\omega = \omega_2 Q_2 + \int \mathrm{d}^3x \left[\vec{\nabla}\phi_2 \cdot \vec{\nabla}\phi_2 + g(\phi_2) + h(\bar{\phi}_1, \phi_2) - \omega_2^2 q_2^2 \phi_2^2 \right]. \tag{6.9}$$

Minimisation with respect to the spatial profile yields a differential equation governing a "bounce" solution associated to the formation of vacuum bubbles during phase transitions [22, 30, 32]. These equations are well-studied and, for a set of boundary conditions appropriate for Q-balls, are known to yield spherically symmetric solutions for the lowest energy configurations.

6.2.2 The Thick-Wall Limit

We now pursue the thick-wall limit of this analysis, which is also known as the small field limit.[3] To proceed, we expand ϕ_2 to its lowest order terms. As stated above,

[3] We note that "small-field" here only relates to ϕ_2, as it is from this that this Q-ball is being formed.

this analysis is essentially identical to a single field case and so is bound by the requirement that the next-to-quadratic term must be cubic in the bounce potential. We thus assume that this term exists. We therefore have, in the small-field limit, that

$$g(\phi_2) + h(\bar{\phi}_1, \phi_2) \approx \left(\mu^2 + h_2(\bar{\phi}_1)\right)\phi_2^2 - \left(h_3(\bar{\phi}_1) - A\right)\phi_2^3, \tag{6.10}$$

where $h_2(\bar{\phi}_1)$ and $h_3(\bar{\phi}_1)$ are the components, functionally dependent on $\bar{\phi}_2$, of the terms quadratic and cubic in ϕ_2 contained within $h(\bar{\phi}_1, \phi_2)$, respectively, and similarly for μ^2 and A in $g(\phi_2)$. We assume that some positive definite term of a higher order exists to stabilise the potential at large field. In this scenario, a Q-ball may only form if the coefficients of the quadratic and cubic terms are positive and negative, respectively:

$$\mu^2 + h_2(\bar{\phi}_1) > 0 \quad \text{and} \quad h_3(\bar{\phi}_1) - A > 0. \tag{6.11}$$

However, recall that we demanded that the pure Φ_2 potential could not support Q-ball solutions. This sets $A \geq 0$, hence the sign assignment on the cubic term.

For notational purposes, we will write the effective quadratic and cubic couplings in the background as

$$\mu_{\text{eff}}^2(\bar{\phi}_1) \equiv \mu^2 + h_2(\bar{\phi}_1) \quad \text{and} \quad A_{\text{eff}}(\bar{\phi}_1) \equiv h_3(\bar{\phi}_1) - A, \tag{6.12}$$

noting that both of these new parameters are positive definite. The bounce potential can now be written in the familiar form,

$$U_\omega(\bar{\phi}_1, \phi_2) \approx (\mu_{\text{eff}}^2 - \omega_2^2 q_2^2)\phi_2^2 - A_{\text{eff}}\phi_2^3. \tag{6.13}$$

For a barrier to form, and thus for a bounce solution to exist, we see that

$$\omega_2^2 < \frac{\mu_{\text{eff}}^2}{q_2^2}, \tag{6.14}$$

which is the familiar requirement of Q-ball solutions. The thick-wall limit is thus equivalent to the limit $\omega_2 q_2 \to \mu_{\text{eff}}^-$.

We redefine the spatial coordinate and field by choosing

$$\begin{aligned} \xi_i &= \left(\mu_{\text{eff}}^2 - \omega_2^2 q_2^2\right)^{1/2} x_i \\ \psi &= \left(\mu_{\text{eff}}^2 - \omega_2^2 q_2^2\right)^{-1} A_{\text{eff}}\phi_2. \end{aligned} \tag{6.15}$$

Our functional of study thus reduces to

$$\mathcal{E}_\omega = \mu_{\text{eff}}^3 \frac{\left(1 - \Omega^2\right)^{3/2}}{A_{\text{eff}}^2} S_\psi + \omega_2 Q_2, \tag{6.16}$$

where we have defined $\Omega \equiv \omega_2 q_2/\mu_{\rm eff}$ and

$$S_\psi = \int \mathrm{d}^3\xi \left[\vec{\nabla}_\xi\psi \cdot \vec{\nabla}_\xi\psi + \psi^2 - \psi^3\right] \tag{6.17}$$

is a dimensionless integral that may be minimised numerically. This has been found to be 38.8 [104].

A stable Q-ball in the background of $\bar{\phi}_1$ is found when minimising this expression with respect to Ω under the constraint that $\Omega^2 < 1$. If this constraint is not satisfied, it is more energetically favourable for the quanta of Φ_2 to remain seperate within the background of $\bar{\phi}_1$. This requirement leads us to the condition

$$\epsilon = \Omega(1-\Omega^2)^{1/2}, \tag{6.18}$$

where we define

$$\epsilon \equiv \frac{1}{3S_\varphi}\frac{Q_2}{q_2}\frac{A_{\rm eff}^2}{\mu_{\rm eff}^2}. \tag{6.19}$$

The solution to this condition is that

$$\Omega^2 = \frac{1+\sqrt{1-4\epsilon^2}}{2}, \tag{6.20}$$

where $0 < \epsilon < 1/2$. The mass of the resulting Q-ball is then given by

$$m_Q = \mu_{\rm eff}\frac{Q_2}{q_2}\left(1 - \frac{1}{6}\epsilon^2 + \mathcal{O}(\epsilon^4)\right). \tag{6.21}$$

We note that

$$m_Q < \mu_{\rm eff}\frac{Q_2}{q_2}, \tag{6.22}$$

which is precisely the requirement for classical stability of this Q-ball within the background of $\bar{\phi}_1$. The radius of the resulting Q-ball is given by $\xi \sim 1$, and so

$$R^{-1} \sim \epsilon\mu_{\rm eff}\left(1 + \mathcal{O}\left(\epsilon^2\right)\right). \tag{6.23}$$

This solution is also subject to the constraint that $\epsilon < 1/2$, which translates to the requirement on the charge that

$$\frac{Q_2}{q_2} < 58.2\frac{\mu_{\rm eff}}{A_{\rm eff}^2}. \tag{6.24}$$

The solution is also subject to the constraint that the higher order term that stabilises the potential is indeed small enough inside the Q-ball to ignore in our analysis – see Section 2.4 for details.

6.2.3 The Thin-Wall Limit

For completeness, we now include the thin-wall analysis, despite not using the results in what remains of this chapter. A thin-wall Q-ball's physical properties are well-described by those of its homogeneous core. We thus write

$$\mathcal{E}_\omega \approx \bar{\omega}_2 Q_2 + V\left[g(\bar{\phi}_2) + h(\bar{\phi}_1, \bar{\phi}_2) - \bar{\omega}_2^2 q_2^2 \bar{\phi}_2^2\right], \tag{6.25}$$

where V is the volume of the core, and we use bars to represent values of variables within the core. Minimisation of this with respect to the Lagrange multiplier yields, as expected, the expression for the charge of this configuration,

$$Q_2 = 2\bar{\omega}_2 q_2^2 \bar{\phi}_2^2 V. \tag{6.26}$$

Eliminating $\bar{\omega}_2$ and minimising with respect to the volume leads to

$$V^2 = \frac{Q_2^2}{4q_2^2\bar{\phi}_2^2} \frac{1}{\left[g(\bar{\phi}_2) + h(\bar{\phi}_1, \bar{\phi}_2)\right]}. \tag{6.27}$$

Finally, upon elimination of the volume, we obtain the rest mass of the configuration

$$m_Q = Q_2 \sqrt{\frac{g(\bar{\phi}_2) + h(\bar{\phi}_1, \bar{\phi}_2)}{q_2^2 \bar{\phi}_2^2}}, \tag{6.28}$$

which is completely expected from the single-field theory, since $U(\bar{\phi}_2) = g(\bar{\phi}_2) + h(\bar{\phi}_1, \bar{\phi}_2)$. For the resultant Q-ball to be stable in the background of the VEV of Φ_1, we must have that

$$m_Q < \mu_{\text{eff}} \frac{Q_2}{q_2}, \tag{6.29}$$

where $\mu_{\text{eff}}(\bar{\phi}_1)$ is defined as in the previous section. The VEV of $\bar{\phi}_2$ must obey the differential equation given by

$$\frac{\partial g}{\partial \bar{\phi}_2} + \frac{\partial h}{\partial \bar{\phi}_2} = 2\left(\frac{g}{\bar{\phi}_2} + \frac{h}{\bar{\phi}_2}\right). \tag{6.30}$$

This concludes the thin-wall analysis of this theory.

6.3 Cored Q-balls

We assume that the potential $f(\Phi_1)$ admits Q-balls composed of the field Φ_1. In the thin-wall limit, these Q-balls are spherically-symmetric, extended objects comprised of a large core of homogeneous "Q-matter", and a thin shell which interpolates between the core and the vacuum of the theory. The VEV in the core is therefore the

origin of the VEV of Φ_1 in the previous section. The physical properties of the Q-ball – it's mass and volume – are well-approximated by the properties of the core in this limit. Inside the Q-ball, where the field is homogeneous, Φ_1 takes on the well-known functional form

$$\Phi_1(t) = e^{iq_1\omega t}\bar{\phi}_1, \tag{6.31}$$

where $\bar{\phi}_1 \in \mathbb{R}$. The rest mass and volume of the Q-ball are then given by

$$m_Q = Q_1\sqrt{\frac{f(\bar{\phi}_1)}{q_1^2\phi_1^2}} \quad \text{and} \quad V = \frac{Q_1}{2\sqrt{q_1^2\bar{\phi}_1^2 f(\bar{\phi}_1)}}, \tag{6.32}$$

where $\bar{\phi}_1$ must satisfy

$$\frac{\partial f(\bar{\phi}_1)}{\partial\bar{\phi}_1} = \frac{2f(\bar{\phi}_1)}{\bar{\phi}_1}, \tag{6.33}$$

such that E/Q_1 must be less than the mass per unit charge of individual quanta of the Φ_1 field. It is in this way that these Q-balls are said to be classically stable.

We assume that, if anything, $h(\Phi_1, \Phi_2)$ provides, at most, a small perturbation to this Q-ball solution. For definiteness, we assume that $g(\Phi_2)$ does not admit Q-ball solutions in isolation from Φ_1, and we further assume, for simplicity, that $U(\Phi_1, \Phi_2)$ does not admit Q-balls charged under both symmetries when all terms are considered.

Now, consider a configuration where a thin-wall Q-ball composed of Φ_1 is surrounded by quanta of the field Φ_2. The potential $h(\Phi_1, \Phi_2)$ defines how these entities interact. Let us consider an attractive potential such that the quanta of Φ_2 become bound within the Q-ball. We will only consider a small amount entering the Q-ball such that the value of $\bar{\phi}_1$ is still consistent with that defined above. Though the core of the Q-ball is, in principle, homogeneous, the presence of the new quanta slightly breaks this homogeneity, and we expect these to settle in the core of the Q-ball as this is the symmetric point of the Q-ball.[4]

If enough quanta are collected, it is reasonable to ask whether a Q-ball composed of Φ_2, in the background of $\bar{\phi}_1$, can form. Moreover, if this Q-ball does not get too large, such that the terms in $h(\Phi_1, \Phi_2)$ greatly perturb the Q-ball background, it should not greatly affect the value of $\bar{\phi}_1$. We will assume that the core is a thick-wall Q-ball, as this is more consistent with our assumption that the new Q-ball does not overly affect the value of $\bar{\phi}_1$, since the VEV is smaller. We can take the results directly from the previous section.

[4]We could also consider the case that many thick-wall Q-balls form within the homogeneous background of the thin-wall Q-ball. However, we do not consider this "speckled" Q-ball here.

We require that the whole system be energetically stable against classical decay to quanta of both fields. The total mass of the cored Q-ball is

$$E_{\rm tot} = \frac{Q_1}{q_1}\sqrt{\frac{f(\bar{\phi}_1)}{\bar{\phi}_1^2}} + \frac{Q_2}{q_2}\mu_{\rm eff}\left(1 - \frac{1}{6}\epsilon^2\right). \tag{6.34}$$

For this to be classically stable against decay to the quanta of both of the fields, we require that

$$E_{\rm tot} < \frac{Q_1}{q_1}m + \frac{Q_2}{q_2}\mu, \tag{6.35}$$

where m is the mass of quanta of the field Φ_1 and, as before, μ is the mass of the quanta of the field Φ_2 in the vacuum of the theory, $\Phi_1 = 0$. Note that, the first term of the total energy is less than the first term of this constraint. If $\mu_{\rm eff} < \mu$, then this constraint is satisfied. If this is not true, then a sufficient condition is for[5]

$$\mu_{\rm eff}\left(1 - \frac{1}{6}\epsilon^2\right) < \mu. \tag{6.37}$$

This constraint, in terms of the charge of the thick-wall Q-ball, evaluates to

$$\frac{Q_2}{q_2} > 201.6\sqrt{h_2(\bar{\phi}_1)}\frac{\mu_{\rm eff}}{A_{\rm eff}^2}. \tag{6.38}$$

This implies that, for this structure to be classically stable, there is a minimum charge that must accumulate in the thick-wall core. For this to be compatible with Eq. (6.24), we require that

$$11h_2 < \mu. \tag{6.39}$$

We thus see that we require that the coupling between the two fields not be too large. If this is satisfied, then it is sufficient to prove that this structure is classically stable over some range of charge. The total system is therefore adequately described as a thin-wall Q-ball, stabilised by the conservation of some charge, with a core composed of a thick-wall Q-ball, stabilised by the conservation of some other charge, over the background field of the thin-wall Q-ball. This is because the field ϕ_2 will remain "small" and thus will not overly affect the background field, $\bar{\phi}_1$.

[5]The necessary condition is that the the binding energy of the thin-wall Q-ball is greater than any energy cost that the thick-wall Q-ball expanded in the background of $\bar{\phi}_1$ brings over the vacuum of the theory,

$$\frac{Q_1}{q_1}\left(m - \sqrt{\frac{f(\bar{\phi}_1)}{\bar{\phi}_1^2}}\right) > \frac{Q_2}{q_2}\left[\mu_{\rm eff}\left(1 - \frac{1}{6}\epsilon^2\right) - \mu\right]. \tag{6.36}$$

This is a model-dependent condition, so we say nothing more of this here.

By definition, a Q-ball is the state that minimises the energy per unit charge of a sector of a theory. Thus, the combination of energy and Noether charge conservation implies that this configuration is more stable than emitting the individual quanta of Φ_2 outside the Q-ball formed from Φ_1. One could also question whether a Q-ball composed of Φ_1 and Φ_2 could be emitted as a decay channel. However, the ability for the potential defined through $g(\Phi_2)$ and $h(\Phi_1, \Phi_2)$ in the background of $\bar{\phi}_1$ to house stable Q-ball solutions does not imply that the full potential $U(\Phi_1, \Phi_2)$ will allow for stable "doubly-charged" Q-balls to exist in isolation. In the absence of this decay mode, the cored Q-ball is indeed stable.

We also require that the Q-ball in the core be smaller than the thin-wall Q-ball it resides in, as otherwise we cannot assume the results of the previous section. From the sizes of the respective Q-balls given in Eqs. (6.23) and (6.32), together with the definition for ϵ given in Eq. (6.19), we find that

$$36\pi(S_\varphi)^3 \frac{q_2^3}{Q_2^3} \frac{\mu_{\text{eff}}^3}{A_{\text{eff}}^6} \ll \frac{Q_1}{2\sqrt{q_1^2 \bar{\phi}_1^2 f(\bar{\phi}_1)}}, \tag{6.40}$$

which is a model-dependent condition which relates the charge accumulation of both Q-balls.

6.4 Summary

In this chapter, we heuristically studied a new type of object that we called a "cored Q-ball". This is a thin-wall Q-ball whose homogeneous interior acts as a stabilising background VEV for a thick-wall Q-ball composed of another field. In this work, we merely concerned ourselves with the question of stability of these objects. Realistic theories that lead to the formation of these objects is a direction for future work. Specifically, a phenomenological analysis is required in which all timescales are taken into account, together with a mechanism for the release of the additional energy. Moreover, one could also extend the ideas here to the case where a stable, "doubly-charged" Q-ball can exist – see the previous chapter. This would open up the decay channel whereby a mixed Q-ball is emitted, leaving behind a pure thin-wall Q-ball.

Intriguingly, these objects could be important in DM experiments. Consider the case that the Q-ball at the core is charged under the SM, whereas the larger thin-wall Q-ball is not directly coupled to the SM. If this object were to pass through a direct detection experiment, we would only see the core, and not the Q-ball at large. This would cause a misidentification of the DM until experiments are sensitive enough

to determine the other component, which could indirectly couple to the SM via the cored field.

Part III

Q-balls from Chiral Symmetry Breaking in the Standard Model and Beyond

Chapter 7

Q-balls in the Standard Model

7.1 Introduction

Within the theoretical structure of the SM, there exists two classes of scalar. The first, the Higgs, cannot house stable Q-ball solutions by virtue of its potential: each piece of the potential comes with a positive-definite coefficient, which we know cannot allow for Q-ball solutions to exist. Moreover, there is no global Higgs charge once the Yukawa couplings are included. The other class of scalar in the SM are the mesons which arise from chiral symmetry breaking. We analyse the latter sector in this chapter.

As we saw in Section 1.3.4, ChPT is a low-energy effective theory of the interactions of the pseudoscalar mesons in the SM. The theory incorporates the breaking of an approximate, global chiral symmetry: $\mathrm{SU}(N_f)_L \times \mathrm{SU}(N_f)_R \to \mathrm{SU}(N_f)_V$. This symmetry is only approximate as the quark masses explicitly break it, mixing the left- and right-handed components of the quark degrees of freedom. The pseudoscalar mesons are realised as pNGBs in the theory, with the approximate chiral symmetry the reason for their relative lightness.

The degrees of freedom of ChPT are pseudoscalars, and this sector can possess global symmetries. For example, SU(3) ChPT contains an approximate global strangeness symmetry in the limit that we ignore strangeness-violating decays mediated through the massive weak bosons. If the Q-ball background kinematically forbids these decays, much like the stability of neutrons in the nucleus, then we can describe Q-balls in the usual way. Thus, it is a reasonable to question whether Q-balls can be present in this type of sector. This is a particularly interesting question in ChPT because the scalars in the theory are composite objects.

In this chapter, we analyse the "pure" ChPT for Q-balls, that is, the unmodified ChPT as found in the SM and discussed in Section 1.3.4. We will focus on the two-

flavour case: SU(2) ChPT.[1] We perform the minimisation procedure in Section 7.2, with the thick-wall analysis following in Section 7.3 and the thin-wall analysis in Section 7.4. This analysis is relevant for both the SM and hidden sectors containing a copy of QCD. We will consider a certain hidden sector in the next chapter.

ChPT has already been analysed for thin-wall Q-balls in [44]. The thick-wall analysis, however, is original. It can be found in the appendix of Ref. [18]. It should be noted that ChPT represents a multi-field theory with non-canonical kinetic terms, and so the analyses of previous chapters cannot be used here.

7.2 Minimising the Energy in a Sector of Fixed Charge

In the SM, there are three quarks that possess masses small enough – below the chiral symmetry breaking scales – such that their low energy effective theory is well-described by the $SU(3)$ chiral Lagrangian. By Goldstone's theorem, the spontaneously broken chiral symmetry $SU(3)_L \times SU(3)_R$ to the diagonal subgroup $SU(3)_V$ possesses eight massless NGBs that parameterise the coset space $SU(3)_L \times SU(3)_R / SU(3)_V$. These NGBs are, in fact, massive (and referred to as pNGBs) as the chiral symmetry is only approximate – it is explicitly broken by the mass matrix, M. The mass matrix further breaks the surviving $SU(3)_V$ symmetry if it is not proportional to the identity matrix: the surviving global symmetry is then $U(1) \times U(1)$ – in general, $U(1)^{N_f-1}$.

Given the non-trivial nature of the potential contained within the chiral Lagrangian, and the existence of a global symmetry, it is reasonable to question whether this theory admits Q-ball states. This was first performed in Ref. [44]. In this paper, the kaon $SU(2)$ subgroup of the chiral Lagrangian was examined together with the surviving $U(1)$ symmetry of strangeness. This is mathematically equivalent to studying the $SU(2)$ chiral Lagrangian from the offset and not associating the surviving $U(1)$ symmetry with electromagnetism, as would be the case in the pion sector of the SM. In this case, the pions of the theory, related to Σ through Eq. (1.26), will take

[1] As mentioned below, we discuss this case as it it simpler mathematically and has the exact same results as for the $SU(3)$ case. However, it should be noted that, in the SM, Q-balls formed from the charged pions are charged under electromagnetism, and thus are more properly considered as gauged Q-balls. However, considerations of the electromagnetic force would only render them more unstable. Since, in the absence of electromagnetism, they are not stable in the first place, as we shall see, we omit this from our discussion. Moreover, these Q-balls would decay as the charged pions themselves are unstable – they decay to, primarily, muons. As discussed in Chapter 1, these decays would be surface-area limited as this a fermionic decay channel.

the form of the usual Q-ball ansatz,

$$\pi^{\pm}(\vec{x},t) = e^{\pm i\omega t}\pi(r) \quad \text{and} \quad \pi^0(\vec{x},t) = \pi^0(r), \tag{7.1}$$

where the spatial profiles obey a bounce equation. We will present this form of the analysis here due, in part, to Chapter 8 in which we study a hidden sector containing pions for Q-ball states. The mathematics is simpler if we perform the analysis with the Σ field and so we proceed from this point of view.

As discussed in Section 1.3.4, the unitary matrix field Σ transforms under the vectorial symmetry as

$$\Sigma \to \exp(-i\alpha X)\Sigma\exp(i\alpha X), \tag{7.2}$$

where X is Hermitian and traceless, and $\alpha \in \mathbb{R}$. For small α, this transformation is

$$\Sigma \to \Sigma + i\alpha\,[\Sigma, X] + \mathcal{O}(\alpha^2), \tag{7.3}$$

where $[\cdot,\cdot]$ denotes the commutator of two matrices. The Noether current density associated to this transformation is then

$$\begin{aligned} j^\mu &= \lim_{\alpha\to 0} \mathrm{tr}\left(\frac{\partial\mathcal{L}}{\partial(\partial_\mu\Sigma)}\frac{\delta\Sigma}{\alpha} + \frac{\partial\mathcal{L}}{\partial\partial(\partial_\mu\Sigma^\dagger)}\frac{\delta\Sigma^\dagger}{\alpha}\right) \\ &= i\frac{f^2}{4}\mathrm{tr}\left(\partial^\mu\Sigma^\dagger[\Sigma,X] + \partial^\mu\Sigma[\Sigma^\dagger,X]\right). \end{aligned} \tag{7.4}$$

For generic diagonal M, this transformation is a symmetry when X is diagonal – it is this matrix that generates the surviving global $U(1)$ symmetry of the theory. We fix this to $X = \sigma_3/2$, without loss of generality.

Q-balls represent the states of a theory that possess the lowest energy for a given charge. The Hamiltonian associated to the leading order chiral Lagrangian, in Eq. (1.32), is given by

$$\begin{aligned} H &= \int \mathrm{d}^3x \left[\mathrm{tr}\left(\frac{\partial\mathcal{L}}{\partial\dot{\Sigma}}\dot{\Sigma} + \frac{\partial\mathcal{L}}{\partial\dot{\Sigma}^\dagger}\dot{\Sigma}^\dagger\right) - \mathcal{L}\right] \\ &= \int \mathrm{d}^3x \left[\frac{f^2}{4}\mathrm{tr}\left(\dot{\Sigma}\dot{\Sigma}^\dagger + \vec{\nabla}\Sigma\cdot\vec{\nabla}\Sigma^\dagger\right) - \frac{B_0 f^2}{2}\mathrm{tr}\left(M(\Sigma+\Sigma^\dagger-2)\right)\right]. \end{aligned} \tag{7.5}$$

To analyse this Hamiltonian for Q-ball states, we introduce a Lagrange multiplier, ω, that fixes the charge, as in Ref. [90]. We thus analyse the functional given by

$$\mathcal{E}_\omega = H + \omega\left(Q - \int \mathrm{d}^3x j^0\right), \tag{7.6}$$

where j^0 is the 0-th component of the Noether current density associated with the U(1) symmetry given in Eq. (7.4). Strictly, there is an additional component to the energy – the pions are composite particles made up of quark/anti-quark pairs. The pion wavefunctions cannot overlap arbitrarily as there is a Fermi repulsion. However, as this would only add to the energy of the Q-balls, we omit this from the current analysis since Q-balls cannot form in this theory even in the absence of Fermi repulsion. We will come back to this component of the energy when we study a hidden sector containing pions in the next chapter.

The functional described above evaluates to

$$\begin{aligned}\mathcal{E}_\omega = \omega Q + \int \mathrm{d}^3x \, \Bigg[& \frac{f^2}{4}\mathrm{tr}\left(\left|\dot{\Sigma} - i\omega[\Sigma, X]\right|^2 + \vec{\nabla}\Sigma^\dagger \cdot \vec{\nabla}\Sigma - \omega^2[\Sigma, X][X, \Sigma^\dagger]\right) \\ & - \frac{B_0 f^2}{2}\mathrm{tr}\left(M(\Sigma + \Sigma^\dagger - 2)\right)\Bigg].\end{aligned} \tag{7.7}$$

The first term under the integral is the sole term with explicit time-dependence. This term is positive semi-definite, and so is minimised if it vanishes, i.e., if

$$\Sigma(\vec{x}, t) = \exp(-i\omega X t)\Sigma(\vec{x})\exp(i\omega X t). \tag{7.8}$$

As stated above, the spatial profiles of the underlying pion fields obey a bounce equation [22, 30, 32], and so we can assume that the profile is spherically symmetric. As ever, we now continue analytically by studying the thick- and thin-wall limits.

7.3 Thick-Wall Analysis

Here we show that thick-wall Q-balls cannot exist within the leading order $SU(2)$ chiral Lagrangian – this analysis is original and was presented in Ref. [18]. To do this, we need to show that the functional in Eq. (7.7), together with the ansatz given in Eq. (7.8), has no minima for $Q \neq 0$ in the small field limit. Substituting Eq. (7.8) into Eq. (7.7) and expanding Σ to the next-to-quadratic order in the constituent pion field, while choosing $X = \sigma_3/2$, we find

$$\begin{aligned}\mathcal{E}_\omega = \int \mathrm{d}^3x \, \Bigg[& \left(\frac{1}{2}\vec{\nabla}\pi^0 \cdot \vec{\nabla}\pi^0 + \vec{\nabla}\pi^+ \cdot \vec{\nabla}\pi^-\right)\left(1 - \frac{1}{3f^2}\left(\pi^0\pi^0 + 2\pi^+\pi^-\right)\right) \\ & + \frac{1}{6f^2}\left(\pi^0\vec{\nabla}\pi^0 + \pi^+\vec{\nabla}\pi^- + \pi^-\vec{\nabla}\pi^+\right)^2 + \frac{1}{2}m_\pi^2\pi^0\pi^0 + (m_\pi^2 - \omega^2)\pi^+\pi^- \\ & - \frac{m_\pi^2}{24f^2}(\pi^0)^4 - \frac{1}{6f^2}(m_\pi^2 - 2\omega^2)(\pi^0\pi^0)(\pi^+\pi^-) - \frac{1}{6f^2}\left(m_\pi^2 - 4\omega^2\right)(\pi^+\pi^-)^2\Bigg] \\ & + \omega Q,\end{aligned} \tag{7.9}$$

where we have defined $m_\pi^2 \equiv B_0 \mathrm{tr} M$, and expanded Σ to quartic order in the π fields on account that there are no cubic terms in the chiral Lagrangian. As is usual in the thick-wall analysis, we ignore higher-order terms, which will stabilise the potential.

The quartic terms containing derivatives are suppressed relative to the kinetic terms by a factor of f^2 and to the other quartic terms by spatial gradients, which are small. We will hence ignore these terms.

Notice that in the limit $\omega \to m_\pi$, i.e., the thick-wall or small-field limit, the last two quartic terms have positive coefficients. In order for a potential barrier to exist (and, therefore, a bounce solution to exist), we require that the overall contribution of all three quartic terms be negative. Consequently, the VEV of the neutral pion in the centre of the Q-ball must be large relative to that of the charged pions, but since this will contribute a large amount of mass to the Q-ball without contributing to its charge, we might expect that no stable Q-balls exist.

To see this quantitatively, we relate the profiles of the pion fields as in Chapter 4: $\pi^0(x) = \beta\pi(x)$ and $\pi^\pm(x) = \pi(x)$. We thus find that

$$\begin{aligned}\mathcal{E}_\omega = \int \mathrm{d}^3x \left[\left(1 + \frac{1}{2}\beta^2\right)\vec{\nabla}\pi \cdot \vec{\nabla}\pi + m_\pi^2\left(1 + \frac{1}{2}\beta^2 - \Omega^2\right)\pi^2 - \lambda(\Omega,\beta)\pi^4\right] \\ + \Omega Q m_\pi,\end{aligned} \tag{7.10}$$

where $\Omega \equiv \omega/m_\pi$, and

$$\lambda(\Omega,\beta) \equiv \frac{m_\pi^2}{6f^2}\left[\frac{\beta^4}{4} - \beta^2(2\Omega^2 - 1) - (4\Omega^2 - 1)\right] \tag{7.11}$$

is the quartic coupling, which must be positive. Choosing

$$\begin{aligned}\xi_i &= m_\pi\left(1 + \frac{1}{2}\beta^2\right)^{-1/2}\left(1 + \frac{1}{2}\beta^2 - \Omega^2\right)^{1/2} x_i, \\ \psi &= \frac{1}{m_\pi}\left(1 + \frac{1}{2}\beta^2 - \Omega^2\right)^{-1/2}\lambda(\Omega,\beta)^{1/2}\,\pi,\end{aligned} \tag{7.12}$$

we may transform $\mathcal{E}_\omega$ to

$$\mathcal{E}_\omega = m_\pi \frac{\left(1 + \beta^2/2\right)^{3/2}\left(1 + \beta^2/2 - \Omega^2\right)^{1/2}}{\lambda(\Omega,\beta)} S_{\psi,4} + \Omega Q m_\pi, \tag{7.13}$$

where

$$S_{\psi,4} = \int \mathrm{d}^3\xi \left[\vec{\nabla}_\xi\psi \cdot \vec{\nabla}_\xi\psi + \psi^2 - \psi^4\right] \tag{7.14}$$

is a positive, dimensionless number [104], whose precise value will not concern us in the following.

Now $\mathcal{E}_\omega$ must be minimised with respect to Ω and β. Minimising with respect to Ω yields

$$0 = \frac{\partial \mathcal{E}_\omega}{\partial \Omega} = \frac{7 m_\pi^3 S_{\psi,4} \Omega}{6 f^2 \lambda(\Omega,\beta)^2} \frac{(1+\beta^2/2)^{5/2}}{(1+\beta^2/2-\Omega^2)^{1/2}} \left(1 + \frac{1}{2}\beta^2 - \frac{4}{7}\Omega^2\right) + Q m_\pi. \tag{7.15}$$

This is positive semidefinite for $\Omega \in [0,1]$, vanishing only when $Q = 0$ and $\Omega = 0$. As such, there is no Q-ball solution.

7.4 Thin-Wall Analysis

The absence of a thick-wall limit does not necessarily preclude the existence of thin-wall Q-balls in the spectrum of the theory. However, it was shown in Ref. [44] that this theory still does not include thin-wall Q-balls. We present this analysis here.

A thin-wall Q-ball is characterised by a core of a homogeneous state, named Q-matter, and a thin outer shell. The mass of the thin-wall Q-ball is dominated by this core. We let $\Sigma(r) = \Sigma_0$ be a constant spatial profile of the field inside the core of the Q-ball, such that Eq. (7.7), together with the ansatz given in Eq. (7.8), becomes

$$\mathcal{E}_\omega \approx \omega Q - \omega^2 \frac{f^2}{4} \mathrm{tr}\left([\Sigma_0, X][X, \Sigma_0^\dagger]\right) V - \frac{B_0 f^2}{2} \mathrm{tr}\left(M(\Sigma_0 + \Sigma_0^\dagger - 2)\right) V \tag{7.16}$$

where V is the volume of the core of the Q-ball.

To determine the mass of the resulting Q-ball, this expression must be minimised with respect to the field content, as well as the volume and the Lagrange multiplier. To proceed further, we take advantage of the fact that $\Sigma_0 \in \mathrm{SU}(2)$,

$$\Sigma_0 = \exp\left(i\varphi \hat{n}\cdot\sigma\right) = \cos\varphi + i\left(\hat{n}\cdot\sigma\right)\sin\varphi, \tag{7.17}$$

where it is understood that $\cos\varphi$ multiplies a unit 2×2 matrix, and $\hat{n} = (n_1,\, n_2,\, n_3)$ is a unit vector, $\hat{n}^2 = 1$. In what follows, we explicitly take $X = \sigma_3/2$. Under this specification, the traces evaluate to

$$\begin{aligned} \mathrm{tr}\left([\Sigma_0, X][X, \Sigma_0^\dagger]\right) &= 2\sin^2\varphi(1-n_3^2), \\ \mathrm{tr}\left(M(\Sigma_0 + \Sigma_0^\dagger - 2)\right) &= -2(1-\cos\varphi)\mathrm{tr}\left(M\right). \end{aligned} \tag{7.18}$$

Inserting these into Eq. (7.16) yields

$$\mathcal{E}_\omega = \omega Q - \omega^2 \frac{f^2}{2} \sin^2\varphi(1-n_3^2)V + m_\pi^2 f^2 (1-\cos\varphi)V \tag{7.19}$$

where we define the pion mass in the usual way, $m_\pi^2 \equiv B_0 \mathrm{tr}\,(M)$. Minimising this expression with respect to the Lagrange multiplier yields

$$Q = f^2 \omega (1 - n_3^2) \sin^2 \varphi V \,. \tag{7.20}$$

This expression corresponds precisely to the one for the charge as determined from Eq. (7.4). We use this to eliminate ω, giving

$$E = \frac{Q^2}{2f^2(1 - n_3^2)\sin^2 \varphi V} + m_\pi^2 f^2 (1 - \cos\varphi) V. \tag{7.21}$$

The only dependence on the direction of the VEV of Σ is the factor n_3 in the first term. The energy of the Q-ball is minimized for $n_3 = 0$, which corresponds to zero VEV for the neutral pions. This behaviour is expected since a neutral pion VEV inside the Q-ball contributes to its mass but not to its charge. Therefore, it increases the mass per unit charge of the Q-ball which is the opposite of the desired behaviour.

Minimising the energy with respect to the volume yields

$$V = \frac{Q}{\sqrt{2 m_\pi^2 f^4 \sin^2 \varphi (1 - \cos\varphi)}}. \tag{7.22}$$

Reinserting this expression into the formula for E yields

$$E = Q m_\pi \sqrt{\frac{2(1 - \cos\varphi)}{\sin^2 \varphi}}. \tag{7.23}$$

Minimising this expression with respect to φ yields the condition

$$\frac{\sin^4(\varphi/2)}{\sin^3 \varphi} \sqrt{1 + \cos\varphi} = 0. \tag{7.24}$$

However, this requires that $\varphi = 2n\pi$, where $n \in \mathbb{Z}$, which returns precisely the vacuum of the theory, $\Sigma_0 = \mathbb{1}$. Thus, we infer that no thin-wall Q-balls can exist in the chiral Lagrangian, at least to leading order.

7.5 Summary

The only known scalar fields in nature, aside from the Higgs boson, are the pseudoscalar mesons of ChPT. The Higgs boson does not possess a potential that allows Q-balls to form. Given the complexity of the potential in the chiral Lagrangian, it is reasonable to ask whether this sector possesses Q-ball solutions. In this chapter, we have performed this analysis on the leading order chiral Lagrangian and found that neither thin- nor thick-wall Q-balls can form.

Since we have only studied the leading terms in the theory, it would be interesting to study the next-to-leading order to determine whether these additional pieces allow Q-ball states to form. In Ref. [44], it was claimed that this was plausible with certain parameter values. However, this was performed over 30 years ago and the parameters of the model are now determined to a higher precision. Thus, it would be useful to return to this study and update it. If it is found that the next-to-leading terms allow thin-wall Q-balls to form, we expect the thick-wall analysis to still be valid. This is because the additional terms are suppressed relative to the leading-order terms, and so in the small-field limit should still be irrelevant.

Chapter 8

Higgs Assisted Q-balls from Pseudo-Nambu-Goldstone Bosons

8.1 Introduction

In most studies of Q-ball solutions, the scalar fields making up the Q-ball are explicitly or implicitly assumed to be elementary. In this chapter we show that Q-balls can exist in theories where the charged scalar fields that make up the Q-ball are not elementary but rather composite states, with non-perturbative dynamics leading to a low-energy effective theory described by light pion-like pNGBs carrying a $U(1)$ global quantum number. In particular, with an eye towards future possible applications to BSM and DM physics, we consider theories which contain a strongly-interacting hidden sector at TeV-scales or above, and which feature a spontaneous breaking of a non-Abelian global symmetry similar to that of the chiral symmetry breaking of QCD, but occurring at $f \sim$ TeV energies or greater, rather than the scale $f \sim 100$ MeV as for QCD. When small explicit breaking of the original global symmetry is included, the previously massless NGBs acquire small masses. Importantly, these, now pseudo-NGBs, can be much lighter than all other mass scales associated with the strongly-coupled sector, and so we can treat their low-energy dynamics separately from all other degrees of freedom originating from the strongly-coupled theory.

As we saw in the previous chapter, these pNGBs alone were found to not form Q-ball states, despite the complexity of their potential. Fortunately, in the situation we study in this chapter, the pNGBs are not the only relevant light fields. In general the SM Higgs field is even lighter than the hidden pNGBs and, as we show in Section 8.2, interacts with them in a particular way via a Higgs-portal interaction. The form of the resulting pNGB-Higgs interactions is not arbitrary, but constrained by the breaking of scale symmetry [27, 139, 140]. This then leads to an interacting system of both

charge-carrying and charge-neutral scalar fields that we show in Sections 8.4 and 8.5 possesses Q-ball solutions for a range of underlying parameter values.

Before turning to the details of our particular model and the existence of Q-ball solutions, we emphasise that the underlying UV strong-coupling dynamics plays almost no role in the analysis,[1] the existence and detailed properties of the Q-ball solutions depending solely on the leading-order low-energy effective Lagrangian interactions between the pNGBs themselves and with the Higgs. We therefore expect that similar Q-ball solutions will occur in a wide range of effective field theories described by the Callan-Coleman-Wess-Zumino coset construction [23, 34] supplemented by Higgs interactions. In particular it would be interesting to study the possible existence of stable or metastable Q-balls in models where the Higgs doublet itself is realised as a pNGB, along with other light pNGB fields [7, 17, 46, 66, 83, 84].

The contents of this chapter are original. The work was split between two papers: Ref. [18] contains work performed alongside Johnson, Bishara and March-Russell; Ref. [19] contains work performed alongside Bishara. Specifically, the numerical simulations contained within these papers, and, consequently, this chapter, were performed by Bishara.

8.2 The Hidden Sector

We assume that there are two sectors: the SM and a hidden sector (HS). As described in the Introduction, the HS possesses a spontaneously broken almost-exact global symmetry, which gives rise to pNGBs. The HS also possesses an unbroken global $U(1)$, under which some of these pNGBs transform. In this section we describe the origin of the Higgs coupling to the HS pions resulting in the Lagrangian in Eq. (8.20).

8.2.1 Structure of the hidden sector

For definiteness, we consider a HS with a QCD-like $SU(N_c)$ Yang-Mills theory with N_f flavours of HS 'quarks' in the fundamental of $SU(N_c)$. This theory possesses an $SU(N_f)_L \times SU(N_f)_R$ chiral flavour symmetry which is spontaneously broken to the diagonal subgroup $SU(N_f)_V$.[2] Then, by Goldstone's theorem, there will be $N_f^2 - 1$ massless NGBs that parameterise the coset space $SU(N_f)_L \times SU(N_f)_R / SU(N_f)_V$.

[1] The exception being the presence or otherwise of a Fermi repulsion term depending on the fermion or boson nature of the underlying matter degrees of freedom in the UV theory.

[2] We ignore the fact that the symmetry group is generally $U(N_f)_L \times U(N_f)_R$ since the one non-anomalous $U(1)$ from the $U(N_f)_L \times U(N_f)_R$, that in the SM case corresponds to baryon number, acts trivially on the pNGBs, so it is not of interest to us here.

Furthermore, the HS quark mass matrix, M, explicitly breaks the chiral symmetry, which becomes only approximate in this limit. The NGBs will therefore acquire a non-zero mass, i.e., they become pNGBs. The mass matrix M also breaks $SU(N_f)_V$ if it is not proportional to the unit matrix: in the situation that no two HS quark masses are equal, the surviving global symmetry acting on the pNGBs is $U(1)^{N_f-1}$, in the absence of other interactions.

As usual, we can describe the light pNGBs transforming under the non-linearly realised $SU(N_f)_L \times SU(N_f)_R$ symmetry by a unitary matrix field of unit determinant built from the $N_f^2 - 1$ pNGBs, π^a:

$$\Sigma = \exp\big(i\pi^a T^a / f\big). \tag{8.1}$$

Then, under the global vectorial symmetry, Σ transforms as

$$\Sigma \to \Sigma' = V\,\Sigma\,V^\dagger, \tag{8.2}$$

where V is in general given by $V = \exp(-i\alpha X)$ with X Hermitian and traceless. The Noether current density associated to this transformation is

$$j^\mu = i\frac{f^2}{4}\mathrm{tr}\left([\Sigma^\dagger, X]\partial^\mu\Sigma + [\Sigma, X]\partial^\mu\Sigma^\dagger\right), \tag{8.3}$$

where we have assumed the usual leading order chiral Lagrangian

$$\mathcal{L} = \frac{f^2}{4}\mathrm{tr}\left(\partial_\mu\Sigma\partial^\mu\Sigma^\dagger\right) + \frac{B_0 f^2}{2}\mathrm{tr}\left(M(\Sigma + \Sigma^\dagger - 2)\right). \tag{8.4}$$

For generic diagonal M, the transformation Eq. (8.2) is a symmetry when X is one of the possible $N_f - 1$ diagonal matrices. The pseudoscalar sector can both possess global symmetries, and have a non-trivial potential given by the second term in Eq. (8.4), but as we have seen in Chapter 7, this theory as it is cannot house Q-ball states. However, in this scenario, we need to be more specific about the coupling of this HS to the SM, and also about the HS itself, as well as the exact form of the global $U(1)$ that we will be using.

For concreteness, suppose that the HS is very similar in form to the SM itself, but with the analogue of $U(1)_Y$ *ungauged*. Thus we take the HS gauge group to be $SU(3)' \times SU(2)'$ with, minimally, one 'generation' of matter fermions in the same $SU(3)' \times SU(2)'$ representations as the SM matter fields. This guarantees the anomaly freedom of the matter content with respect to these two symmetries. We also require the HS quarks to acquire bare masses, so the HS must also have an $SU(2)'$-doublet scalar state, S, which acquires a VEV, analogous to the Higgs doublet in the SM

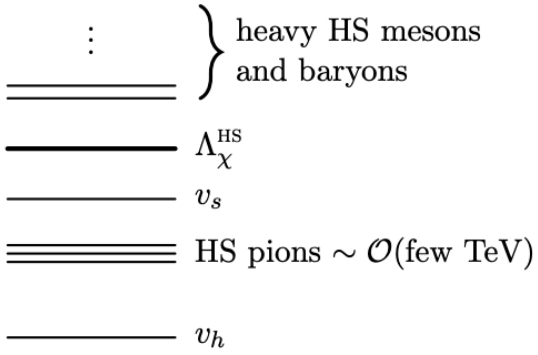

Figure 8.1: Spectrum of hidden sector states.

sector. This scalar doublet is coupled via Yukawa interactions to HS chiral quarks which acquire a mass upon the spontaneous breaking of $SU(2)'$. The Yukawa terms in our HS Lagrangian are

$$\mathcal{L}^{\rm HS} \supset y_{ij}\overline{Q}_{L,i}Sq_{R,j} + \text{h.c.}, \tag{8.5}$$

where Q (q) are the doublet (singlet) HS quarks and y_{ij} are Yukawa couplings.

The $SU(3)'$ is asymptotically free and confines at low energies with a corresponding confinement scale $\Lambda_\chi^{\rm HS}$. We require the HS quarks of the first generation to be light relative to $\Lambda_\chi^{\rm HS}$ and assume that any additional generations beyond the first are heavy.[3] The light HS quarks will then hadronise into a massive but light triplet of HS pions as a consequence of chiral symmetry breaking – see Fig. 8.1 for a schematic of the spectrum.

To ensure that the HS pions are absolutely stable in the presence of $SU(2)'$ interactions, the HS 'leptons' – minimally one generation – must have masses above the HS pion masses.

8.2.2 Coupling the two sectors

The leading interaction between the two sectors is due to a Higgs-portal interaction. Specifically, the scalar potential for the SM Higgs and the HS doublet is given by

$$V(H,S) = -\mu_h^2 H^\dagger H + \lambda_h (H^\dagger H)^2 - \mu_s^2 S^\dagger S + \lambda_s (S^\dagger S)^2 + \lambda_p (H^\dagger H)(S^\dagger S)\,. \tag{8.6}$$

[3]This setup has obvious similarities with Mirror World [54, 55, 87] and Twin Higgs [24–26] scenarios, and in particular the Fraternal Twin Higgs models [36, 37, 53, 60, 61], although in our case we are taking the HS $SU(3)'$ dynamical scale $\Lambda_\chi^{\rm HS} \gtrsim 1\,\text{TeV}$ rather than the few GeV appropriate for the Twin Higgs models.

This potential induces spontaneous symmetry breaking in both sectors. We write the VEV of S as $\langle S\rangle = v_s/\sqrt{2}$ and the VEV of H as $\langle H\rangle = v_h/\sqrt{2}$, with $v_h = 246\,\text{GeV}$ the electroweak VEV.

We introduced a portal term in the above Lagrangian with a coupling λ_p. This is a marginal operator which can arise from integrating out heavier degrees of freedom and is allowed by the symmetries of the two sectors. The portal coupling results in the mixing of the SM and HS Higgs gauge eigenstates h' and s' into the mass eigenstates h and s.

The scalar potential given in Eq. (8.6) is generically minimised when both $|H|$ and $|S|$ acquire non-zero VEVs. Expanding around these VEVs and diagonalising the resulting quadratic terms in the potential gives the masses m_h and m_s of the light and heavy scalar mass eigenstates of the theory. These can be read-off directly from Ref. [15]. We have

$$m_h^2 = \lambda_h v_h^2 + \lambda_s v_s^2 - \sqrt{\mathcal{D}} \tag{8.7}$$

$$m_s^2 = \lambda_h v_h^2 + \lambda_s v_s^2 + \sqrt{\mathcal{D}}, \tag{8.8}$$

where

$$\mathcal{D} = \left(\lambda_h v_h^2 - \lambda_s v_s^2\right)^2 + \lambda_p^2 v_h^2 v_s^2. \tag{8.9}$$

The two scalar mass eigenstates h and s are related to the gauge eigenstates h' and s' by the rotation that enacts the aforementioned diagonalisation. That is to say,

$$\begin{pmatrix} h' & s' \end{pmatrix} \cdot M^2 \cdot \begin{pmatrix} h' \\ s' \end{pmatrix} = \begin{pmatrix} h & s \end{pmatrix} \cdot \widehat{M}^2 \cdot \begin{pmatrix} h \\ s \end{pmatrix} \tag{8.10}$$

where $\widehat{M} = \text{diag}(m_h, m_s)$ and

$$\begin{pmatrix} h \\ s \end{pmatrix} = \begin{pmatrix} \cos\theta & -\sin\theta \\ \sin\theta & \cos\theta \end{pmatrix} \begin{pmatrix} h' \\ s' \end{pmatrix}, \tag{8.11}$$

We identify the lightest scalar mass eigenstate, h, as the SM Higgs. It is the coupling of the pions to this particle that is of most interest to us, on account that it can mediate a long-range attractive force between the pions by virtue of its relative lightness. Given that it is the HS gauge eigenstate s' which couples to the pions, it is necessary to find an expression for the mixing angle θ. We have

$$\tan(2\theta) = \frac{\lambda_p z}{\lambda_s z^2 - \lambda_h}, \tag{8.12}$$

where z is defined as ratio of the VEVs, $z \equiv v_s/v_h$. For z large, assuming λ_h and λ_s are comparable in size, we can write the mixing angle in Eq. (8.12) in terms of the small parameter $\zeta \equiv z^{-1}$,

$$\tan(2\theta) = \frac{\lambda_p \zeta}{\lambda_s - \lambda_h \zeta^2} = \frac{\lambda_p}{\lambda_s}\zeta + \mathcal{O}(\zeta^3). \tag{8.13}$$

In this limit, the small angle approximation for θ is also valid and we find that

$$\theta \approx \frac{\lambda_p v_h}{2\lambda_s v_s}. \tag{8.14}$$

Finally, we can write the SM Higgs cubic coupling λv_h in terms of the couplings in the scalar potential. We have

$$\lambda v_h = \lambda_h v_h \cos^3\theta - \lambda_s v_s \sin^3\theta + \frac{\lambda_p}{2}\left(v_h \cos\theta \sin^2\theta - v_s \sin\theta \cos^2\theta\right), \tag{8.15}$$

and so

$$\lambda \approx \lambda_h - \frac{\lambda_p^2}{4\lambda_s}. \tag{8.16}$$

In the small mixing angle limit, $\theta \ll 1$, s' can be written in terms of the mass eigenstates as

$$s' \approx s - \theta h \approx s - \frac{\lambda_p v_h}{2\lambda_s v_s} h. \tag{8.17}$$

Furthermore, when the HS pions are heavier than the lightest mass eigenstate h, the form of the couplings of h to the HS pions is fully determined by the breaking of scale symmetry in the HS theory. In particular, following the work of Voloshin and Zakharov [139,140], later explicated by Chivukula et al. [27], we may first write down the effective chiral Lagrangian for the interactions with the HS gauge eigenstate s', which is given at leading order by

$$\begin{aligned}\mathcal{L} = &\left(1 + \frac{4n_h}{3\beta_0}\frac{s'}{v_s}\right)\frac{f^2}{4}\mathrm{tr}\left(\partial_\mu \Sigma \partial^\mu \Sigma^\dagger\right) \\ &+ \left(1 + \left[1 + \frac{2n_h}{\beta_0}\right]\frac{s'}{v_s}\right)\frac{B_0 f^2}{2}\mathrm{tr}\left(M(\Sigma + \Sigma^\dagger - 2)\right).\end{aligned} \tag{8.18}$$

Here, n_h is the number of heavy flavours – i.e., the number of quarks q with $m_q > \Lambda_\chi^{\mathrm{HS}}$ – and β_0 is the one-loop beta function in the HS, given for general $SU(N_c)$ with n_ℓ light flavours by

$$\beta_0 = \frac{1}{3}\left(11 C_A - 4 T_F n_\ell\right), \tag{8.19}$$

where $C_A = N_c$ and $T_F = 1/2$ sets the normalisation of the generators. In all that follows, we assume that $n_\ell = 2$, and so we consider the $SU(2)$ chiral Lagrangian.

The additional terms in Eq. (8.18) that couple s' to the HS pions originate either from integrating out heavy quarks (terms proportional to n_h) or via the Yukawa terms in Eq. (8.5) – for details of the numerical coefficients, see Ref. [27]. Finally, the Lagrangian in Eq. (8.18) can be rewritten in favour of h/v_s using the relation in Eq. (8.17) as

$$\begin{aligned}\mathcal{L} = &\left(1 - \theta\frac{2\eta}{3}\frac{h}{v_s}\right)\frac{f^2}{4}\mathrm{tr}\left(\partial_\mu\Sigma\partial^\mu\Sigma^\dagger\right) \\ &+ \left(1 - \theta\left(1+\eta\right)\frac{h}{v_s}\right)\frac{B_0 f^2}{2}\mathrm{tr}\left(M(\Sigma + \Sigma^\dagger - 2)\right) \\ &+ \frac{1}{2}\partial_\mu h\partial^\mu h - U(h),\end{aligned} \tag{8.20}$$

where we have defined $\eta \equiv 2n_h/\beta_0$ (and neglected interactions with the scalar s on the grounds that it is much heavier than the other scalar states), and we have now included the Higgs potential,

$$U(h) = \frac{1}{2}m_h^2 h^2 + \lambda v_h h^3 + \frac{1}{4}\lambda h^4. \tag{8.21}$$

We will show in the following sections that the field theory defined by the Lagrangian Eq. (8.20) admits thick- and thin-wall Q-ball solutions for some values of the parameters.

8.3 Minimising the Energy in a Sector of Fixed Charge

A Q-ball is the state with minimum energy for a given charge in a theory of scalar fields. The Hamiltonian for the theory defined by Eq. (8.20) is given by

$$\begin{aligned}H = \int \mathrm{d}^3x &\left(1 - \theta\frac{2\eta}{3}\frac{h}{v_s}\right)\frac{f^2}{4}\mathrm{tr}\left(\dot\Sigma\dot\Sigma^\dagger + \nabla\Sigma\cdot\nabla\Sigma^\dagger\right) \\ &- \left(1 - \theta\left(1+\eta\right)\frac{h}{v_s}\right)\frac{B_0 f^2}{2}\mathrm{tr}\left(M(\Sigma + \Sigma^\dagger - 2)\right) \\ &+ \frac{1}{2}\left(\dot h^2 + \nabla h\cdot\nabla h\right) + U(h).\end{aligned} \tag{8.22}$$

This yields the energy of a configuration according to the low energy description of the theory. However, since the scalar fields are composites of fermions, their wave functions cannot arbitrarily overlap due to Fermi repulsion. This will add a component to the total energy of the Q-ball, which we denote $\mathcal{E}_F$. The average energy contributed to

the Q-ball per constituent fermion, derived by considering the occupancy of a phase space volume,[4] is

$$\frac{3}{5}E_F = \frac{3}{10m_f}(3\pi^2 n)^{2/3} \tag{8.23}$$

where E_F is the Fermi energy, n is the number density of a fermionic species, and m_f is the dressed quark mass, i.e., the mass of an excitation with the same quantum numbers as a quark, within the Q-ball medium. Typically, $m_f \sim \Lambda_\chi^{\rm HS}$, which is not set in our theory and so can in principle be large relative to other scales.[5] The total energy contributed to the Q-ball is thus

$$\mathcal{E}_F = \frac{1}{5m_f}\left(243\pi^4\frac{Q^5}{V^2}\right)^{1/3}, \tag{8.24}$$

where V is the volume of the Q-ball, and Q the total charge.

To determine the state with the lowest energy for a given charge, we introduce a Lagrange multiplier, ω, to the Hamiltonian to enforce charge conservation, as per the analysis given in Ref. [90]. Combining the above elements, the functional we wish to study is given by

$$\mathcal{E}_\omega = H + \mathcal{E}_F + \omega\left(Q - \int \mathrm{d}^3x\, j^0\right), \tag{8.25}$$

where minimisation with respect to the Lagrange multiplier yields the definition of the charge Q for a given field configuration. The mass of the Q-ball is determined through minimisation with respect to the field content of the theory.[6] The charge functional is found by considering the 0-th component of the Noether current density, j^μ, associated to the transformation

$$\Sigma \to \exp(-i\alpha X)\Sigma\exp(i\alpha X) \quad \text{and} \quad h \to h, \tag{8.26}$$

where $X = X^\dagger$. In what follows, we will take $X = \sigma_3/2$, but we leave it as X at present for notational convenience. The charge functional is given by

$$\int \mathrm{d}^3x\, j^0 = i\int \mathrm{d}^3x\left(1 - \theta\frac{2\eta}{3}\frac{h}{v_s}\right)\frac{f^2}{4}\mathrm{tr}\left(\dot\Sigma[\Sigma, X] + \dot\Sigma^\dagger[\Sigma^\dagger, X]\right). \tag{8.27}$$

[4] See, for example, Ref. [86], for a full derivation and discussion of the origin of the Fermi energy.

[5] If the chiral symmetry breaking scale is sufficiently high, one might wonder if it might give rise to unnaturally large corrections to the Higgs mass through pion loops. The cubic Higgs-pion coupling gives rise to corrections that are logarithmic in $\Lambda_\chi^{\rm HS}/m_\pi$, however, and therefore naturalness is not a problem in this case.

[6] The field configuration $\Sigma(\vec{r}, t) = \mathbb{1}$ and $h(\vec{r}, t) = 0$ leads to $Q = 0$. Thus, a configuration with non-zero charge must differ from 0 in some domain.

We can isolate the explicit time-dependence by rewriting Eq. (8.25) as

$$\begin{aligned}\mathcal{E}_\omega = \int \mathrm{d}^3x \left(1-\theta\frac{2\eta}{3}\frac{h}{v_s}\right)\frac{f^2}{4}\mathrm{tr}\left(|\dot{\Sigma}-i\omega[\Sigma,X]|^2-\omega^2[\Sigma,X][X,\Sigma^\dagger]+\nabla\Sigma\cdot\nabla\Sigma^\dagger\right)\\ -\left(1-\theta\,(1+\eta)\,\frac{h}{v_s}\right)\frac{B_0 f^2}{2}\mathrm{tr}\left(M(\Sigma+\Sigma^\dagger-2)\right)\\ +\frac{1}{2}\left(\dot{h}^2+\nabla h\cdot\nabla h\right)+U(h)\\ +\omega Q+\mathcal{E}_F.\end{aligned} \tag{8.28}$$

The two terms with explicit time-dependence are minimised if they vanish, and so

$$\Sigma(\vec{r},t)=\exp(-i\omega Xt)\Sigma(\vec{r})\exp(i\omega Xt)\quad\text{and}\quad h(\vec{r},t)=h(\vec{r}). \tag{8.29}$$

Though written in favour of a matrix representation, the earlier choice of $X=\sigma_3/2$ reproduces the well-known fact about Q-balls: the charged constituent scalars (here $\pi^\pm$) rotate in field space with angular speed proportional to ω and their respective charge under the symmetry.

As usual, upon reinsertion of the Q-ball ansatz into the energy functional, what remains is impossible to solve analytically for Q-balls in general. However, progress can be made in the thick- and thin-wall limits. We present both of these limits in the forthcoming sections. These are original work and can be found in Ref. [18] and Ref. [19], respectively.

8.4 Thick-Wall Q-balls

We will show in this section that thick-wall Q-balls formed from the light scalars of the theory (the HS pions and the SM Higgs) can exist. We will present two cases: an analytic example with no heavy quarks in the HS, and a numerical example with arbitrarily many heavy quarks. As found in the previous chapter, the chiral Lagrangian alone, i.e., with no coupling to the Higgs field, does not admit thick-wall Q-balls.

8.4.1 The Thick-Wall Analysis

The thick-wall Q-ball limit corresponds to the limit in which the field values at the centre of the Q-ball are small such that terms quartic (and higher) in the fields can be neglected [89]. In what follows, we will neglect the contribution to the energy of the Fermi repulsion and will consider that effect separately below. We take, without loss

of generality, the $U(1)$ symmetry of the Chiral Lagrangian to act on the underlying pNGBs as

$$\pi^{\pm} \to e^{\pm i\alpha}\pi^{\pm} \quad \text{and} \quad \pi^0 \to \pi^0. \tag{8.30}$$

The labels on the pions thus refer to their charge under this $U(1)$ symmetry, not to their electromagnetic charge.

Expanding Σ in the functional given in Eq. (8.28), using Eq. (8.1), and including terms involving the Higgs alone gives, to cubic order,

$$\begin{aligned}\mathcal{E}_\omega = \int \mathrm{d}^3x \; \Bigg[& \left(1 - \theta\frac{2\eta}{3}\frac{h}{v_s}\right)\left(\left|\dot{\pi}^+ - i\omega\pi^+\right|^2 + \frac{1}{2}\dot{\pi}^0\dot{\pi}^0\right) + \frac{1}{2}\dot{h}^2 \\ & + \left(1 - \theta\frac{2\eta}{3}\frac{h}{v_s}\right)\left(\vec{\nabla}\pi^+ \cdot \vec{\nabla}\pi^- + \frac{1}{2}\vec{\nabla}\pi^0 \cdot \vec{\nabla}\pi^0\right) \\ & + \frac{1}{2}\vec{\nabla}h \cdot \vec{\nabla}h + \widehat{U}(\vec{\pi}, h)\Bigg] \\ & + \omega Q,\end{aligned} \tag{8.31}$$

where

$$\begin{aligned}\widehat{U}(\vec{\pi}, h) = & \, m_\pi^2\left(1 - \theta\,(1+\eta)\,\frac{h}{v_s}\right)\left(\pi^+\pi^- + \frac{1}{2}\pi^0\pi^0\right) + \frac{1}{2}m_h^2h^2 + \lambda v_h h^3 \\ & - \left(1 - \theta\frac{2\eta}{3}\frac{h}{v_s}\right)\omega^2\pi^+\pi^-.\end{aligned} \tag{8.32}$$

The only explicit time dependence of $\mathcal{E}_\omega$ has been isolated in the first line of Eq. (8.31). This integral is positive semidefinite, and to minimise its contribution to the energy the fields must have the following time dependence:

$$\pi^{\pm}(x,t) = e^{\pm i\omega t}\pi^{\pm}(x), \quad \pi^0(x,t) = \pi^0(x), \quad h(x,t) = h(x). \tag{8.33}$$

Our problem now involves four real degrees of freedom: $\pi^{\pm}(x)$, $\pi^0(x)$, and $h(x)$. To proceed, we assume that the spatial profile of each of the fields has, up to normalisations, the same form:

$$\pi^{\pm}(x) = \pi(x), \qquad \pi^0(x) = \beta\pi(x), \qquad h(x) = \alpha\pi(x)\,, \tag{8.34}$$

where we allow for α and/or β to be zero. This ansatz is sufficient for the purpose of demonstrating the existence of Q-balls; in reality, the spatial profiles of the fields might differ, but this extra freedom in the minimisation process can only further lower the Q-ball energy. With these proportionality relations, we can write $\mathcal{E}_\omega$ solely

in terms of the field $\pi(x)$. In addition to the gradient-squared and field-squared terms, we also have the cross-term

$$-\theta\frac{2\eta}{3}\frac{\alpha}{v_s}\left(1+\frac{1}{2}\beta^2\right)\pi(\vec{\nabla}\pi)^2. \tag{8.35}$$

This term can be dropped to leading order in a self-consistent approximation scheme for the Q-ball solution. This is because it is suppressed relative to the $(\vec{\nabla}\pi)^2$ term by the mixing angle and $\langle\pi\rangle/v_s$, where $\langle\pi\rangle$ is the maximum value of the pion VEV inside the Q-ball, and to the π^3 term in Eq. (8.32) by spatial gradients, which we will *a posteriori* check to be small. This term is also exactly absent when $\eta \propto n_h = 0$.

It now remains to minimise the energy functional with respect to the function $\pi(x)$ and the three variables α, β, and ω. To do this, it is useful to redefine the fields and the coordinates in Eq. (8.31) in order to isolate them in a dimensionless integral:

$$\begin{aligned}
\xi_i &= m_\pi \frac{\left(1+\frac{1}{2}\beta^2+\frac{1}{2}\frac{m_h^2}{m_\pi^2}\alpha^2-\Omega^2\right)^{1/2}}{\left(1+\frac{1}{2}\beta^2+\frac{1}{2}\alpha^2\right)^{1/2}}\, x_i, \\
\psi &= \alpha\frac{\frac{m_\pi}{v_s}\theta(1+\eta)\left(1+\frac{1}{2}\beta^2-\frac{2\eta}{3(1+\eta)}\Omega^2\right)-\frac{\lambda v_h}{m_\pi}\alpha^2}{m_\pi\left(1+\frac{1}{2}\beta^2+\frac{1}{2}\frac{m_h^2}{m_\pi^2}\alpha^2-\Omega^2\right)}\,\pi.
\end{aligned} \tag{8.36}$$

After these redefinitions, the energy functional becomes

$$\frac{\mathcal{E}_\omega}{Qm_\pi} = \frac{S_\psi}{Q\alpha^2}\frac{\left(1+\frac{1}{2}\beta^2+\frac{1}{2}\frac{m_h^2}{m_\pi^2}\alpha^2-\Omega^2\right)^{3/2}\left(1+\frac{1}{2}\beta^2+\frac{1}{2}\alpha^2\right)^{3/2}}{\left(\frac{m_\pi}{v_s}\theta(1+\eta)\left[1+\frac{1}{2}\beta^2-\frac{2\eta}{3(1+\eta)}\Omega^2\right]-\frac{\lambda v_h}{m_\pi}\alpha^2\right)^2}+\Omega, \tag{8.37}$$

where $\Omega \equiv \omega/m_\pi$ and S_ψ is given by

$$S_\psi = \int \mathrm{d}^3\xi\left(\vec{\nabla}_\xi\psi\cdot\vec{\nabla}_\xi\psi+\psi^2-\psi^3\right), \tag{8.38}$$

where ξ and ψ are the spatial coordinate and field in dimensionless units, defined in Eq. (8.36). This has the same form as the bounce action for an analogous Euclidean tunnelling problem in three dimensions, and so we can make use of previous results on this subject [22, 30, 32]. In particular, the integral is minimised when the field

is spherically symmetric, and thus we expect all Q-ball solutions to be spherically symmetric. The value of Eq. (8.38) when minimised is approximately 38.8 [104].

A global minimum with $\mathcal{E}_\omega/Qm_\pi < 1$ corresponds to a classically stable Q-ball solution. After minimisation with respect to ω, which enforces the fixed-charge constraint, and α and β, the Q-ball has a mass $M_Q = \mathcal{E}_\omega$. The radius, R_Q, of the Q-ball is ~ 1 in terms of the dimensionless coordinate ξ. Translated into the parameters of the model, it is given by

$$R_Q^{-1} \sim m_\pi \frac{\left(1 + \frac{1}{2}\beta^2 + \frac{1}{2}\frac{m_h^2}{m_\pi^2}\alpha^2 - \Omega^2\right)^{1/2}}{\left(1 + \frac{1}{2}\beta^2 + \frac{1}{2}\alpha^2\right)^{1/2}}. \tag{8.39}$$

We will minimise $\mathcal{E}_\omega$ in two cases: first, we will analytically study the case that there are no additional quarks with masses above the chiral symmetry breaking scale in the HS, and with the Higgs acting as a massless mediator; second, we will numerically study the case that there are arbitrarily many heavy quarks in the HS, allowing the Higgs mass and self-coupling to be non-zero.

The qualitative dependence of the energy functional on α and β is shown in Fig. 8.2, for typical parameter choices. Physically we expect that, for $m_h^2/m_\pi^2 \ll 1$, β will be zero for the following reason. The neutral pion has no cubic interactions with the charged pions, unlike the Higgs, and thus no direct way to lower the energy of the Q-ball. It does, however, have a cubic interaction with the Higgs, which will acquire a VEV at the centre of the Q-ball along with the charged pions, and this cubic interaction may favour the neutral pion acquiring a VEV of its own. However, since this interaction is quadratic in the neutral pion, the Higgs VEV in the Q-ball must be sufficiently large that this term dominates the neutral pion mass term. We hence expect that for pions much heavier than the Higgs, the neutral pion will have a VEV of precisely zero. We will see that this is so in both the analytic and the numerical analysis of the subsequent two sections.

8.4.2 An analytic example: no heavy quarks

In order to determine the conditions for the existence of Q-balls in this theory, as well as the nature of the Q-balls should they exist, we must minimise the energy functional given in Eq. (8.37) with respect to Ω, α, and β. This is not possible to do analytically in the general case: minimising with respect to Ω requires finding the roots of a sixth-order polynomial. The barrier to analyticity comes from the term

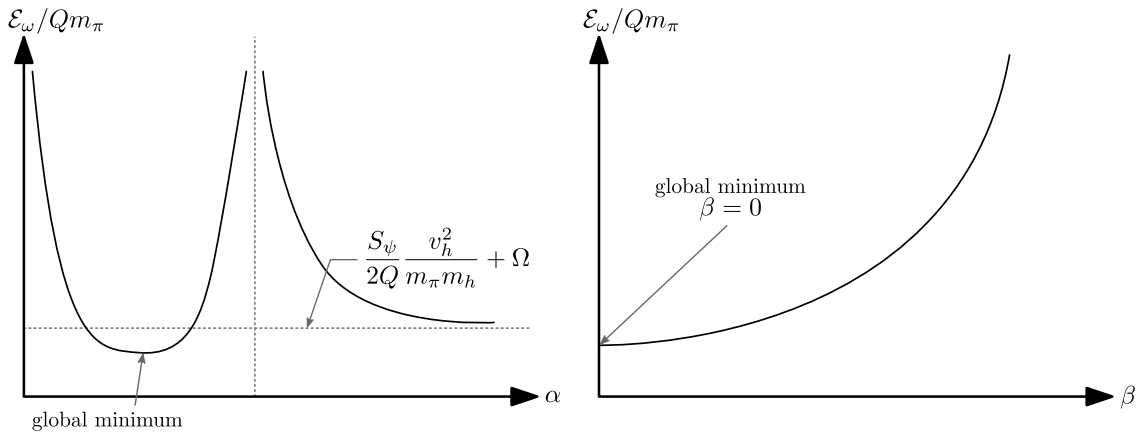

Figure 8.2: The schematic behaviour of the dimensionless energy functional $\mathcal{E}_\omega/Qm_\pi$ in Eq. (8.37) as a function of α and β, for typical choices of parameters. It can be seen that the formation of a Higgs VEV inside the Q-ball is energetically favoured, whilst the formation of a neutral pion VEV is not.

proportional to Ω in the denominator of $\mathcal{E}_\omega$. Thus, to gain an analytic understanding of the Q-ball, we assume that there are no heavy quarks in the HS: this sets $\eta = 0$ and therefore removes the problematic term.[7] To make the results more straightforward and illuminating, we will also take the Higgs mass and cubic self-coupling to zero; it is possible to analytically study the system without this assumption, but at the expense of making the results more opaque. This assumption is valid provided the pion mass terms and the cubic coupling of the pions to the Higgs dominate the aforementioned terms in the Lagrangian; that is,

$$\frac{1}{2}\frac{m_h^2}{m_\pi^2}\alpha^2 \ll 1 \quad \text{and} \quad \frac{\lambda v_h v_s}{\theta m_\pi^2}\alpha^2 \ll 1. \tag{8.40}$$

We will leave a more general discussion of this type of hidden sector until Section 8.4.3, where we relax this assumption and the assumption that $n_h = 0$ with a numerical minimisation of the Q-ball energy, scanning over the parameters of the model.

Setting $\eta = 0$ and $m_h = \lambda = 0$ in Eq. (8.37), we first minimise with respect to α to obtain $\alpha^2 = 4 + 2\beta^2$. Substituting this back into the energy functional, we observe that, for $\Omega^2 > 0$, the expression is a strictly increasing function of β, and hence is

[7]Notice that $\eta \to 0$ removes all couplings of the field to its derivative in Eq. (8.31). Thus, the results of Chapter 4 hold. Since the potential contains terms that are cubic in the field, it is plausible that thick-wall Q-balls exist. Moreover, this theory includes two massive real scalars. Thus, the Q-ball has a lower bound of accumulated charge for stability unless either the VEV of these real scalars vanish inside the Q-ball or the mass is much smaller than the mass of the charged pions.

minimised when $\beta = 0$ (as argued in the previous section). Thus

$$\alpha = 2 \quad \text{and} \quad \beta = 0. \tag{8.41}$$

The energy of the Q-ball is minimised when the VEV of the neutral pion inside the Q-ball is zero, whilst the VEV of the Higgs is double that of the charged pions.

With these substitutions, we have an energy functional of the same form, as a function of Ω, as that given in [89]. We can therefore translate those results across to our case. The energy functional is minimised with respect to Ω if

$$\epsilon \equiv \frac{4}{9\sqrt{3}S_\psi}\frac{Q\theta^2 m_\pi^2}{v_s^2} = \Omega\left(1-\Omega^2\right)^{1/2}, \tag{8.42}$$

which has a solution for Ω provided $0 < \epsilon < 1/2$. The expression for Ω at the minimum is

$$\Omega = \left(\frac{1+\sqrt{1-4\epsilon^2}}{2}\right)^{1/2}. \tag{8.43}$$

Substituting this back into the energy functional and expanding in ϵ yields

$$\frac{M_Q}{Qm_\pi} = 1 - \frac{1}{6}\epsilon^2 - \mathcal{O}(\epsilon^4), \tag{8.44}$$

where M_Q is the energy of the Q-ball. The expression on the right-hand side is clearly less than unity for $\epsilon > 0$. Thus, this solution is (classically) stable for $Q > 0$.[8]

From Eq. (8.39) we find that the radius of the Q-ball is given by

$$R_Q^{-1} \sim \frac{\epsilon m_\pi}{\sqrt{3}}\left(1 + \frac{1}{2}\epsilon^2 + \mathcal{O}\left(\epsilon^4\right)\right). \tag{8.45}$$

This characteristic (inverse) length scale is proportional to the small parameter ϵ, thus justifying our earlier assertion that spatial derivatives are suppressed in the thick-wall case.

Finally, the maximal value of the charged pion VEV occurs in the centre of the Q-ball and takes the value

$$\langle\pi(0)\rangle \sim \left(1-\Omega^2\right)\frac{v_s}{2\theta} \sim \left(2\times 10^{-5}\right) Q^2\theta^3\left(\frac{m_\pi}{v_s}\right)^3 m_\pi. \tag{8.46}$$

[8] If the Higgs mass is appreciable compared to that of the pions, there is a lower bound on the charge Q due to the fact that the Higgs provides an unfavourable contribution to the mass-to-charge ratio of the Q-ball – see below. Note also that the charge needs to be sufficiently large that quantum fluctuations are under control and the semiclassical approximation is valid. Here we take this to imply $Q \gtrsim 10$.

This solution is subject to the following theoretical constraints. Firstly, we require the charge to be sufficiently small that the thick-wall analysis is valid. Secondly, we must check that the Q-ball number density is not so large that the Fermi degeneracy pressure due to the quarks which constitute the pions becomes important. Finally, the fact that the Higgs is actually massive introduces a lower bound on the charge aggregated to form a stable Q-ball.

Thick-wall validity

The thick-wall analysis is only valid in the low charge regime. This is represented by the condition that $\epsilon < 1/2$, which can be rearranged to give

$$Q \lesssim 76 \left(\frac{v_s}{\theta m_\pi} \right)^2 . \tag{8.47}$$

We have assumed that the quartic terms in the energy functional are small compared to the quadratic and cubic terms, which are approximately equal in size in the centre of the Q-ball. There are two types of quartic term we need to consider: the π^4 term and the h^4 term.[9] Demanding that the Higgs quartic is indeed negligible when the pion VEV is given by its maximum value, Eq. (8.46), yields

$$Q \ll 150 \frac{v_s}{\theta m_\pi \sqrt{\lambda}}. \tag{8.48}$$

Demanding that the pion quartics are negligible likewise gives the constraint

$$Q \ll 430 \frac{v_s f}{\theta m_\pi^2}. \tag{8.49}$$

Note that these constraints merely place limits on the validity of the thick-wall analysis, not on the existence of a Q-ball of any description. If these constraints are strongly violated, then stable Q-balls are best described using the thin-wall analysis [31,90]. We will return to the issue of existence and properties of thin-wall Q-balls in this class of hidden sector models in the next section. In the intermediate charge region, we expect that stable Q-balls will still exist, though these will be of neither thick- nor thin-wall type.

[9] In principle, there is also an $h^2\pi^2$ term, but this arises due to a dimension-six operator suppressed by an independent mass scale. This scale can naturally be much larger than Λ_χ^{HS}, thus decoupling this quartic interaction.

Fermi degeneracy pressure

Another important consideration arises due to the fact that the scalars from which these Q-balls are built are in fact composites of fermions, the HS quarks. If the density of pions in the Q-ball is too high, Fermi degeneracy pressure due to these quarks can become significant. In this case, we expect that the radius of the Q-ball will increase to counteract this pressure and reduce the contribution to the Q-ball energy from the filled Fermi sphere. Nevertheless, we can put a conservative upper bound on the charge of the Q-ball by demanding that, for the Q-ball radius as calculated above, such energy contributions are lower than the binding energy.

In the non-relativistic limit, the average additional energy contributed to the Q-ball per constituent fermion is

$$E = \frac{3}{5}E_F = \frac{3}{10m_f}(3\pi^2 n)^{2/3}, \tag{8.50}$$

where m_f is the fermion mass and n its number density. We will demand that

$$2QE < Qm_\pi - M_Q. \tag{8.51}$$

This leads to

$$Q \lesssim 0.1 \left(\frac{m_f}{m_\pi}\right)^{3/2}. \tag{8.52}$$

We hence see that Fermi degeneracy pressure can be quite significant. Given that the pions are pseudo-Nambu-Goldstone bosons of an approximate spontaneously-broken chiral flavour symmetry, we expect them to be relatively light compared to the other scales in the theory. In particular, the appropriate masses of the constituent (dressed) quarks should be of order the chiral symmetry breaking scale, Λ_χ^{HS}. This is undetermined and can in principle be arbitrarily high; as such, we will not worry further about this constraint.

The Higgs Mass

In Chapter 4, we remarked that if a thick-wall Q-ball is partially composed of a massive real scalar, then there will be a lower bound on the charge for the Q-ball to be stable. This is because the mass of the real scalar only contributes to the energy of the Q-ball without an increase in charge, and thus enough charge must accumulate for the system to be stable. Given that the Higgs is assumed as having a small mass relative to the HS pions, we may approximate this lower bound by perturbing

about the analytic solution given here. Specifically, we consider Eq. (8.37), under the constraint

$$\frac{\mathcal{E}_\omega}{m_\pi Q} < 1, \tag{8.53}$$

with the parameter values $\eta \to 0$, $\lambda \to 0$, $\alpha \to 2$, $\beta \to 0$, and Ω given by Eq. (8.43). We find that the approximate lower bound on the charge due to the Higgs mass is

$$Q > 186.8 \frac{m_h v_s^2}{\theta^2 m_\pi^3}, \tag{8.54}$$

which, as expected, vanishes in the limit that $m_h/m_\pi \to 0$. Moreover, we would also expect a bound due to the Higgs cubic, as this similarly provides the Q-ball with additional mass without a corresponding increase to the charge. However, we do not include this here.

8.4.3 A numerical example: arbitrarily many heavy quarks

The task of analytically minimising the energy functional, Eq. (8.31), is intractable in the general case, but can be done numerically. In this section we present the results of a numerical minimisation of the energy functional with respect to α, β, and Ω for various choices of n_h, scanning over the parameters in Eq. (8.31). Across the entirety of parameter space we find that the energy functional is minimised when $\beta = 0$. This is in line with the heuristic argument presented in Section 8.4.2 that the neutral pion should not acquire a VEV inside the Q-ball.

The results are almost entirely independent of the number of heavy quarks. This is perhaps to be expected, since the number of heavy quarks enters only through a small modification to the denominator of Eq. (8.37). Consequently, we have chosen to use $n_h = 4$ as an illustrative example of the full numerical analysis; the most important differences between the analytic and numerical results arise from neglecting the Higgs mass and cubic coupling in the former case. We therefore also present a numerical analysis where we take $n_h = 0$, $m_h/m_\pi \to 0$ and $\lambda \to 0$; this 'minimal' case is meant as a cross-check against the analytic example discussed in Section 8.4.2.

The parameters were randomly sampled uniformly on a logarithmic scale. They are listed, along with their lower and upper bounds used for the scan, in Table 8.1. A set of randomly chosen parameters was rejected if it resulted in an energetically unfavourable solution – i.e., if Eq. (8.31) had no minimum such that $\mathcal{E}_\omega/Qm_\pi < 1$. The Higgs cubic coupling λ was treated as an independent parameter since it is poorly constrained by LHC Higgs measurements [1, 2].

Parameter	Range	Distribution
Q	$[1, 10^8]$	log-uniform
v_s [TeV]	$[1, 10]$	log-uniform
m_π [TeV]	$[0.5, 2v_s]$	log-uniform
θ	$[10^{-4}, 0.1]$	log-uniform
λ	$[10^{-6}, 10^{-1}]$	log-uniform

Table 8.1: Scan parameters and their ranges. Log-uniform means uniformly distributed on a logarithmic scale.

In the following figures, the solutions are clustered in cells and the cell brightness is directly proportional to the number of solutions it contains; the lighter (more yellow) the cell, the larger the number of solutions contained in it. In each figure, the left (right) panel shows the results for the minimal (full) case.

Figure 8.3 shows the result of the scan for the fractional binding energy, $1 - M_Q/Qm_\pi$, versus the total Q-ball charge. The figure shows that thick wall Q-balls exist for a wide range of charges (indeed, across the entire range of charges scanned over), with (for small charges) there being a preference for larger binding energy the larger the charge. This is consistent with the expression Eq. (8.44) in the analytic example. When the Higgs mass is appreciable, there is some preference for larger binding energy, across a range of charges. This can be attributed to the fact that the Higgs mass results in an unfavourable contribution to the Q-ball energy, and so favourable contributions from the other terms in the energy functional are required to be larger to offset this. The typical scale of the binding energy is thus increased.

Figures 8.4 and 8.5 show the behaviour of the physical Q-ball parameters, namely its mass and radius, with respect to the charge of the Q-ball. In Fig. 8.4 there is a strong linear correlation between the mass and charge of the Q-ball in both the minimal case and the full case. This is consistent with expression Eq. (8.44) in the analytic example, which predicts a linear relation between the mass and charge, to leading order.

Figure 8.5 shows that, for a given charge, there are Q-ball solutions with radii ranging from around 10^{-3} fm to around 1 fm in the minimal case. The radius (for small charges) tends to be larger on average for smaller Q; this is consistent with the expression Eq. (8.45) in the analytic example. We also note that the radius is bounded above by about 10^{-2} fm in the full case, when the Higgs mass is accounted for. This effect can be traced back to Eq. (8.39), with m_h acting to reduce the radius of the Q-ball. Indeed, if we take the limit $\Omega \to 1$, then whilst the Q-ball gets arbitrarily

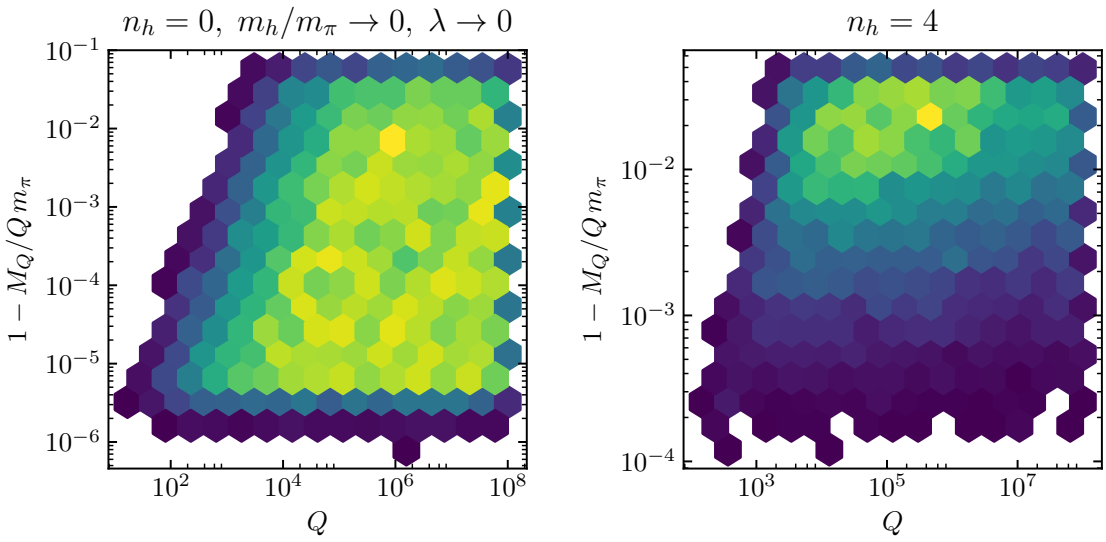

Figure 8.3: Number of Q-ball solutions with different fractional binding energies for different choices of Q-ball charge. The shade of a given cell corresponds to the number of solutions in that cell; a lighter (more yellow) shade corresponds to more solutions. The left and right panels show the result of the scan for the minimal case and the full case respectively.

large in the minimal case, its radius is bounded above by $\sim m_h/m_\pi$ in the full case. Physically we expect a lighter Higgs to yield a longer range attractive force, in turn stabilising bigger Q-balls.

Figure 8.6 shows the relationship between the Q-ball fractional binding energy and radius, in units of the pion mass. In the minimal case there is an exact relation between these two quantities; note that Eq. (8.44) and Eq. (8.45) are both functions solely of ϵ. To leading order this relation is linear with gradient -2. In the full case there is no such fixed relation, but nevertheless the binding energy is bounded above for a given radius, with there being a preference for binding energies close to this bound.

8.5 Thin-Wall Q-balls

A thin-wall Q-ball is characterised by a core of a homogeneous state, named Q-matter, and a thin outer shell. The mass of a thin-wall Q-ball is dominated by this core.[10] We let $\Sigma(\vec{r}) = \Sigma_0$ and $h(\vec{r}) = h_0$ be constant spatial profiles of the fields inside the

[10]This statement holds apart from in the case where the underlying fields comprising the Q-ball take on configurations such that the potential energy vanishes inside the homogeneous core (see Ref. [130]). In this case, the mass of the resulting Q-ball is dependent only on its surface energy.

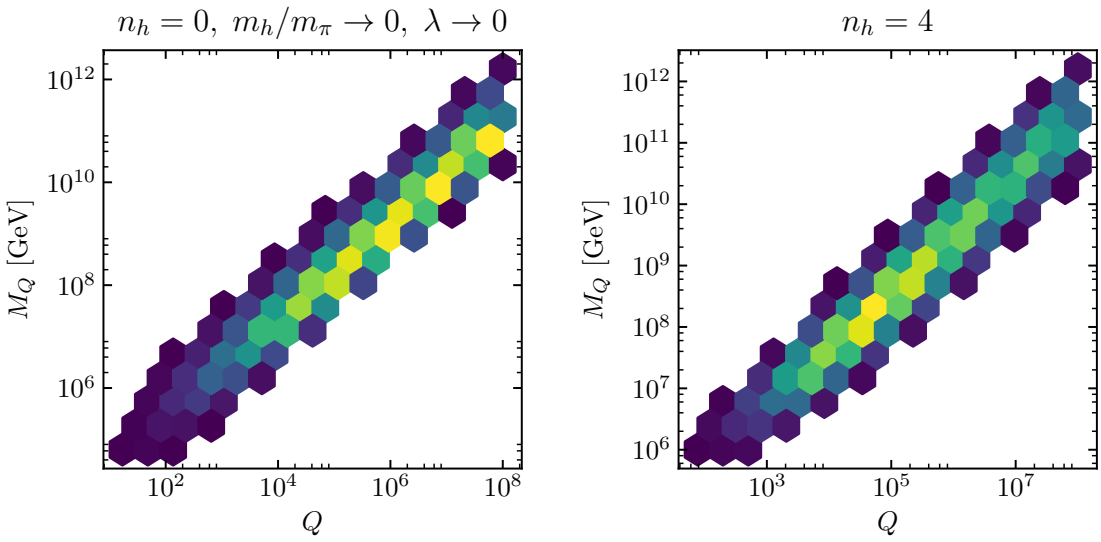

Figure 8.4: The distribution of Q-ball solutions in the mass-charge plane. See caption of Fig. 8.3 for more details.

core of the Q-ball, such that

$$\begin{aligned}\mathcal{E}_\omega \approx &-\omega^2\left(1-\theta\frac{2\eta}{3}\frac{h_0}{v_s}\right)\frac{f^2}{4}\mathrm{tr}\left([\Sigma_0,X][X,\Sigma_0^\dagger]\right)V\\ &-\left(1-\theta\,(1+\eta)\,\frac{h_0}{v_s}\right)\frac{B_0 f^2}{2}\mathrm{tr}\left(M(\Sigma_0+\Sigma_0^\dagger-2)\right)V\\ &+U(h_0)V+\omega Q+\mathcal{E}_F,\end{aligned} \tag{8.55}$$

where V is the volume of the core of the Q-ball.

To determine the mass of the resulting Q-ball, this expression must be minimised with respect to the field content, as well as the volume and the Lagrange multiplier. As we are working in the regime that there are two light quarks, we take advantage of the fact that $\Sigma_0 \in \mathrm{SU}(2)$ to proceed further,

$$\Sigma_0 = \exp\left(i\varphi\hat{n}\cdot\sigma\right) = \cos\varphi + i\,(\hat{n}\cdot\sigma)\sin\varphi, \tag{8.56}$$

where it is understood that $\cos\varphi$ multiplies a unit 2×2 matrix, and $\hat{n} = (n_1,\, n_2,\, n_3)$ is a unit vector, $\hat{n}^2 = 1$.

For convenience, we introduce a small parameter, ϵ, defined as,

$$\epsilon \equiv \theta\frac{h_0}{v_s}\,. \tag{8.57}$$

Here, we recall that θ is the mixing angle between the SM and HS Higgses and is less than unity following our choice to work in the small angle limit. Furthermore, the

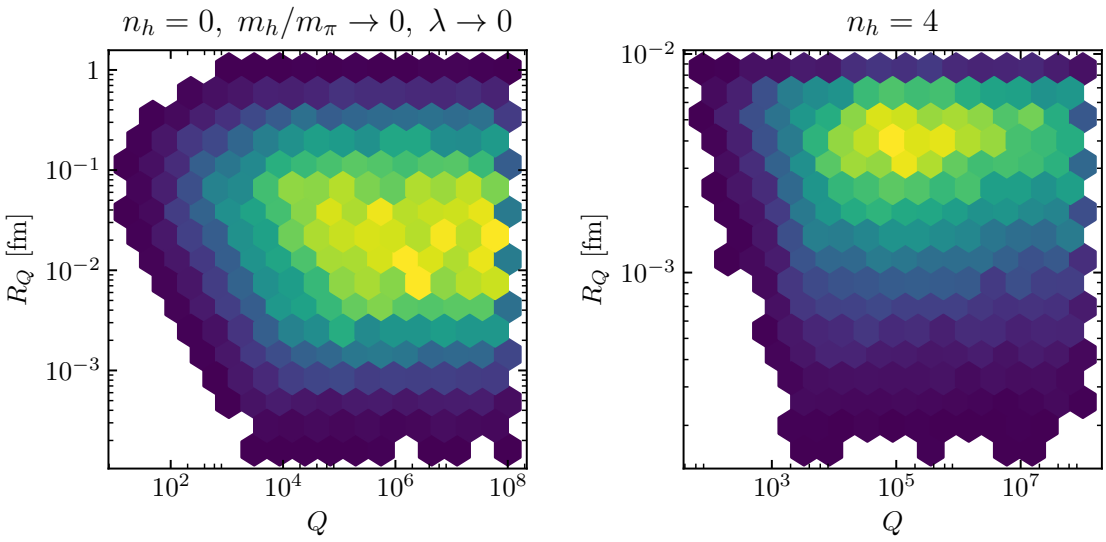

Figure 8.5: The distribution of Q-ball solutions in the radius-charge plane. See caption of Fig. 8.3 for more details.

ratio of VEVs h_0/v_s must also be small otherwise the effective field theory describing our system is not valid. Therefore, we also have that $\epsilon \ll 1$. Minimising with respect to the Lagrange multiplier, ω, yields

$$Q = \left(1 - \frac{2\eta}{3}\epsilon\right) f^2 \omega (1 - n_3^2) \sin^2 \varphi V \,. \tag{8.58}$$

This expression corresponds precisely to the one for the charge as determined from Eq. (8.27). We use this to eliminate ω, giving

$$\begin{aligned} E = &\frac{Q^2}{2\left(1 - \frac{2\eta}{3}\epsilon\right) f^2 (1 - n_3^2) \sin^2 \varphi V} + \left(1 - (1+\eta)\,\epsilon\right) m_\pi^2 f^2 (1 - \cos\varphi) V \\ &+ U(h_0)\, V + \frac{1}{5 m_f} \left(243 \pi^4 \frac{Q^5}{V^2}\right)^{1/3} . \end{aligned} \tag{8.59}$$

The only dependence on the direction of the VEV of Σ is the factor n_3 in the first term. The energy of the Q-ball is minimized for $n_3 = 0$, which corresponds to zero VEV for the neutral pions. This behaviour is unsurprising since a neutral pion VEV inside the Q-ball contributes to its mass but not to its charge – unlike the SM Higgs, the neutral pion does not offer a way to reduce the mass of the resulting Q-ball for a given charge.

We further note that, in the expression that must be minimised, E/Q, the volume and charge of the Q-ball always appear in the form V/Q. Thus, we infer that V

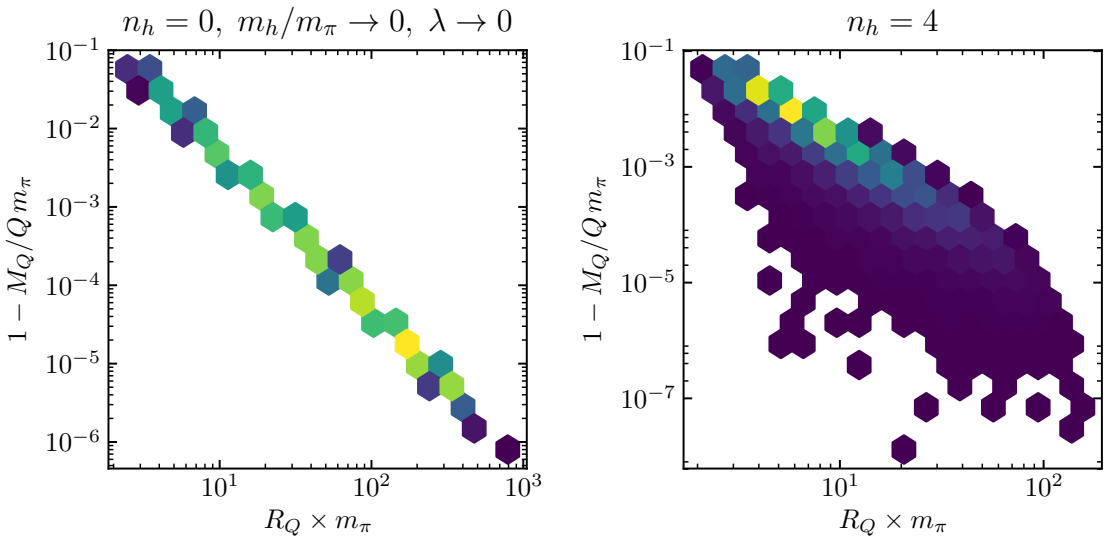

Figure 8.6: The distribution of Q-ball solutions with different fractional binding energies and radii (in units of the pion mass). See caption of Fig. 8.3 for more details.

scales linearly with Q for thin-wall Q-balls, even in the presence of Fermi degeneracy pressure. This is in contrast with the thick-wall case, where $V \sim Q^{-3}$, for small Q [18, 89].

Before we continue, we note the complications in proceeding analytically. Due to the non-trivial dependence on V, it is not feasible to analytically minimise the energy of the Q-ball with respect to the volume exactly. This is entirely due to the presence of the Fermi degeneracy pressure. Furthermore, the presence of n_h heavy quarks in Eq. (8.59) does not qualitatively affect the Q-ball solution since it only contributes an additional (and slightly larger) coupling between the HS Higgs and pions. Therefore, in the following, we will set $n_h = 0$ to simplify our expressions – we will reintroduce this parameter in our numerical results. The Higgs potential is also a barrier to obtaining exact analytical expression. We will discuss this as we proceed below.

For notational convenience, let us define the dimensionless variables,

$$\hat{E} \equiv \frac{E}{m_\pi\, Q} \qquad \text{and} \qquad \nu \equiv \frac{m_\pi\, f^2\, V}{Q}\,, \tag{8.60}$$

together with the dimensionless parameters

$$A \equiv \frac{(243\pi^4)^{1/3}}{5}\left(\frac{f^4}{m_f^3\, m_\pi}\right)^{1/3} \tag{8.61}$$

$$B \equiv \frac{1}{4}\frac{\lambda}{\theta^4}\frac{v_s^4}{m_\pi^2\, f^2} \tag{8.62}$$

$$C \equiv \theta\frac{v_h}{v_s} \tag{8.63}$$

These parameters effectively control the size of the contribution to the Q-ball mass due to the presence of Fermi degeneracy pressure, and the SM Higgs potential. Note that C is not entirely independent of B – they are related through

$$BC^4 = \frac{\lambda}{4}\frac{v_h^4}{m_\pi^2 f^2}. \tag{8.64}$$

This relation is always satisfied for some parameter values in each theory. Moreover, by Eq. (8.14), we see that $C \propto \theta^2$, and so it is related to the mixing between the SM and the HS. Thus, we see that C is naturally small.

Consider the example of $m_\pi \sim f \sim 4v_h$ and $\lambda \sim 0.1$, then $BC^4 \sim 10^{-4}$. Since, in the small angle approximation, $\theta \lesssim 10^{-1}$, we also have that

$$B \gtrsim 10^3\left(\frac{v_s}{f}\right)^4, \quad C \lesssim 10^{-1}\left(\frac{v_h}{v_s}\right), \quad \frac{\lambda_p}{\lambda_s}\left(\frac{v_h}{v_s}\right) \lesssim 10^{-1}, \tag{8.65}$$

where the final inequality comes from the definition of θ in Eq. (8.14). If there is no hierarchy between the two parameters λ_p and λ_s, then we see that $C \lesssim 10^{-2}$ and $B \gtrsim 10^4$, which in turn requires that $v_s \gtrsim f$ – this latter constraint is consistent with the idea that the "heavy Higgs" is massive enough that we need not include it in our effective theory. Realistically, the parameters can be different from these assignments, but we use values similar to these in our numerical study below.

Q-ball stability requires, at the minimum of the energy, that $\hat{E} < 1$; that is, the mass of the Q-ball must be less than the product of the total charge and the HS pion mass such that it cannot classically decay into pions. With these definitions, the energy of the Q-ball reads,

$$\widehat{E} = \frac{1}{2\sin^2\varphi\,\nu} + (1-\epsilon)(1-\cos\varphi)\,\nu + B\left(4C^2\epsilon^2 + 4C\epsilon^3 + \epsilon^4\right)\,\nu + \frac{A}{\nu^{2/3}}\,, \tag{8.66}$$

where we have set $\eta = 0$, as discussed above. Minimising this expression with respect

to ϵ, φ and ν yields, respectively,

$$\begin{aligned} 4B\left(2C^2\epsilon + 3C\epsilon^2 + \epsilon^3\right) &= (1-\cos\varphi) \\ (1-\epsilon)\nu^2 &= \frac{\cos\varphi}{(1-\cos^2\varphi)^2} \\ (1-\epsilon)(1-\cos\varphi) + B\left(4C^2\epsilon^2 + 4C\epsilon^3 + \epsilon^4\right) &= \frac{1}{2(1-\cos^2\varphi)\nu^2} + \frac{2}{3}\frac{A}{\nu^{5/3}}. \end{aligned} \tag{8.67}$$

It is not possible to simultaneously solve these equations analytically due to the combination of the terms proportional to ν^{-2} and $\nu^{-5/3}$, as well as the Higgs self-interactions.[11] We must therefore proceed numerically obtaining, at best, analytical approximations in certain limits.

Naively, we might expect that, since they represent contributions to the Q-ball energy without a corresponding contribution to the charge, the parameters A, B and C, defined in Eqs. (8.61), (8.62), and (8.63), should be as small as possible for a stable Q-ball to form. However, note that if we set $B \to 0$ in the above, then $\varphi \to 0$. This represents the vacuum solution, i.e., no stable Q-ball forms. Thus, counterintuitively, the Higgs potential is a necessary component in the stabilisation of these Q-balls; it is not enough for the Higgs to merely couple linearly to the pNGBs.

In the limit of $A \to 0$ and $C \to 0$, with B non-zero, these equations can be readily solved for a stable Q-ball solution. We find that, to leading order,

$$\varphi^2 \approx 8B\epsilon^3, \quad \nu \approx \frac{1}{8B\epsilon^3} \quad \text{and} \quad \epsilon \approx \frac{1}{(8B)^{1/2}}. \tag{8.68}$$

The resulting physical properties of the Q-balls are given by

$$m_Q \approx m_\pi Q\left(1 - \frac{1}{8}\frac{1}{(2B)^{1/2}}\right) \quad \text{and} \quad V \approx \frac{Q}{m_\pi f^2}(8B)^{1/2}. \tag{8.69}$$

We see that the resulting Q-balls are stable, provided that $B > 1/128$. In fact, $B > \mathcal{O}(1)$ since the expansion is in terms of $\epsilon \ll 1$, and so this condition is always satisfied whenever the expansion in ϵ is valid.

For the resulting Q-balls to be well-approximated by this idealised solution, we require that $A \ll 1$ and that the Higgs potential be well-defined by its quartic term in the centre of the Q-ball, i.e., that $4C \ll \epsilon$. Considering the definition of C and ϵ given above, this translates to $v_h \ll h_0$, and so the VEV of the Higgs inside the Q-ball must be much greater than its VEV outside it. This occurs if the separation between

[11] One might naively expect that, in the large volume limit, we might ignore the term proportional to ν^2, however, this becomes equivalent to the limits, either $\epsilon \to 1$, $\phi \to 0$, or $\nu \to 0$, which are all inconsistent with our assumptions ($\epsilon < 1$) or the requirements for a stable Q-ball solution ($\phi \neq 0$ and $\nu > 0$).

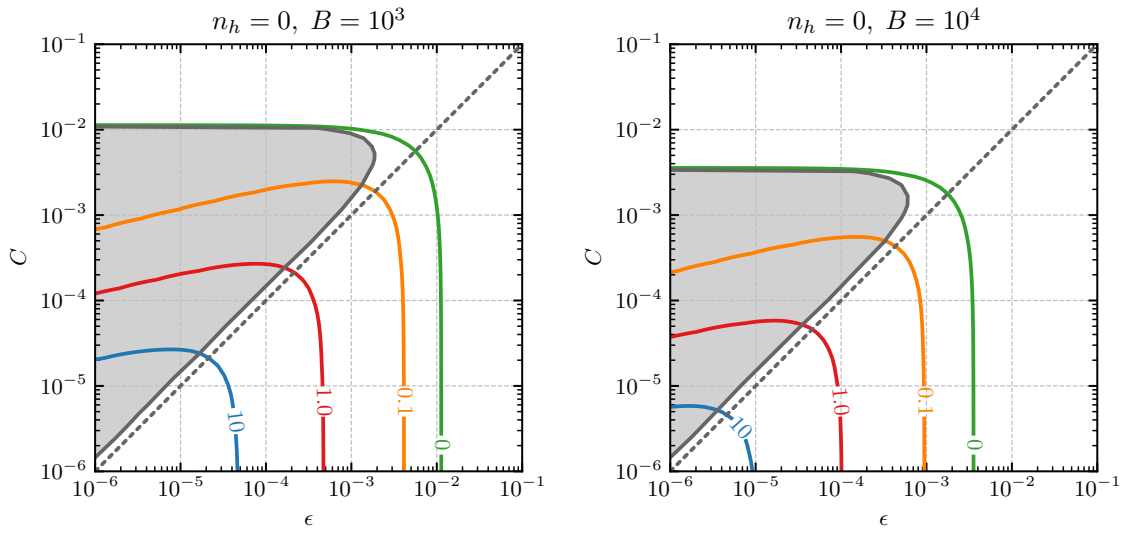

Figure 8.7: The C vs. ϵ plane. Each line corresponds to a family of Q-ball solutions for different values of the parameter A each given on their respective line. The dotted line denotes $C = \epsilon$. The excluded zone is the region where the binding energy goes negative – this corresponds with $C \gg \epsilon$, as discussed in the main text.

the scale of the Higgs and the scale of the HS pNGBs is large. To corroborate this, we examine this inequality in terms of the solution above,

$$8\sqrt{2}B^{1/2}C \ll 1, \tag{8.70}$$

which, in terms of the fundamental parameters of the theory, is

$$\frac{v_s^2}{m_\pi f} \ll 1, \tag{8.71}$$

where we have assumed that no hierarchy exists between the parameters λ_s and λ_p, and taken $\lambda \sim 0.1$. Thus, we see that, for this limit to be realistic, we require a hierarchy between the scale of the pNGBs and the VEV of the *heavier* HS Higgs. Moreover, since we ignored the HS Higgs from our analysis, for this to be self-consistent, we would require a large splitting between m_π and f. We thus see that this limit is highly idealised (and is contrary to our realistic parameter values discussed above).

A realistic analysis, however, must consider non-zero A and C. And, regarding the latter, for A positive definite, there is a maximum value of C beyond which the Q-ball becomes unbound because large values of C make the contribution of the Higgs potential to the Q-ball mass large. For a given value of A and B, we can numerically determine the relationship between ϵ and C by solving the set of equations in Eq. (8.67) simultaneously. These contours are shown in Fig. 8.7. The shaded region in the figure delineates where the Q-ball solutions become unstable

because C becomes too large.[12] Note that for the case where $A = 0$, the Q-ball solutions are always bound for any value of C up to its asymptotic value.

The vertical asymptotes[13] on the right of the plot represent the case that $C \to 0$. For $A \to 0$, this corresponds to the idealised case given above. When C is appreciable with respect to ϵ – when the curve differs slightly from the vertical asymptote – we find that

$$\epsilon \approx \frac{1}{(8B)^{1/2}} - C. \tag{8.72}$$

Given that $1 - \hat{E} \sim \epsilon$, we thus see that the binding energy of the Q-balls is reduced, which is as expected – though the Higgs is a necessary component for the stability of these Q-balls, the Higgs self-interactions only increase the mass without increasing the charge, and so the turning on of additional terms in the potential should always relatively reduce the binding energy. For $A \gtrsim 1$, we find that the asymptotes are given by

$$\epsilon \approx \frac{3}{64AB^{2/3}}. \tag{8.73}$$

In these cases, $1 - \hat{E} \sim \epsilon$ once more, and so we see that the binding energy of these Q-balls reduces quickly with increasing A or, equivalently, the greater the contribution the Fermi repulsion has, the less bound the Q-ball is.

We now turn our attention to the Fermi repulsion, its corresponding parameter, A, and the properties of realistic Q-balls. In Figs. 8.8 and 8.9, we plot the fractional binding energy, $1 - \hat{E}$, and the resulting Q-ball radius, as functions of A for different values of B and C – we use the fact that B and C are related through Eq. (8.64). We see that there are two limiting regimes. For $A \ll 1$ – the Fermi repulsion provides a negligible component to the energy – there is no dependence of the physical parameters on A: for $C \to 0$, this regime corresponds to our idealised scenario above. In the high A regime, the binding energy and radius scales as

$$m_Q \approx m_\pi Q \left(1 - \frac{9}{1024}\frac{1}{AB^{2/3}}\right) \quad \text{and} \quad V \approx \frac{Q}{m_\pi f^2}\left(\frac{32}{3}\right)^3 A^3 B. \tag{8.74}$$

As we can see in the latter case, together with the plots in Figs. 8.8 and 8.9, the effect of the Fermi repulsion is profound on the physical properties of the Q-ball. The binding energy reduces quickly with increased A and the Q-ball radius increases

[12] In this plane, this can be thought of as the region where $\epsilon \ll C$ – this is equivalent to the limit $h_0 \ll v_h$, i.e., that the Higgs VEV inside the Q-ball is negligible. As noted above, the Higgs is a necessary component to the stability of these Q-balls, and so it is expected that this limit would not produce a meaningful solution.

[13] The asymptotes in the shaded region are unphysical, and so we do not mention them further.

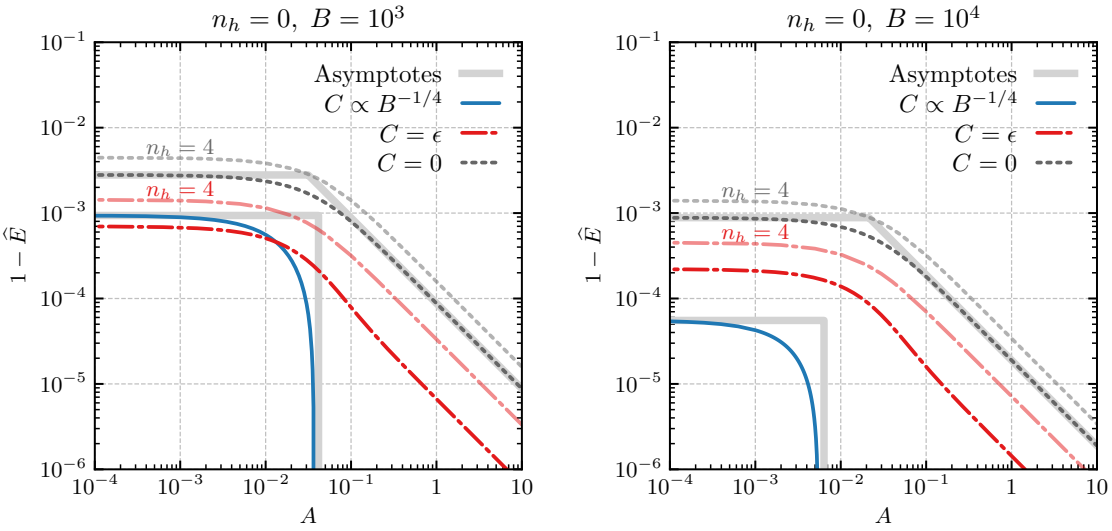

Figure 8.8: The fractional binding energy with no heavy quarks (left panel) and three heavy quarks (right panel). The three curves correspond to different values of the constant B; see text for details. The thick grey lines behind each curve (left panel) are obtained from the analytic expressions in the two limits of large and small A.

quickly with increased A. Note, when $C \sim \epsilon$, we obtain a function of A that is almost parallel to the case of $C \to 0$. When $C > \epsilon$, we see that as A gets larger, it becomes too large of a component of the energy of the Q-ball, and it renders it unstable. There is thus a maximum value of A that allows for stable Q-balls to form – this maximum can only be found numerically and is model-dependent, and so we do not state any values here.

We also include in these plots the binding energy curve for non-zero heavy quarks. Here, we choose $n_h = 4$ to mimic the SM. We find that the shape of the curves are unchanged by the addition of the heavy quarks and they merely introduce a shift to the curve towards higher binding energy. This behaviour is consistent with our earlier discussion, namely that the addition of heavy quarks effectively introduces an additional, slightly larger, coupling between the HS Higgs and pions.

Finally, we comment on the phenomenology of these Q-balls if they form a component of the observed DM abundance. In order to give an analytic understanding, we consider the idealised scenario of $A \to 0$ and $C \to 0$ in what follows. Upon including gravity, Q-balls may not have arbitrarily large charge [124, 133, 134]. A constraint on the maximum charge of Q-balls comes from demanding that the radius is always larger than the corresponding Schwarzschild radius, $R_Q > 2M_Q/M_{\rm Pl}^2$. This gives a

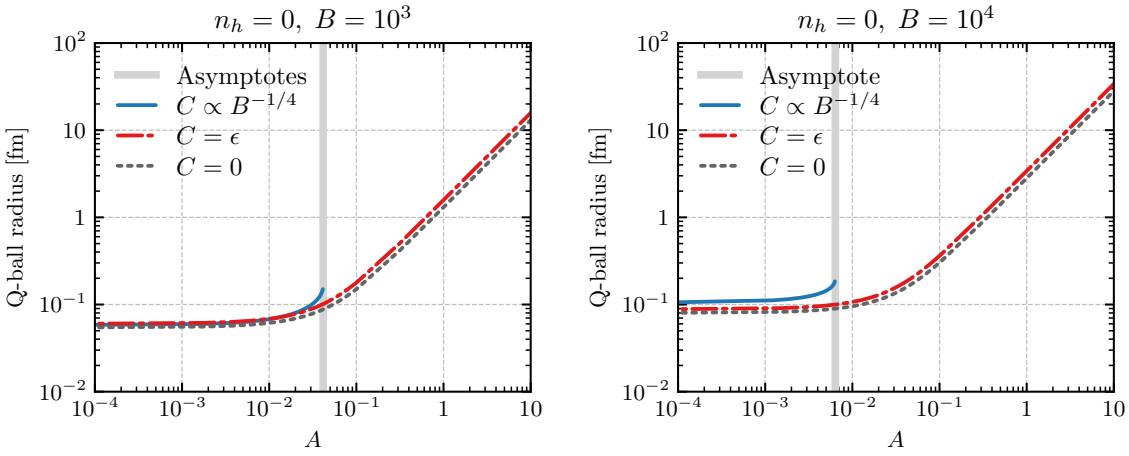

Figure 8.9: The Q-ball radius in [fm] with $Q = 10^6$. The three curves correspond to different values of the constant B; see text for details. The thick grey lines behind each curve (left panel) are obtained from the analytic expressions in the two limits of large and small A.

constraint on the charge to be

$$Q < \left[\frac{3\sqrt{2}}{16\pi}\right]^{1/2} \frac{M_{\rm Pl}^3}{m_\pi^2 f} B^{1/4}. \tag{8.75}$$

Since both the volume and energy of the Q-balls we studied scale with the charge, this in turn sets an upper bound on the mass and volume of these Q-balls before they collapse into black holes:

$$m_Q < \left[\frac{3\sqrt{2}}{16\pi}\right]^{1/2} \frac{M_{\rm Pl}^3}{m_\pi f} B^{1/4} \tag{8.76}$$

and

$$R_Q < \frac{1}{2}\left[\frac{54\sqrt{2}}{\pi^3}\right]^{1/6} \frac{M_{\rm Pl}}{m_\pi f} B^{1/4}. \tag{8.77}$$

For some typical values for the idealised case of $m_\pi \sim$ TeV, $f \sim 10$TeV, $v_s \sim 5$TeV, $\theta \sim 0.01$ and $\lambda \sim 0.1$, this sets an upper bound of $\sim 10\,$cm! These Q-balls can therefore be phenomenologically relevant, far below their upper bound in size, in DM experiments seeking direct detection, as they are in principle distinguishable from point-like particle states due to form factor suppression at moderately-high momentum transfer. The question, therefore, is how can such large Q-balls be formed in the early Universe? The build-up of Q-balls from collisions with constituent quanta, coined 'solitosynthesis' [59, 69], is unlikely to result in such large Q-balls, or even Q-balls that are large enough to be distinguished phenomenologically. This question is the subject of ongoing study.

8.6 Summary

In this work we have demonstrated, by both analytic and numerical methods, the existence of Q-ball solutions in an interacting, hidden sector pNGB-Higgs boson system. The specific class of low-energy effective Lagrangians we study, Eq. (8.20), are simple generalisations of the usual chiral Lagrangian to hidden sector QCD-like strong dynamics, supplemented by Higgs-portal-mediated interactions with the (lighter) physical Higgs boson. We find that both thick- and thin-wall Q-balls exist in this sector, subject to certain constraints given throughout the chapter. We emphasise that we have shown that Q-balls can exist in theories where the global charge-carrying states are composite, rather than elementary, scalars.

Such Q-ball solutions may be relevant to DM properties in a variety of BSM theories, in particular those of asymmetric dark matter and pNGB-Higgs theories. To assess whether this is the case requires a dedicated study of Q-ball production dynamics in the early Universe. Naively, there is no analogue of a decay of an Affleck-Dine condensate [50, 93] as applies in supersymmetric Q-ball models of dark matter. Thus we are left with solitosynthesis and aggregation build up along the lines of [59, 69, 72] as the likely dominant mechanism, though the details are different, or even a new mechanism altogether. This is the subject of future work.

Chapter 9

Concluding Remarks and Future Prospects

To reiterate Chapter 1, this thesis represented a study on the formal properties of field theories to determine which class of theories admit Q-ball solutions. Consequently, its goals were two-fold:

- To constrain the theories that possess stable Q-ball states by: (i) determining the differential equations that govern the VEV of the constituent scalar in the thin-wall limit, together with the physical properties of the resulting Q-ball; (ii) constraining the small-field expansions that lead to stable thick-wall Q-balls by demanding that the minimum of energy be classically stable against decay to the underlying quanta of the scalar field;
- To determine whether stable Q-balls, in both the thick- and thin-wall limit, can form from scalar mesons arising from the breaking of an approximate chiral symmetry in the SM and in a particular BSM theory.

We did not discuss the phenomenology of these theories in this thesis. We addressed the first point in Parts I and II, and the second point in Part III.

We have studied a wide class of theories and characterised the requirements for stable Q-balls to form. Specifically, we have studied: single-field theories possessing a single stabilising symmetry whose potential possesses interactions that are powers of the field, and for theories with non-canonical kinetic terms; and multi-field theories with either a single or multiple symmetries. Specifically, in the class of single-field theories we studied, we obtained necessary conditions for stable thick-wall Q-balls to exist. In our studies of multi-field theories, we only obtained sufficient conditions for stable thick-wall Q-balls to exist. We have also introduced a new class of object:

cored Q-balls, in which a larger Q-ball possesses another Q-ball, composed of another field, in its core.

As an example of a multi-field theory with non-canonical kinetic terms, we studied ChPT both in the SM and in a new hidden sector. We found that, to leading order, the SM does not admit Q-ball states. However, we found that a particular hidden sector, with mirror-world-like properties, could house Q-ball states that are stabilised by the SM Higgs.

There is still much work to be done. Firstly, a common result in our analyses of thick-wall Q-balls was that the next-to-quadratic term had to have an index p, such that $2 < p < 10/3$. That this same result appeared time and again would imply something deeper about thick-wall Q-balls in general. Whether or not this is the case is worthy of study. However, this could just be an artefact of our assumptions throughout – we often reduced the complexity of the system by making it as close to a single-field theory as possible, and so one could have predicted the results found.

Given that theories that violate this bound on p possess a thin-wall limit – including the theory whose potential contains terms with indices that are 2-4-6, which is often studied – it is implied that there exists a minimum charge in order for stable Q-balls to exist. The value of this charge is important to know, particularly in the scenario that realistic Q-balls are formed through aggregation of charge in the early universe. The requirement here is that, until this minimum charge is reached, the timescale of formation must be much less than the timescale of dissolution of the unstable thick-wall state.

The analysis of theories contained in this thesis can be generalised to more complex theories. This includes theories which couple the field to higher derivatives, or a more complex scenario involving multiple fields and a product group of symmetries.

A key component of the study of multi-field theories in the thick-wall limit was the assumption that the spatial profiles only differ by a positive normalisation constant. This must be tested numerically to see whether the properties of the Q-balls found are accurate or at least approximately so. It should be emphasised that relaxing this assumption should only make the true binding energy greater, and thus the Q-balls are more likely to form over a wider range of parameter space.

Much of this thesis has been concerned with characterising the types of theories that possess Q-ball states. We are physicists and we care about real-world theories that describe known phenomena. It would therefore be beneficial – if not crucial – to find actual theories that allow these Q-balls to exists, particularly in the case of multi-charged and cored Q-balls.

On the subject of realistic theories, ChPT contains terms beyond the leading order piece studied in this thesis. It is important to understand whether the addition of these terms leads to stable Q-ball states in the SM itself.

The Higgs-assisted Q-balls studied here are stable. As such, they can be relevant DM candidates. A dedicated study is required in order to determine their viability, as well as the formation properties in the early universe.

In his 1876 article, *On Waves*, Lord Rayleigh states that [131]:

> "Airy, in his treatise on Tides and Waves, still probably the best authority on the subject, appears not to recognize anything distinctive in the solitary wave."

We hope that this thesis has shown that solitons, specifically Q-balls, are distinctive and of much interest with still so much to learn about them, from their formal properties in field theories to whether our universe allows them to exist at all.

Bibliography

[1] *Prospects for measuring Higgs pair production in the channel $H(\to \gamma\gamma)H(\to b\bar{b})$ using the ATLAS detector at the HL-LHC*. Geneva, Oct 2014.

[2] *Higgs Pair Production in the $H(\to \tau\tau)H(\to b\bar{b})$ channel at the High-Luminosity LHC*. Geneva, Nov 2015.

[3] B. P. Abbott et al. Observation of Gravitational Waves from a Binary Black Hole Merger. *Phys. Rev. Lett.*, 116(6):061102, 2016.

[4] Steven Abel and Alex Kehagias. Q-branes. *JHEP*, 11:096, 2015.

[5] P. A. R. Ade et al. Planck 2015 results. XIII. Cosmological parameters. 2015.

[6] Ian Affleck and Michael Dine. A New Mechanism for Baryogenesis. *Nucl. Phys.*, B249:361–380, 1985.

[7] Kaustubh Agashe, Roberto Contino, and Alex Pomarol. The Minimal composite Higgs model. *Nucl. Phys.*, B719:165–187, 2005.

[8] Mark G. Alford. Q-clouds. *Nucl. Phys.*, B298:323–332, 1988.

[9] Rouzbeh Allahverdi, James Dent, and Jacek Osinski. Nonthermal production of dark matter from primordial black holes. *Phys. Rev. D*, 97(5):055013, 2018.

[10] M. Ambrosio et al. Nuclearite search with the macro detector at Gran Sasso. *Eur. Phys. J.*, C13:453–458, 2000.

[11] J. Arafune, T. Yoshida, S. Nakamura, and K. Ogure. Experimental bounds on masses and fluxes of nontopological solitons. *Phys. Rev.*, D62:105013, 2000.

[12] H. Arodz and J. Lis. Compact Q-balls and Q-shells in a scalar electrodynamics. *Phys. Rev. D*, 79:045002, 2009.

[13] Minos Axenides, Emmanuel Floratos, and Alexandros Kehagias. NonAbelian Q balls in supersymmetric theories. *Phys. Lett.*, B444:190–195, 1998.

[14] Vijay Balasubramanian, Bartlomiej Czech, Klaus Larjo, and Thomas S. Levi. Vacuum decay in multidimensional field landscapes: thin, thick and intersecting walls. *Phys. Rev. D*, 84:025019, 2011.

[15] Vernon Barger, Paul Langacker, Mathew McCaskey, Michael Ramsey-Musolf, and Gabe Shaughnessy. Complex Singlet Extension of the Standard Model. *Phys. Rev.*, D79:015018, 2009.

[16] Jacob D. Bekenstein. Relativistic gravitation theory for the MOND paradigm. *Phys. Rev.*, D70:083509, 2004. [Erratum: Phys. Rev.D71,069901(2005)].

[17] Brando Bellazzini, Csaba Csáki, and Javi Serra. Composite Higgses. *Eur. Phys. J.*, C74(5):2766, 2014.

[18] Fady Bishara, George Johnson, Olivier Lennon, and John March-Russell. Higgs Assisted Q-balls from Pseudo-Nambu-Goldstone Bosons. *JHEP*, 11:179, 2017.

[19] Fady Bishara and Olivier Lennon. Thin-Walled Higgs Assisted Q-balls from Pseudo-Nambu-Goldstone Bosons. arXiv:2110.02236.

[20] J. R. Bond and G. Efstathiou. Cosmic background radiation anisotropies in universes dominated by nonbaryonic dark matter. *Astrophys. J.*, 285:L45–L48, 1984.

[21] Annamaria Borriello and Paolo Salucci. The Dark matter distribution in disk galaxies. *Mon. Not. Roy. Astron. Soc.*, 323:285, 2001.

[22] Curtis G. Callan, Jr. and Sidney R. Coleman. The Fate of the False Vacuum. 2. First Quantum Corrections. *Phys. Rev.*, D16:1762–1768, 1977.

[23] Curtis G. Callan, Jr., Sidney R. Coleman, J. Wess, and Bruno Zumino. Structure of phenomenological Lagrangians. 2. *Phys. Rev.*, 177:2247–2250, 1969.

[24] Z. Chacko, Hock-Seng Goh, and Roni Harnik. A Twin Higgs model from left-right symmetry. *JHEP*, 01:108, 2006.

[25] Z. Chacko, Hock-Seng Goh, and Roni Harnik. The Twin Higgs: Natural electroweak breaking from mirror symmetry. *Phys. Rev. Lett.*, 96:231802, 2006.

[26] Z. Chacko, Yasunori Nomura, Michele Papucci, and Gilad Perez. Natural little hierarchy from a partially goldstone twin Higgs. *JHEP*, 01:126, 2006.

[27] R. S. Chivukula, Andrew G. Cohen, H. Georgi, Benjamin Grinstein, and A. V. Manohar. Higgs decay into goldstone bosons. *Annals Phys.*, 192:93–103, 1989.

[28] Douglas Clowe, Marusa Bradac, Anthony H. Gonzalez, Maxim Markevitch, Scott W. Randall, Christine Jones, and Dennis Zaritsky. A direct empirical proof of the existence of dark matter. *Astrophys. J.*, 648:L109–L113, 2006.

[29] Andrew G. Cohen, Sidney R. Coleman, Howard Georgi, and Aneesh Manohar. The Evaporation of Q Balls. *Nucl. Phys.*, B272:301–321, 1986.

[30] Sidney R. Coleman. The Fate of the False Vacuum. 1. Semiclassical Theory. *Phys. Rev.*, D15:2929–2936, 1977. [Erratum: Phys. Rev.D16,1248(1977)].

[31] Sidney R. Coleman. Q Balls. *Nucl. Phys.*, B262:263, 1985. [Erratum: Nucl. Phys.B269,744(1986)].

[32] Sidney R. Coleman, V. Glaser, and Andre Martin. Action Minima Among Solutions to a Class of Euclidean Scalar Field Equations. *Commun. Math. Phys.*, 58:211, 1978.

[33] Sidney R. Coleman and J. Mandula. All Possible Symmetries of the S Matrix. *Phys. Rev.*, 159:1251–1256, 1967.

[34] Sidney R. Coleman, J. Wess, and Bruno Zumino. Structure of phenomenological Lagrangians. 1. *Phys. Rev.*, 177:2239–2247, 1969.

[35] Edmund J. Copeland, Paul M. Saffin, and Shuang-Yong Zhou. Charge-Swapping Q-balls. *Phys. Rev. Lett.*, 113(23):231603, 2014.

[36] Nathaniel Craig and Andrey Katz. The Fraternal WIMP Miracle. *JCAP*, 1510(10):054, 2015.

[37] Nathaniel Craig, Andrey Katz, Matt Strassler, and Raman Sundrum. Naturalness in the Dark at the LHC. *JHEP*, 07:105, 2015.

[38] Bartlomiej Czech. A Novel Channel for Vacuum Decay. *Phys. Lett. B*, 713:331–334, 2012.

[39] Haakon Dahle. A compilation of weak gravitational lensing studies of clusters of galaxies. 2007.

[40] Durmus A. Demir. Stable Q balls from extra dimensions. *Phys. Lett.*, B495:357–362, 2000.

[41] A. Derevianko and M. Pospelov. Hunting for topological dark matter with atomic clocks. *Nature Phys.*, 10:933, 2014.

[42] Michael Dine, Lisa Randall, and Scott D. Thomas. Supersymmetry breaking in the early universe. *Phys. Rev. Lett.*, 75:398–401, 1995.

[43] Michael Dine, Lisa Randall, and Scott D. Thomas. Baryogenesis from flat directions of the supersymmetric standard model. *Nucl. Phys.*, B458:291–326, 1996.

[44] Jacques Distler, Brian Russell Hill, and Donald Spector. K Balls in the Chiral Lagrangian. *Phys. Lett.*, B182:71–74, 1986.

[45] Scott Dodelson and Michele Liguori. Can Cosmic Structure form without Dark Matter? *Phys. Rev. Lett.*, 97:231301, 2006.

[46] Michael J. Dugan, Howard Georgi, and David B. Kaplan. Anatomy of a Composite Higgs Model. *Nucl. Phys.*, B254:299–326, 1985.

[47] John R. Ellis, K. Enqvist, Dimitri V. Nanopoulos, and Keith A. Olive. Can Q Balls Save the Universe From Intermediate Scale Phase Transitions? *Phys. Lett.*, B225:313–318, 1989.

[48] John R. Ellis, S. Kelley, and Dimitri V. Nanopoulos. Precision LEP data, supersymmetric GUTs and string unification. *Phys. Lett. B*, 249:441–448, 1990.

[49] John R. Ellis, Dimitri V. Nanopoulos, and Serge Rudaz. GUTs 3: SUSY GUTs 2. *Nucl. Phys. B*, 202:43–62, 1982.

[50] Kari Enqvist and John McDonald. Q balls and baryogenesis in the MSSM. *Phys. Lett.*, B425:309–321, 1998.

[51] Nick Evans and Konstantinos S. Rigatos. Chiral symmetry breaking and confinement: separating the scales. *Phys. Rev. D*, 103:094022, 2021.

[52] Benoit Famaey and Stacy McGaugh. Modified Newtonian Dynamics (MOND): Observational Phenomenology and Relativistic Extensions. *Living Rev. Rel.*, 15:10, 2012.

[53] Marco Farina, Angelo Monteux, and Chang Sub Shin. Twin mechanism for baryon and dark matter asymmetries. *Phys. Rev.*, D94(3):035017, 2016.

[54] R. Foot. Mirror dark matter: Cosmology, galaxy structure and direct detection. *Int. J. Mod. Phys.*, A29:1430013, 2014.

[55] Robert Foot, H. Lew, and R. R. Volkas. A Model with fundamental improper space-time symmetries. *Phys. Lett.*, B272:67–70, 1991.

[56] Katherine Freese. Review of Observational Evidence for Dark Matter in the Universe and in upcoming searches for Dark Stars. *EAS Publ. Ser.*, 36:113–126, 2009.

[57] R. Friedberg, T. D. Lee, and A. Sirlin. A Class of Scalar-Field Soliton Solutions in Three Space Dimensions. *Phys. Rev. D*, 13:2739–2761, 1976.

[58] Joshua A. Frieman, G. B. Gelmini, Marcelo Gleiser, and Edward W. Kolb. Solitogenesis: Primordial Origin of Nontopological Solitons. *Phys. Rev. Lett.*, 60:2101, 1988.

[59] Joshua A. Frieman, Angela V. Olinto, Marcelo Gleiser, and Charles Alcock. Cosmic Evolution of Nontopological Solitons. 1. *Phys. Rev.*, D40:3241, 1989.

[60] Isabel Garcia Garcia, Robert Lasenby, and John March-Russell. Twin Higgs Asymmetric Dark Matter. *Phys. Rev. Lett.*, 115(12):121801, 2015.

[61] Isabel Garcia Garcia, Robert Lasenby, and John March-Russell. Twin Higgs WIMP Dark Matter. *Phys. Rev.*, D92(5):055034, 2015.

[62] Graciela Gelmini, Alexander Kusenko, and Shmuel Nussinov. Experimental identification of nonpointlike dark matter candidates. *Phys. Rev. Lett.*, 89:101302, 2002.

[63] Graciela B. Gelmini. TASI 2014 Lectures: The Hunt for Dark Matter. In *Theoretical Advanced Study Institute in Elementary Particle Physics: Journeys Through the Precision Frontier: Amplitudes for Colliders (TASI 2014) Boulder, Colorado, June 2-27, 2014*, 2015.

[64] H. Georgi. *Weak Interactions and Modern Particle Theory.* 1984.

[65] H. Georgi and S. L. Glashow. Unity of All Elementary Particle Forces. *Phys. Rev. Lett.*, 32:438–441, 1974.

[66] Howard Georgi and David B. Kaplan. Composite Higgs and Custodial SU(2). *Phys. Lett.*, 145B:216–220, 1984.

[67] Paul Gorenstein and Wallace Tucker. Astronomical Signatures of Dark Matter. *Adv. High Energy Phys.*, 2014:878203, 2014.

[68] Peter W. Graham, Surjeet Rajendran, and Jaime Varela. Dark Matter Triggers of Supernovae. *Phys. Rev.*, D92(6):063007, 2015.

[69] Kim Griest and Edward W. Kolb. Solitosynthesis: Cosmological Evolution of Nontopological Solitons. *Phys. Rev.*, D40:3231, 1989.

[70] Kim Griest, Edward W. Kolb, and Alessandro Massarotti. Statistical Fluctuations as the Origin of Nontopological Solitons. *Phys. Rev.*, D40:3529, 1989.

[71] Evan D. Hall, Thomas Callister Valery V. Frolov, Thomas Callister, Holger Mller, Maxim Pospelov, and Rana X Adhikari. Laser Interferometers as Dark Matter Detectors. 2016.

[72] Edward Hardy, Robert Lasenby, John March-Russell, and Stephen M. West. Big Bang Synthesis of Nuclear Dark Matter. *JHEP*, 06:011, 2015.

[73] Saquib Hassan. Private Communication. 2021.

[74] Julian Heeck, Arvind Rajaraman, Rebecca Riley, and Christopher B. Verhaaren. Mapping Gauged Q-Balls. *Phys. Rev. D*, 103(11):116004, 2021.

[75] Julian Heeck, Arvind Rajaraman, Rebecca Riley, and Christopher B. Verhaaren. Understanding Q-Balls Beyond the Thin-Wall Limit. *Phys. Rev. D*, 103(4):045008, 2021.

[76] Julian Heeck, Arvind Rajaraman, and Christopher B. Verhaaren. The Ubiquity of Gauged Q-Shells. arXiv:2105.02893.

[77] Shunsaku Horiuchi, Philip J. Humphrey, Jose Onorbe, Kevork N. Abazajian, Manoj Kaplinghat, and Shea Garrison-Kimmel. Sterile neutrino dark matter bounds from galaxies of the Local Group. *Phys. Rev.*, D89(2):025017, 2014.

[78] Wayne Hu, Rennan Barkana, and Andrei Gruzinov. Cold and fuzzy dark matter. *Phys. Rev. Lett.*, 85:1158–1161, 2000.

[79] Wayne Hu and Scott Dodelson. Cosmic microwave background anisotropies. *Ann. Rev. Astron. Astrophys.*, 40:171–216, 2002.

[80] Wayne Hu and Naoshi Sugiyama. Anisotropies in the cosmic microwave background: An Analytic approach. *Astrophys. J.*, 444:489–506, 1995.

[81] Wayne Hu and Martin J. White. The Damping tail of CMB anisotropies. *Astrophys. J.*, 479:568, 1997.

[82] George Johnson and John March-Russell. Hawking Radiation of Extended Objects. *JHEP*, 04:205, 2020.

[83] David B. Kaplan and Howard Georgi. SU(2)×U(1) Breaking by Vacuum Misalignment. *Phys. Lett.*, 136B:183–186, 1984.

[84] David B. Kaplan, Howard Georgi, and Savas Dimopoulos. Composite Higgs Scalars. *Phys. Lett.*, 136B:187–190, 1984.

[85] Masahiro Kawasaki, Kenichiro Konya, and Fuminobu Takahashi. Q-ball instability due to U(1) breaking. *Phys. Lett.*, B619:233–239, 2005.

[86] C. Kittel, P. McEuen, and John Wiley & Sons. *Introduction to Solid State Physics*. John Wiley & Sons, 2015.

[87] I. Yu. Kobzarev, L. B. Okun, and I. Ya. Pomeranchuk. On the possibility of experimental observation of mirror particles. *Sov. J. Nucl. Phys.*, 3(6):837–841, 1966. [Yad. Fiz.3,1154(1966)].

[88] Alexander Kusenko. Phase transitions precipitated by solitosynthesis. *Phys. Lett.*, B406:26–33, 1997.

[89] Alexander Kusenko. Small Q balls. *Phys. Lett.*, B404:285, 1997.

[90] Alexander Kusenko. Solitons in the supersymmetric extensions of the standard model. *Phys. Lett.*, B405:108, 1997.

[91] Alexander Kusenko, Vadim Kuzmin, Mikhail E. Shaposhnikov, and P. G. Tinyakov. Experimental signatures of supersymmetric dark matter Q balls. *Phys. Rev. Lett.*, 80:3185–3188, 1998.

[92] Alexander Kusenko and Anupam Mazumdar. Gravitational waves from fragmentation of a primordial scalar condensate into Q-balls. *Phys. Rev. Lett.*, 101:211301, 2008.

[93] Alexander Kusenko and Mikhail E. Shaposhnikov. Supersymmetric Q balls as dark matter. *Phys. Lett.*, B418:46–54, 1998.

[94] Alexander Kusenko and Paul J. Steinhardt. Q ball candidates for selfinteracting dark matter. *Phys. Rev. Lett.*, 87:141301, 2001.

[95] M. Laine and Mikhail E. Shaposhnikov. Thermodynamics of nontopological solitons. *Nucl. Phys.*, B532:376–404, 1998.

[96] Ki-Myeong Lee, Jaime A. Stein-Schabes, Richard Watkins, and Lawrence M. Widrow. Gauged q Balls. *Phys. Rev. D*, 39:1665, 1989.

[97] T. D. Lee. *Particle Physics and Introduction to Field Theory*, volume 1. 1981.

[98] T. D. Lee and Y. Pang. Nontopological solitons. *Phys. Rept.*, 221:251–350, 1992. [,169(1991)].

[99] R. A. Leese. Q lumps and their interactions. *Nucl. Phys.*, B366:283–311, 1991.

[100] Olivier Lennon. Multi-Field Q-balls with Real Scalars. arXiv:2112.14263.

[101] Olivier Lennon. Non-Canonical Q-balls. arXiv:2112.12547.

[102] Olivier Lennon. Q-balls with Multiple Charges and Cores. arXiv:2201.00024.

[103] Olivier Lennon, John March-Russell, Rudin Petrossian-Byrne, and Hannah Tillim. Black Hole Genesis of Dark Matter. *JCAP*, 04:009, 2018.

[104] Andrei D. Linde. Decay of the False Vacuum at Finite Temperature. *Nucl. Phys. B*, 216:421, 1983. [Erratum: Nucl.Phys.B 223, 544 (1983)].

[105] Mariangela Lisanti. Lectures on Dark Matter Physics. In *Theoretical Advanced Study Institute in Elementary Particle Physics: New Frontiers in Fields and Strings (TASI 2015) Boulder, CO, USA, June 1-26, 2015*, 2016.

[106] A. K. Lloyd-Stubbs and J. McDonald. Q-balls in Non-Minimally Coupled Palatini Inflation and their Implications for Cosmology. arXiv:2112.09121.

[107] R. B. MacKenzie and Manu B. Paranjape. From Q walls to Q balls. *JHEP*, 08:003, 2001.

[108] M. Milgrom. A Modification of the Newtonian dynamics as a possible alternative to the hidden mass hypothesis. *Astrophys. J.*, 270:365–370, 1983.

[109] T. F. Morris. Class of Nonlinear Klein-Gordon Equations with Localized Solutions. *Phys. Lett. B*, 78:87–89, 1978.

[110] T. F. Morris. Nondissipative Character of Solutions of a Class of Nonlinear Klein-Gordon Equations. *Phys. Lett. B*, 76:337–339, 1978.

[111] Leonidas A. Moustakas and R. Benton Metcalf. Detecting dark matter substructure spectroscopically in strong gravitational lenses. *Mon. Not. Roy. Astron. Soc.*, 339:607, 2003.

[112] K. A. Olive et al. Review of Particle Physics. *Chin. Phys.*, C38:090001, 2014.

[113] Hideharu Otsu and Toshiro Sato. Q balls with Topological Charge. *Nucl. Phys.*, B334:489–505, 1990.

[114] James M. Overduin and P. S. Wesson. Dark matter and background light. *Phys. Rept.*, 402:267–406, 2004.

[115] F. Paccetti Correia and M. G. Schmidt. Q balls: Some analytical results. *Eur. Phys. J. C*, 21:181–191, 2001.

[116] A. G. Panin and M. N. Smolyakov. Problem with classical stability of U(1) gauged Q-balls. *Phys. Rev. D*, 95(6):065006, 2017.

[117] Michael E. Peskin and Daniel V. Schroeder. *An Introduction to quantum field theory*. Addison-Wesley, Reading, USA, 1995.

[118] A. Pich. Chiral perturbation theory. *Rept. Prog. Phys.*, 58:563–610, 1995.

[119] Marieke Postma. Solitosynthesis of Q balls. *Phys. Rev. D*, 65:085035, 2002.

[120] Gerald Rosen. Particlelike Solutions to Nonlinear Complex Scalar Field Theories with Positive-Definite Energy Densities. *J. Math. Phys.*, 9:996, 1968.

[121] Vera C. Rubin and W. Kent Ford, Jr. Rotation of the Andromeda Nebula from a Spectroscopic Survey of Emission Regions. *Astrophys. J.*, 159:379–403, 1970.

[122] Alexander M. Safian. Some More Non-Abelian Q-balls. *Nucl. Phys.*, B304:392–402, 1988.

[123] Alexander M. Safian, Sidney R. Coleman, and Minos Axenides. SOME NON-ABELIAN Q BALLS. *Nucl. Phys.*, B297:498–514, 1988.

[124] Nobuyuki Sakai and Takashi Tamaki. What happens to Q-balls if Q is so large? *Phys. Rev.*, D85:104008, 2012.

[125] A. D. Sakharov. Violation of CP Invariance, c Asymmetry, and Baryon Asymmetry of the Universe. *Pisma Zh. Eksp. Teor. Fiz.*, 5:32–35, 1967. [Usp. Fiz. Nauk161,61(1991)].

[126] James H. C. Scargill. Barnacles and Gravity. *JHEP*, 09:080, 2017.

[127] Matthew D. Schwartz. *Quantum Field Theory and the Standard Model*. Cambridge University Press, 2014.

[128] Douglas Scott, Martin J. White, Joanne D. Cohn, and Elena Pierpaoli. Cosmological difficulties with modified Newtonian dynamics (or, La Fin du MOND?). *Submitted to: Mon. Not. Roy. Astron. Soc.*, 2001.

[129] Uros Seljak. A Two fluid approximation for calculating the cosmic microwave background anisotropies. *Astrophys. J.*, 435:L87–L90, 1994.

[130] Donald Spector. First Order Phase Transitions in a Sector of Fixed Charge. *Phys. Lett. B*, 194:103, 1987.

[131] J. W. Strutt. On waves. *Philos. Mag. Series 5*, 1(4):257–279, 1876.

[132] Y. Takenaga et al. Search for neutral Q-balls in super-Kamiokande II. *Phys. Lett.*, B647:18–22, 2007.

[133] Takashi Tamaki and Nobuyuki Sakai. How does gravity save or kill Q-balls? *Phys. Rev.*, D83:044027, 2011.

[134] Takashi Tamaki and Nobuyuki Sakai. What are universal features of gravitating Q-balls? *Phys. Rev.*, D84:044054, 2011.

[135] Takashi Tamaki and Nobuyuki Sakai. Large gauged Q-balls with regular potential. *Phys. Rev. D*, 90(8):085022, 2014.

[136] Mitsuo I. Tsumagari, Edmund J. Copeland, and Paul M. Saffin. Some stationary properties of a Q-ball in arbitrary space dimensions. *Phys. Rev.*, D78:065021, 2008.

[137] J. Anthony Tyson, Greg P. Kochanski, and Ian P. Dell'Antonio. Detailed mass map of CL0024+1654 from strong lensing. *Astrophys. J.*, 498:L107, 1998.

[138] Edo van Uitert, Henk Hoekstra, Tim Schrabback, David G. Gilbank, Michael D. Gladders, and H. K. C. Yee. Constraints on the shapes of galaxy dark matter haloes from weak gravitational lensing. *Astron. Astrophys.*, 545:A71, 2012.

[139] M. B. Voloshin. Once Again About the Role of Gluonic Mechanism in Interaction of Light Higgs Boson with Hadrons. *Sov. J. Nucl. Phys.*, 44:478, 1986. [Yad. Fiz.44,738(1986)].

[140] Mikhail B. Voloshin and Valentin I. Zakharov. Measuring QCD Anomalies in Hadronic Transitions Between Onium States. *Phys. Rev. Lett.*, 45:688, 1980.

[141] Robert V. Wagoner, William A. Fowler, and Fred Hoyle. On the Synthesis of elements at very high temperatures. *Astrophys. J.*, 148:3–49, 1967.

[142] J. Werle. Localized Solutions of Nonlinear Klein-Gordon Equations. *Phys. Lett. B*, 71:367–368, 1977.

[143] Qi-Xin Xie, Paul M. Saffin, and Shuang-Yong Zhou. Charge-Swapping Q-balls and Their Lifetimes. *JHEP*, 07:062, 2021.

[144] Jaiyul Yoo, Julio Chaname, and Andrew Gould. The end of the MACHO era: limits on halo dark matter from stellar halo wide binaries. *Astrophys. J.*, 601:311–318, 2004.

[145] F. Zwicky. On the Masses of Nebulae and of Clusters of Nebulae. *Astrophys. J.*, 86:217–246, 1937.